Supporting Information

g-C_3N_4 Catalysed Sustainable Synthesis of (Hetero)aryl Acids and Regioselective α- bromo ketones In One Vessel Under Visible Light Catalysis

Sangita Bishi,[a] Mahuya Kar,[b] Tarun K. Mandal[b] and Debayan Sarkar[*c]

[a] Sangita Bishi, Department of Chemistry, National Institute of Technology, Rourkela, Odisha 769008, India. Email-518CY2020@nitrkl.ac.in.
[b] Mahuya Kar, Email-csmk2225@iacs.res.in
Prof. Tarun Kumar Mandal, Email-psutkm@iacs.res.in
School of Chemical Science, Indian Association for the Cultivation of Science, Jadavpur, Kolkata 700032, India.
[c] Corresponding Author- Dr. Debayan Sarkar, Department of Chemistry, Indian Institute of Technology, Indore, Madhya Pradesh 453552, India. http://orcid.org/0000-0003-2221 2912. Email: sarkard@iiti.ac.in

TABLE OF CONTENTS

1. General Information

All starting materials were purchased from Sigma-Aldrich, Avra chemical synthesis, Hi-Media, Spectrochem, TCI chemicals, or Thermo Fisher Scientific and used without further purification unless otherwise indicated. Solvents were purchased from Finar. Carboxylic acids and solvents were used as received. Thin layer chromatography (TLC) was performed on 0.25 mm E. Merck silica gel 60 F254 plates and visualized under UV light (254 nm). Silica flash chromatography was performed on 230−400 mesh silica gel and 100−200 mesh silica gel. The products were confirmed by nuclear magnetic resonance (NMR) spectroscopy and measured in δ values in parts per million (ppm). ^{1}H and ^{13}C NMR spectra were recorded on Bruker, Advance III NMR spectrometer (300 MHz, 400 MHz for ^{1}H and 75 MHz, 100 MHz for ^{13}C). ^{1}H chemical shifts were referenced from the chemical shifts of residual solvent peaks (7.26 ppm for $CDCl_3$, 3.31 ppm for CD_3OD, and 2.50 ppm for DMSO-d_6). ^{13}C NMR spectra were recorded with complete proton decoupling. ^{13}C chemical shifts were referenced from the chemical shifts of $CDCl_3$ (77.16 ppm), CD_3OD (49.00 ppm), or DMSO-d_6 (39.52 ppm). Analytical thin layer chromatography (TLC) was carried out on pre-coated glass silica gel plates, and the spots were visualized under 254 nm UV irradiation and/or staining by vanillin solution. Column chromatography was performed on silica gel (230–400 mesh) using an appropriate eluent system. Coupling constants (*J*) are given in hertz (Hz), and signal multiplicities are described of NMR data as s = singlet, d = doublet, t = triplet, dd = doublet of doublets, dt = doublet of triplets, qd = quartet of doublets, q = quartet, quint, and p = pentet, m = multiplet, and br = broad. High-resolution mass spectra (HRMS) were measured in a Waters Xevo G_2-XS Q-Tof/Tof and a 6200 series TOF/6500 series Q-TOF B.09.00 (B9044.1SP1) mass spectrometer with an orthogonal Z-spray-electrospray interface on a micro mass spectrometer.

Crystal structure of g-C_3N_4 investigated by X-ray diffraction (XRD) spectroscopy (Philips PW3040/00 diffractometer (40 kV and 30 mA, Cu Kα) in a 2θ range from 5° to 80° at a scanning rate of 10°/min. Fourier transform infrared (FTIR) spectra (PerkinElmer spectrometer) were performed between 400 and 4000 cm^{-1} at room temperature. The UV/vis diffuse reflectance spectra (UV/vis DRS) were recorded on a spectrophotometer (Hitachi U-4100) equipped with an integrating sphere assembly using $BaSO_4$ as a reflectance standard material. The Raman spectra of as-prepared samples were recorded on a Renishaw InVia Raman spectrometer (UK model). The morphologies of the samples were observed by Field emission scanning electron microscopy (Hitachi COM-S-4200), transmission electron microscopy (TEM), and high-resolution transmission electron microscopy (JEOL JEM 2100F, operated at 200 kV). The photoluminescence (PL) spectra and time-resolved PL spectra were obtained on an FLS-920T fluorescence spectrophotometer at room temperature. ESR experiment was conducted in Bruker EMX Spectrometer (X-Band, 9-10 GHz) to confirm the radical mechanism of the reaction pathway.

2. Synthetic procedures for the synthesis of photocatalyst g-C_3N_4

The g-C_3N_4 photocatalyst was synthesized by the classic and facile method via the slow pyrolysis of melamine at programmed temperatures in air (Scheme S1). In detail, 5 g melamine was placed in an alumina crucible covered with a lid and heated in a muffle furnace at 450 °C, 500 °C, 550 °C and 600 °C for 3 h at a heating rate of 3 °C/ min. The resultant g-C_3N_4 samples were designated as g-C_3N_4 (450 °C), g-C_3N_4 (500 °C), g-C_3N_4 (550 °C), and g-C_3N_4 (600 °C) according to polymerization temperatures. The white colour of melamine changes from white to yellow, indicating the formation of a g-C_3N_4 nanosheet. The lesser yield of g-C_3N_4 (3.20 g) as part of melamine sublimate before 550 °C. XRD characterization of melamine and g-C_3N_4 confirms the full conversion of melamine to g-C_3N_4(Figure S1).

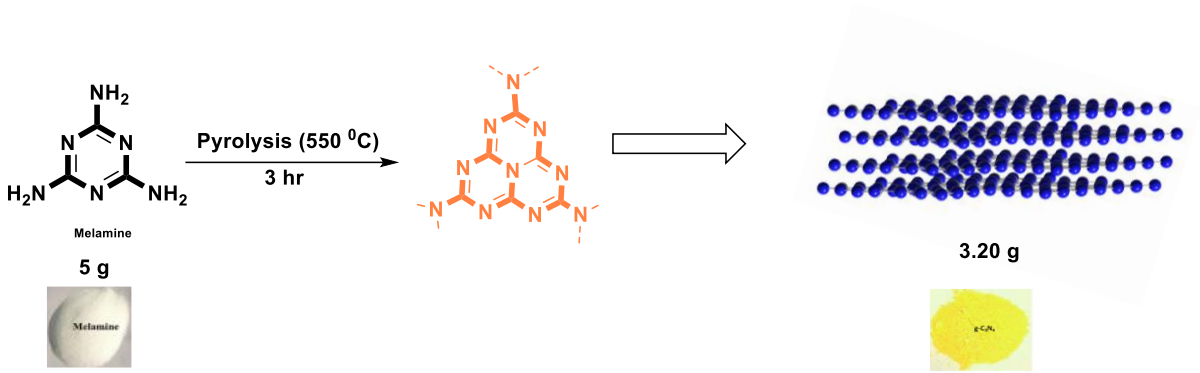

Scheme S1. Graphitic carbon nitride (g-C_3N_4) preparation from melamine through pyrolysis at 550 °C.

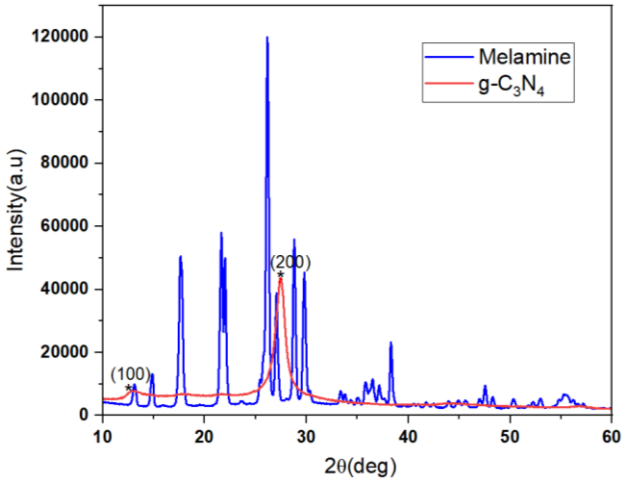

Figure S1. Comparison of XRD pattern of melamine and g-C_3N_4 (550 °C).

3. General method for the preparation of aryl acid and α-bromo ketones

To the reaction mixture of aryl halides 1a 50 mg (0.29 mmol) and g-C_3N_4(5 mg), 4 mL CH_3CN was added into the 5 mL reaction vial while stirring vigorously. After being stirred for another 6 h at room temperature, 1 equiv. of olefin was supplemented and further irradiated to blue LED. After 10 minutes of stirring, the reaction mixture was centrifuged at 1000 rpm and washed with acetonitrile 4 times and then ethanol to separate the catalyst from the reaction mixture. Then the organic layer was dried over anhydrous Na_2SO_4 and concentrated in vacuo for column chromatography. Column chromatography was performed on silica gel (230–400 mesh) using an appropriate eluent system. The catalyst was then washed with ethanol several times to recover the catalyst for further use in the next cycle of reaction.

4. Characterizations of photocatalyst g-C_3N_4

The UV–Vis diffuse reflectance spectrum of the as-prepared sample is depicted in Figure 2(a), which has an absorption edge at about 450 nm, which originates from its bandgap of 2.7 eV. The crystal structure of as-prepared g-C_3N_4 was analyzed by XRD patterns. As presented in Figure 2(b), all the peaks in the XRD patterns of the samples could be easily indexed to the hexagonal phase of g-C_3N_4. The peak at about 27° is due to the stacking of the conjugated aromatic system, which is indexed for graphitic materials as the (002) peak of g-C_3N_4. Another minor diffraction peak around 13° is assigned to the (100) plane associated with the in-plane repeated units of g-C_3N_4. The crystal structure of the g-C_3N_4 can be further confirmed by FTIR spectroscopy. As shown in Figure 2(c) for the pristine g-C_3N_4 sample, the broadband at the range of 3000–3500 cm^{-1} corresponds to the N–H stretching vibration of uncondensed amino groups and O–H vibration from adsorbed water on the surface. The band at 1638 cm^{-1} could be ascribed to C–N stretching and the four bands at 1575 cm^{-1}, 1410 cm^{-1}, 1325 cm^{-1} and

1246 cm^{-1} can attribute to aromatic C–N stretching vibration. The absorption band at 807 cm^{-1} accords with the characteristic breathing mode of triazine units.

Photoluminescence (PL) analysis was helpful to reveal the efficiency of carrier transfer and separation and to study the lifetime of charge carriers. As can be seen, g-C_3N_4 had a strong emission peak centered at around 460 nm Figure S2(a) shows the PL excitation spectrum of g-C_3N_4 exhibiting a broad excitation band covering 200 nm to 420 nm. The evolution of the excitation spectrum matches well with the phase and microstructure evolution as shown in Figure S11(b). The time-resolved fluorescence decay spectrum Figure S2(b) gives information about the photophysical behaviour of photoexcited charge carriers. The fluorescent intensity of the sample decays exponentially with a radiative lifetime of 2.5566 ns, which plays an important role in photocatalytic reactions before recombination. Raman spectroscopy is usually used to search the vibrational properties of carbon materials. There are no significant Raman signals observed on pristine g-C_3N_4 (Figure S2(c)). The band at 1569 cm^{-1} corresponds to the C=N stretching vibration of g-C_3N_4, which is also defined as a graphitic G band, indicating the formation of a graphite-like structure, while the 552 cm^{-1} belongs to the in-plane symmetrical stretching vibration of heptazine heterocycles. The peaks located at 475 cm^{-1}, and 1235 cm^{-1} stem from the vibration modes of CN heterocycles in g-C_3N_4.

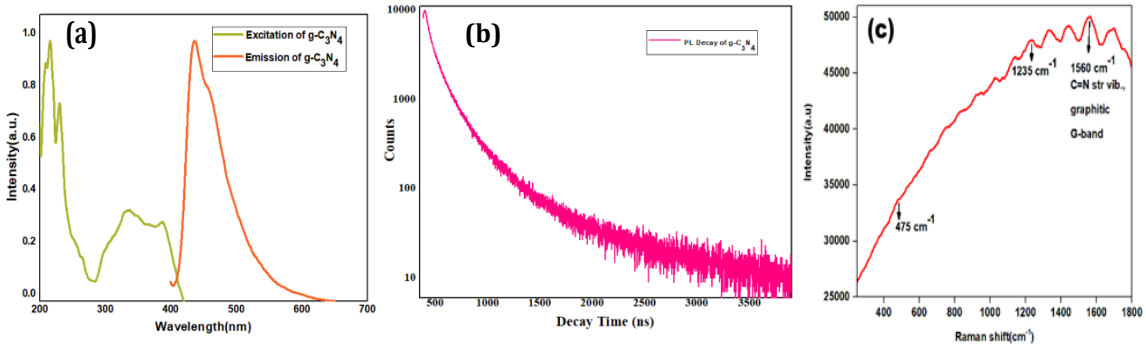

Figure S2. (a) Excitation and emission spectrum, (b) Time-resolved fluorescence decay spectrum, and (c) Raman spectrum of fresh g-C_3N_4.

The more detailed characterization of the morphologies and microstructures of the samples was based on FESEM, TEM, and EDS analyses. Figure S3 represents HR-TEM and SAED images for g-C_3N_4, no obvious crystal fringe is observed, which indicates that the product is amorphous. Further, the mist diffraction ring, shown in the selected area electron diffraction (SEAD) in Figure S3(c) confirms that the product synthesized is amorphous. This result is in good agreement with those of HRTEM and XRD patterns.

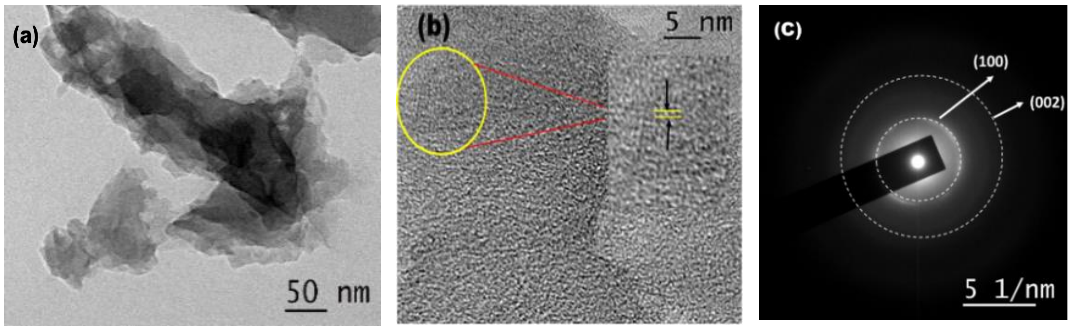

Figure S3. (a) TEM, (b) HR-TEM, and (c) SAED images of g-C_3N_4 synthesized via the thermal condensation of melamine at 550 °C for 3 h.

5. Light on/off experiment

From the light on/off studies, it was observed that product formation occurred only during periods of constant irradiation (Figure S4). Benzyl bromide **1a** (25.0 mg), and g-C_3N_4 (5 mg) were added into a 3 mL vial equipped with a stirring bar under atmosphere. Acetonitrile was added to the reaction tube. The reaction mixture was irradiated by 0. 9 W blue LED. After being irradiated for 1 h, GC yield of **3a** was calculated. Then the reaction

mixture was stirred for 1 h with light-off. All the subsequent GC yields were analysed in the similar way after 1 h light on and off.

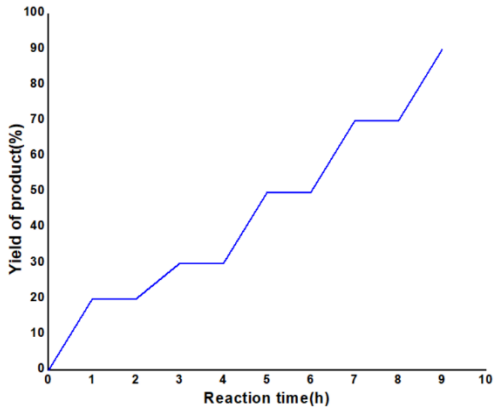

Figure S4. Light ON/OFF experiment for benzyl bromide.

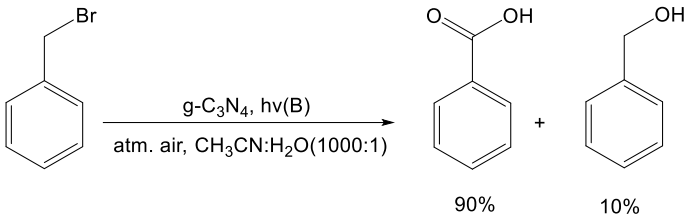

Scheme S2. Solvent H_2O: CH_3CN (1:100) used for photooxidation of benzyl bromide with g-C_3N_4.

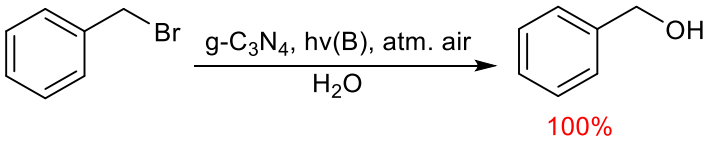

Scheme S3. Solvent H_2O used for photooxidation of benzyl bromide with g-C_3N_4.

Table S1. CAS number of the photocatalyzed product.

SI No.	Compound (No.)	CAS Number
1	Benzoic acid (1)	65-85-0
2	2-chloro benzoic acid (2)	118-91-2
3	4-bromo benzoic acid (3)	586-76-5
4	2-bromo benzoic acid (4)	88-65-3
5	2, 4-dichloro benzoic acid (5)	50-84-0
6	2-Hydroxybenzoic acid (6)	9003-11-6
7	4-Nitrobenzoic acid (7)	62-23-7
8	2-Iodobenzoic acid (8)	88-67-5
9	4- (Trifluoromethyl)benzoic acid (9)	455-24-3
10	Pyridine-3-carboxylic acid (10)	59-67-6

11	3-methoxy benzoic acid (11)	586-38-9
12	2'-Cyano[1,1'-biphenyl]-4-carboxylic acid (12)	5728-44-9
13	Pentafluorobenzoic acid (14)	602-94-8
14	3, 5-Dimethoxybenzoic acid (15)	1132-21-4
15	4-Fluorobenzoic acid (16)	456-22-4
16	3-Cholorobenzoic acid (18)	535-80-8
17	3-Phenoxy benzoic acid (19)	3739-38-6
18	4-Chlorobenzoic acid (20)	74-11-3
19	Benzophenone (22)	119-61-9
20	pyridine-2,6-dicarboxylic acid (23)	499-83-2
21	phthalic acid (24)	88-99-3
22	2,4,6-trimethyl benzoic acid (25)	480-63-7
23	2-aminobenzoic acid (26)	118-92-3
24	2-(diphenylphosphaneyl) benzoic acid (27)	17261-28-8
25	1,2,4,5-Benzenetetracarboxylic acid (28)	89-05-4
26	2-Ethylbenzoic acid (29)	612-19-1
27	Furan-2-carboxylic acid (30)	88-14-2
28	Thiophene-2-carboxylic acid (31)	25112-68-9
29	Valeric acid (32)	109-52-4
30	Cyclopentane carboxylic acid (33)	3400-45-1

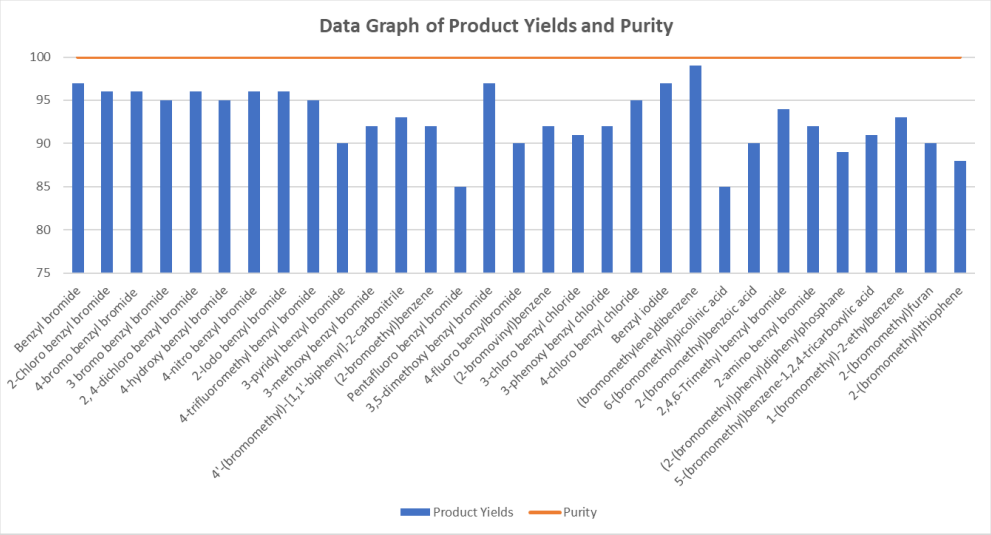

Figure S5. Data graphs of the yield and purity of the target products.

6. Active species trapping reaction

To ensure the reaction mechanism, the reaction system was subjected to scavengers of electrons, holes, and radicals. Under the oxygen atmosphere, the conversion of benzyl bromide in presence of sodium oxalate ($Na_2C_2O_4$) and methanol as holes (h^+) scavenger, tetra-methyl piperidine N-oxide (TEMPO) and 5,5-Dimethyl-1-Pyrroline-N-Oxide (DMPO) as radical scavengers, $K_2S_2O_8$, $AgNO_3$ as electron(e^-) scavenger and benzoquinone (BQ) as superoxide ($^{\bullet}O_2^-$) radical is considerably reduced and a trace amount of benzoic acid is obtained. In the presence of hole scavenger methanol (as solvent) and H_2O, benzyl alcohol is obtained as the major product instead of benzoic acid (Scheme S4).

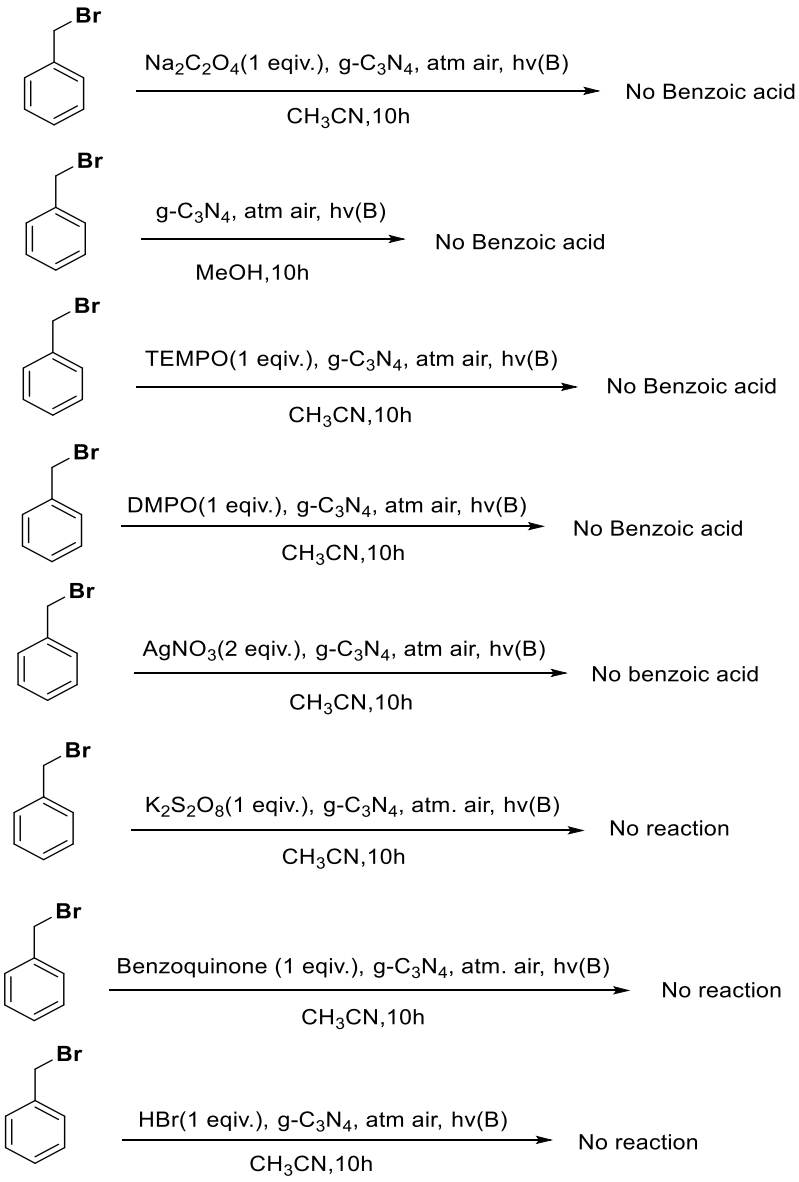

Scheme S4. Active species trapping reaction.

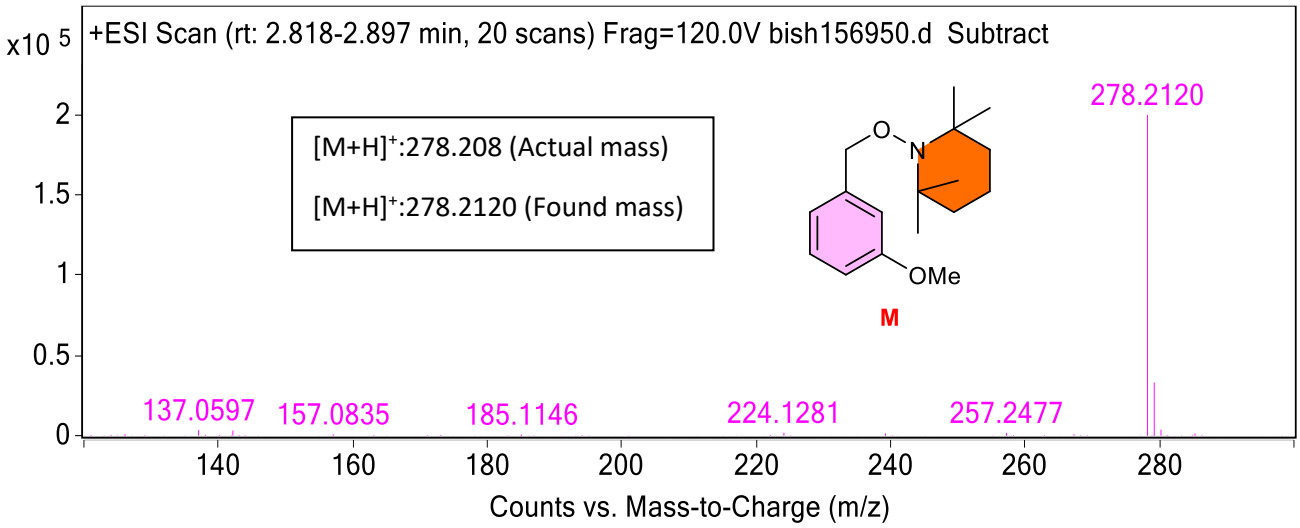

Figure S6. HRMS spectrum of intermediate M.

7. Control experiments for photooxidation of benzyl bromide

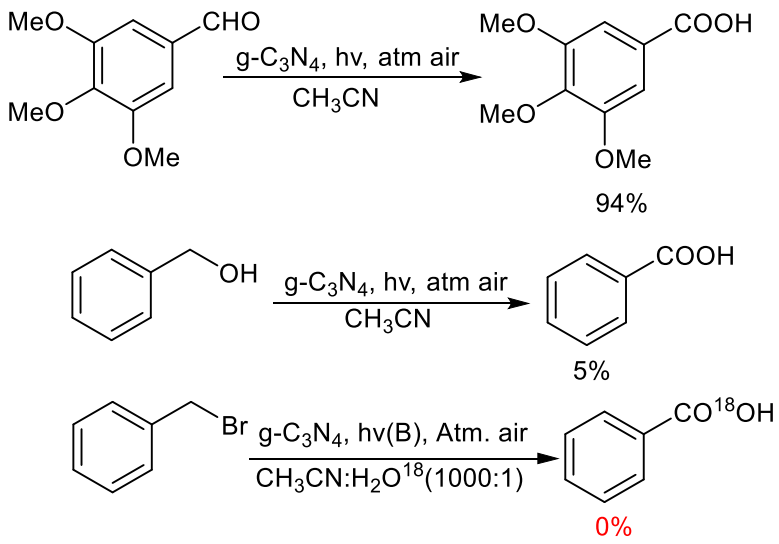

Scheme S5. Control experiments for photooxidation of benzyl bromide.

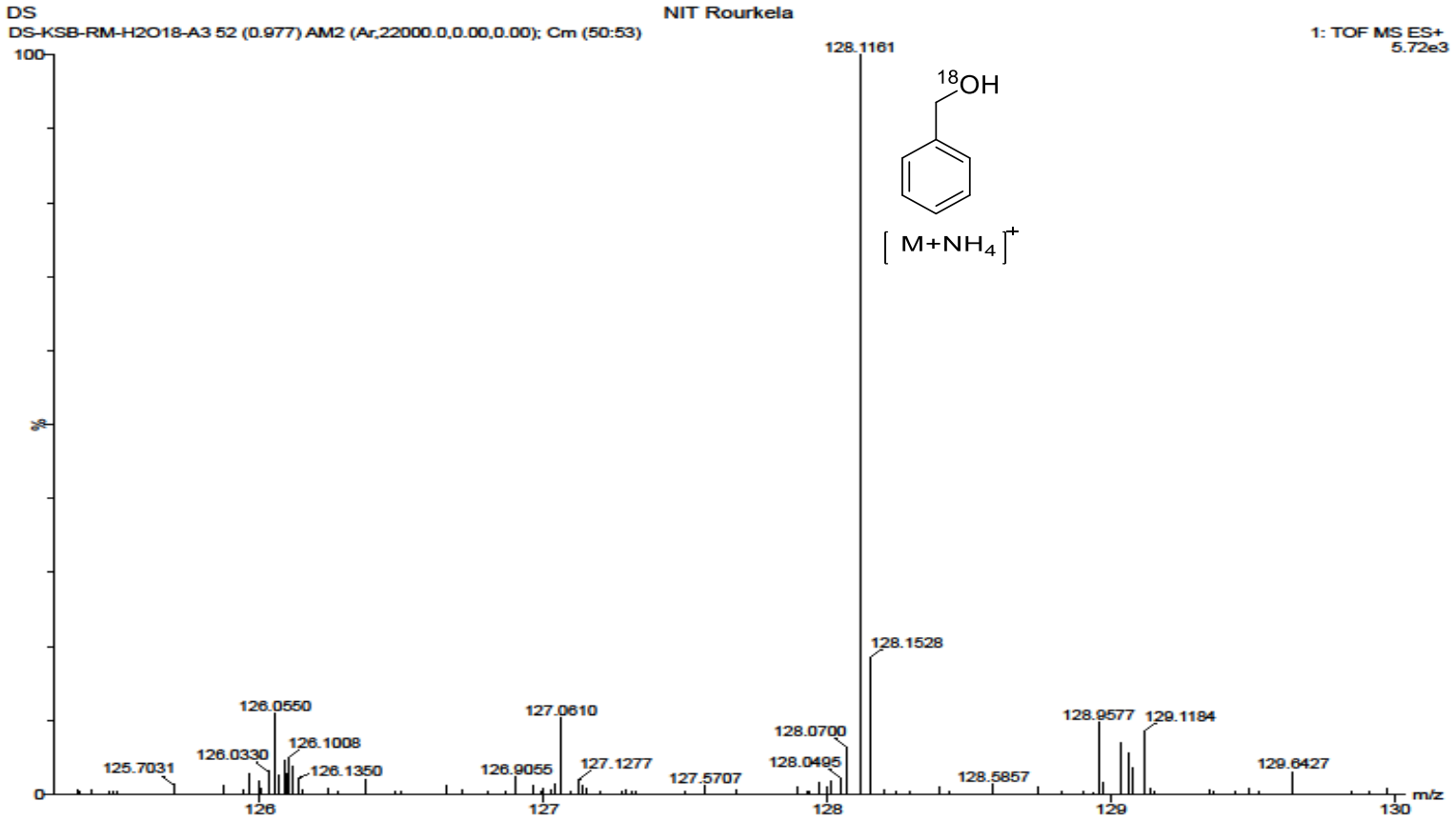

Figure S7. HRMS spectrum of reaction mixture for benzyl bromide photooxidation in $CH_3CN:H_2O^{18}$(1000:1) after 1 h of LED irradiation.

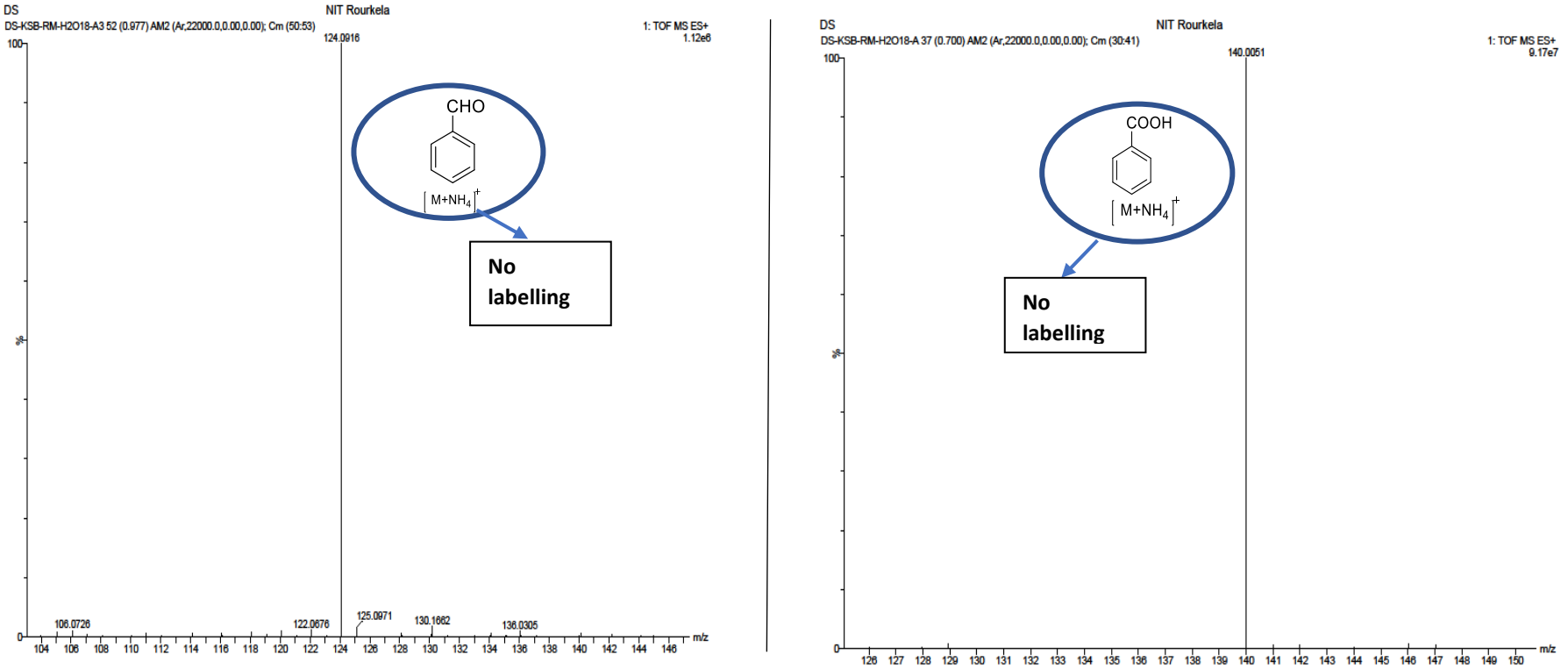

Figure S8. HRMS spectrum of the reaction mixture for benzyl bromide photooxidation in CH_3CN: H_2O^{18} (1000:1) after 1 h of LED irradiation.

8. General information for electron spin resonance spectroscopy study of O_2 radical with DMPO

Continuous-wave (CW) electron paramagnetic resonance (EPR) experiment was carried out in acetonitrile solutions on a Bruker EMX Spectrometer (X-Band, 9-10 GHz) equipped with an ER 083 (200/60) power source electromagnet (0-6000 G). For the measurements, an ER 4104OR/9009 resonant cavity with a resonance frequency of 9.66 GHz was used. To take ESR study 0.025 mmol of benzyl bromide, 1 eq. of DMPO, and 5 mg of g-C_3N_4 catalyst were charged into the 5 ml reaction vial. After 30 min of reaction, 0.3 ml reaction mixture was filled in glass pipettes for measurement, and the EPR spectrum was obtained as a first-order derivative plot.

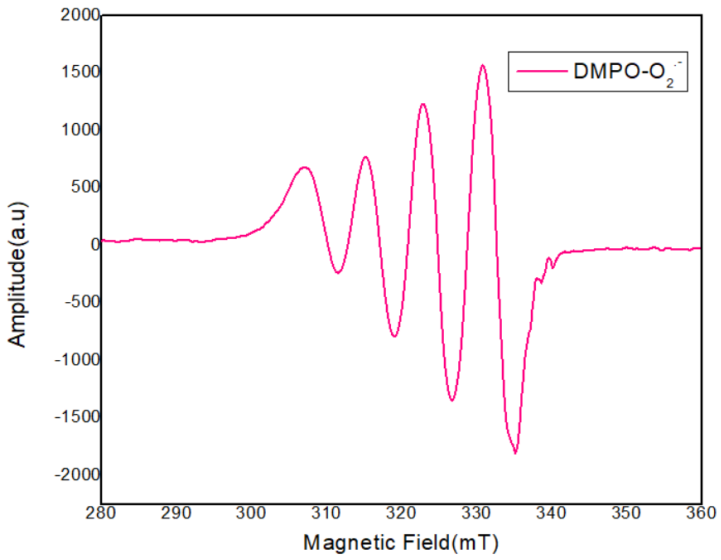

Figure S9. The EPR signals of the DMPO-O_2 $^{\bullet-}$ adduct in acetonitrile in the presence of g-C_3N_4.

9. Control experiments for optimization of photooxidation of styrene

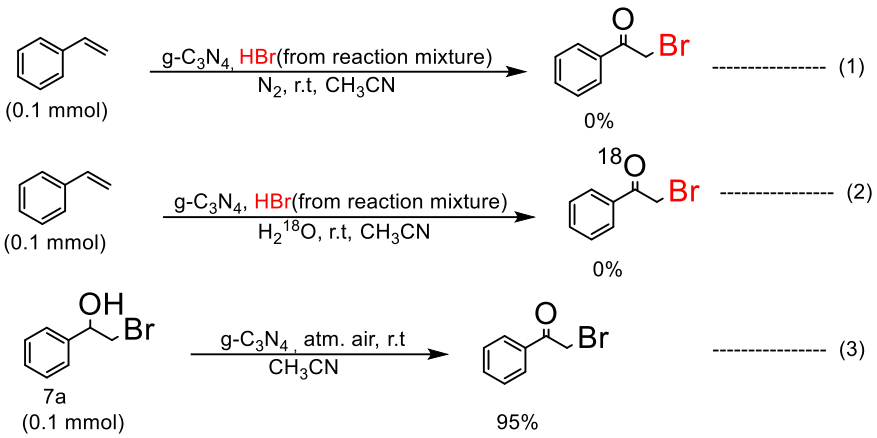

Scheme S6. Control experiments for optimization of photooxidation of styrene.

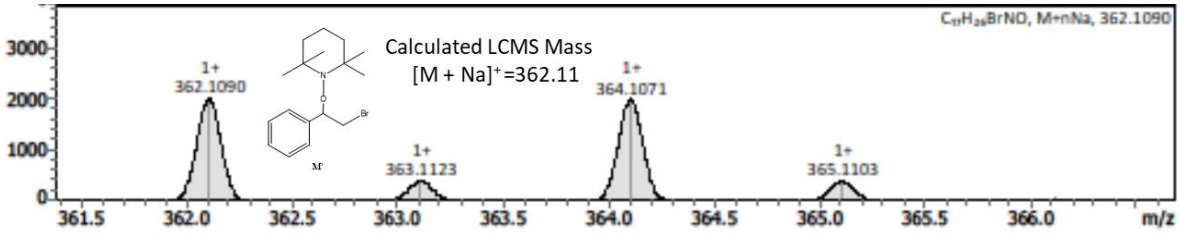

Figure S10. LCMS spectrum of intermediate M'.

10. Recycling of photocatalyst

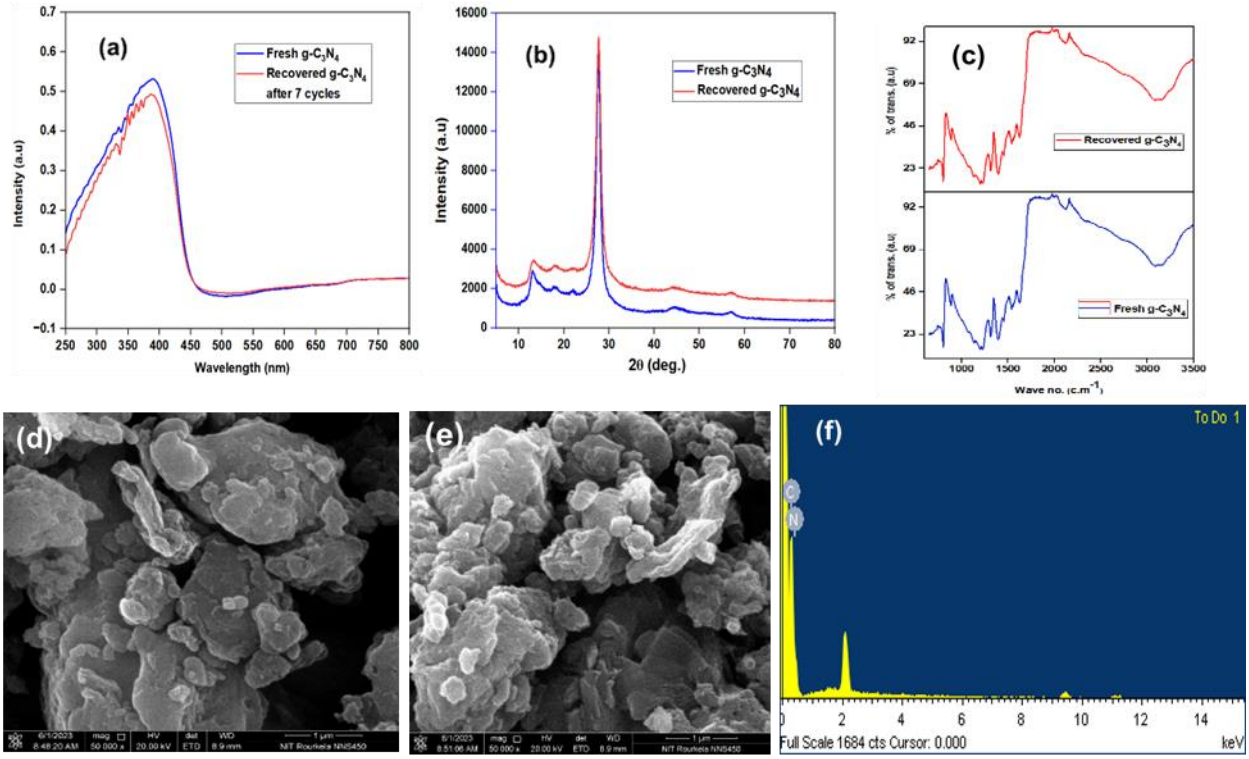

(g)

Entry	Elements	Weight (%)	Atomic (%)
1	C K	42.91	46.71
2	N K	57.09	53.29
Totals		100.00	100.00

Figure S11. (a) UV-vis diffuse reflectance spectra (UV-vis DRS), (b) IR spectra, (c) XRD pattern of fresh g-C_3N_4 and recovered g-C_3N_4 after 7 cycles (d) and (e) SEM images of fresh g-C_3N_4 and recovered g-C_3N_4 after 7 cycles, (f) EDS image and (g) Surface atomic ratios of all elements measured by EDS of fresh g-C_3N_4.

11. Identification of aryl carboxylic acid

Compound 1

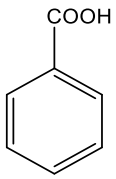

White solid.

^{1}H NMR (400 MHz, Chloroform-*d*) δ 8.15 (dd, *J* = 8.2, 1.2 Hz, 2H), 7.67 – 7.61 (m, 1H), 7.51 (t, *J* = 7.7 Hz, 2H).

^{13}C NMR (101 MHz, Chloroform-*d*) δ 133.77, 130.22, 129.26, 128.50.

Compound 2

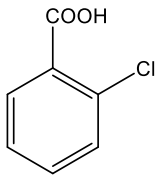

White Solid.
^{1}H NMR (400 MHz, Chloroform-*d*) δ 9.56 (s, 1H), 8.06 (d, *J* = 7.8 Hz, 1H), 7.55 – 7.47 (m, 2H), 7.39 (ddd, *J* = 8.2, 6.3, 2.3 Hz, 1H).
^{13}C NMR (101 MHz, Chloroform-*d*) δ 170.88, 134.80, 133.61, 132.51, 131.53, 128.44, 126.72.

Compound 3

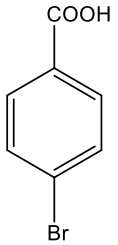

White Solid.
^{1}H NMR (400 MHz, DMSO-d_6) δ 7.87 (d, *J* = 8.5 Hz, 2H), 7.72 (d, *J* = 8.5 Hz, 2H).
^{13}C NMR (101 MHz, DMSO-d_6) δ 171.83, 136.93, 136.51, 135.21, 132.11.

Compound 4

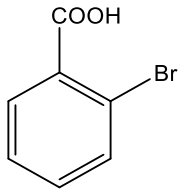

White solid.

^{1}H NMR (300 MHz, Chloroform-*d*) δ 8.05 – 7.97 (m, 1H), 7.76 – 7.68 (m, 1H), 7.46 – 7.35 (m, 2H).
^{13}C NMR (75 MHz, Chloroform-*d*) δ 266.34, 168.25, 134.91, 133.59, 132.48, 127.33.

Compound 5

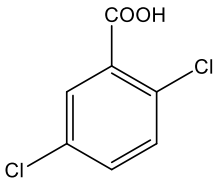

White Solid.
^{1}H NMR (400 MHz, Chloroform-*d*) δ 8.87 – 8.12 (m, 1H), 8.02 (dd, *J* = 2.2, 0.7 Hz, 1H), 7.49 – 7.43 (m, 2H).

^{13}C NMR (101 MHz, Chloroform-*d*) δ 169.39, 133.50, 133.10, 132.79, 132.66, 132.24, 129.73.

Compound 6

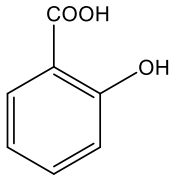

White Solid.
^{1}H NMR (300 MHz, Chloroform-*d*) δ 10.36 (s, 1H), 7.94 (dd, *J* = 8.0, 1.7 Hz, 1H), 7.54 (ddd, *J* = 8.8, 7.2, 1.8 Hz, 1H), 7.02 (dd, *J* = 8.4, 1.1 Hz, 1H), 6.95 (ddd, *J* = 8.2, 7.2, 1.1 Hz, 1H).
^{13}C NMR (75 MHz, Chloroform-*d*) δ 175.01, 162.23, 137.08, 131.00, 119.66, 117.89, 111.29.

Compound 7

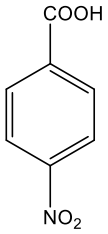

Light Yellow Solid.
^{1}H NMR (400 MHz, DMSO-*d*$_6$) δ 8.35 – 8.29 (m, 2H), 8.21 – 8.15 (m, 2H).
^{13}C NMR (101 MHz, DMSO-*d*$_6$) δ 166.25, 150.57, 131.16, 124.17.

Compound 8

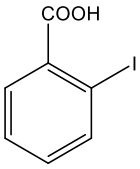

White Solid.
^{1}H NMR (400 MHz, Chloroform-*d*) δ 8.08 (dd, *J* = 7.9, 0.9 Hz, 1H), 8.03 (dd, *J* = 7.8, 1.7 Hz, 1H), 7.47 (td, *J* = 7.7, 1.1 Hz, 1H), 7.23 (td, *J* = 7.8, 1.7 Hz, 1H).
^{13}C NMR (101 MHz, Chloroform-*d*) δ 170.61, 141.97, 133.53, 133.20, 132.05, 128.05, 94.72.

Compound 9

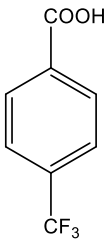

White Solid.

^{1}H NMR (400 MHz, Chloroform-*d*) δ 8.25 (d, *J* = 8.2 Hz, 2H), 7.78 (d, *J* = 8.2 Hz, 2H).
^{13}C NMR (101 MHz, Chloroform-*d*) δ 169.14, 130.60, 125.57, 29.71.

Compound 12

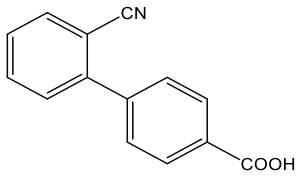

White solid.
^{1}H NMR (400 MHz, DMSO-*d*$_6$) δ 13.17 (s, 1H), 8.12 – 8.06 (m, 2H), 8.03 – 7.98 (m, 1H), 7.84 (td, *J* = 7.7, 1.2 Hz, 1H), 7.72 (d, *J* = 8.3 Hz, 2H), 7.70 – 7.65 (m, 1H), 7.65 – 7.62 (m, 1H).
^{13}C NMR (101 MHz, DMSO-*d*$_6$) δ 167.38, 143.99, 142.45, 134.41, 134.14, 131.37, 130.62, 130.09, 129.54, 129.31, 118.77, 110.68.

Compound 14

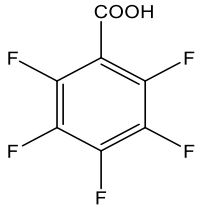

White solid.
^{1}H NMR (400 MHz, Chloroform-*d*) δ 8.83 (s, 1H).
^{13}C NMR (101 MHz, Chloroform-*d*) δ 167.78, 130.89, 129.50, 128.81, 114.07.

Compound 22

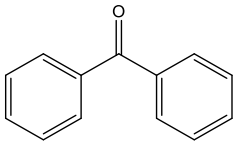

White solid.

^{1}H NMR (400 MHz, Chloroform-*d*) δ 7.83 (d, *J* = 7.5 Hz, 4H), 7.61 (t, *J* = 7.5 Hz, 2H), 7.51 (t, *J* = 7.6 Hz, 4H).
^{13}C NMR (101 MHz, Chloroform-*d*) δ 196.78, 137.62, 132.44, 130.08, 128.30.

Compound 23

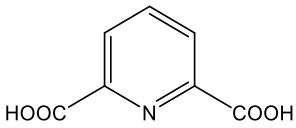

White solid.

^{1}H NMR (400 MHz, DMSO-*d*$_6$) δ 13.41 (s, 2H), 8.25 (d, *J* = 7.3 Hz, 3H), 8.19 (d, *J* = 7.9 Hz, 1H).
^{13}C NMR (101 MHz, DMSO-*d*$_6$) δ 165.96, 148.58, 139.72, 128.01.

Compound 25

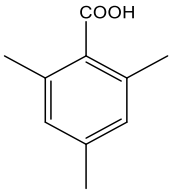

White solid.

^{1}H NMR (300 MHz, Chloroform-*d*) δ 6.90 (s, 2H), 2.43 (s, 6H), 2.31 (s, 3H).
^{13}C NMR (75 MHz, Chloroform-*d*) δ 175.61, 140.13, 136.21, 129.27, 128.83, 21.18, 20.38.

Compound 26

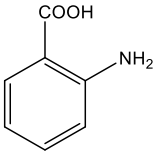

Light yellow solid.
^{1}H NMR (300 MHz, Chloroform-*d*) δ 7.94 (dd, *J* = 8.3, 1.7 Hz, 1H), 7.32 (ddd, *J* = 8.6, 7.1, 1.6 Hz, 2H), 6.74 – 6.62 (m, 2H).
^{13}C NMR (75 MHz, Chloroform-*d*) δ 266.50, 266.35, 173.35, 151.15, 135.15, 132.16, 116.81, 116.49, 109.51.

Compound 27

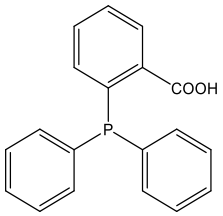

White solid.
^{1}H NMR (400 MHz, DMSO-d_6) δ 12.75 (s, 1H), 8.00 (ddt, *J* = 7.6, 5.6, 4.0 Hz, 1H), 7.49 – 7.40 (m, 2H), 7.34 (qt, *J* = 3.7, 2.1 Hz, 6H), 7.20 – 7.11 (m, 4H), 6.80 (ddd, *J* = 7.3, 3.8, 2.1 Hz, 1H).
^{13}C NMR (101 MHz, DMSO-d_6) δ 168.12, 139.95, 138.74, 138.61, 134.03, 133.97, 133.77, 132.36, 130.92, 130.90, 129.09, 129.06, 129.03, 128.99.
^{31}P NMR (162 MHz, DMSO-d_6) δ -4.48.

Compound 28

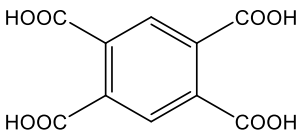

White solid.
^{1}H NMR (400 MHz, DMSO-d_6) δ 7.93 (s, 2H).
^{13}C NMR (101 MHz, DMSO-d_6) δ 167.77, 135.08, 128.94.

Compound 29

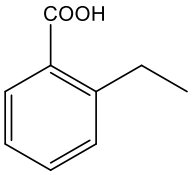

White solid.
^{1}H NMR (300 MHz, Chloroform-*d*) δ 8.05 (dd, *J* = 7.7, 1.5 Hz, 1H), 7.50 (td, *J* = 7.4, 1.5 Hz, 1H), 7.34 – 7.28 (m, 2H), 3.08 (q, *J* = 7.5 Hz, 2H), 1.28 (t, *J* = 7.5 Hz, 3H).
^{13}C NMR (75 MHz, Chloroform-*d*) δ 173.50, 147.30, 133.07, 131.65, 130.50, 128.03, 125.85, 27.77, 15.94.

Compound 30

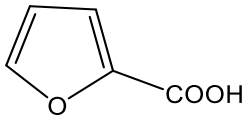

White solid.
^{1}H NMR (300 MHz, Chloroform-*d*) δ 10.02(s, 1H), 7.65 (dd, *J* = 1.7, 0.9 Hz, 1H), 7.34 (dd, *J* = 3.6, 0.9 Hz, 1H), 6.57 (dd, *J* = 3.5, 1.7 Hz, 1H).
^{13}C NMR (75 MHz, Chloroform-*d*) δ 163.58, 147.47, 143.83, 120.20, 112.31.

Compound 31

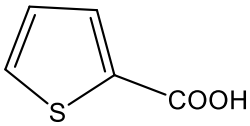

White solid.
^{1}H NMR (300 MHz, Chloroform-*d*) δ 7.91 (dd, *J* = 3.8, 1.3 Hz, 1H), 7.66 (dd, *J* = 5.0, 1.3 Hz, 1H), 7.15 (dd, *J* = 5.0, 3.8 Hz, 1H).
^{13}C NMR (75 MHz, Chloroform-*d*) δ 167.56, 135.05, 134.05, 132.86, 128.10.

12. NMR Spectra of aryl carboxylic acids.

^{1}H NMR spectrum of compound 1.

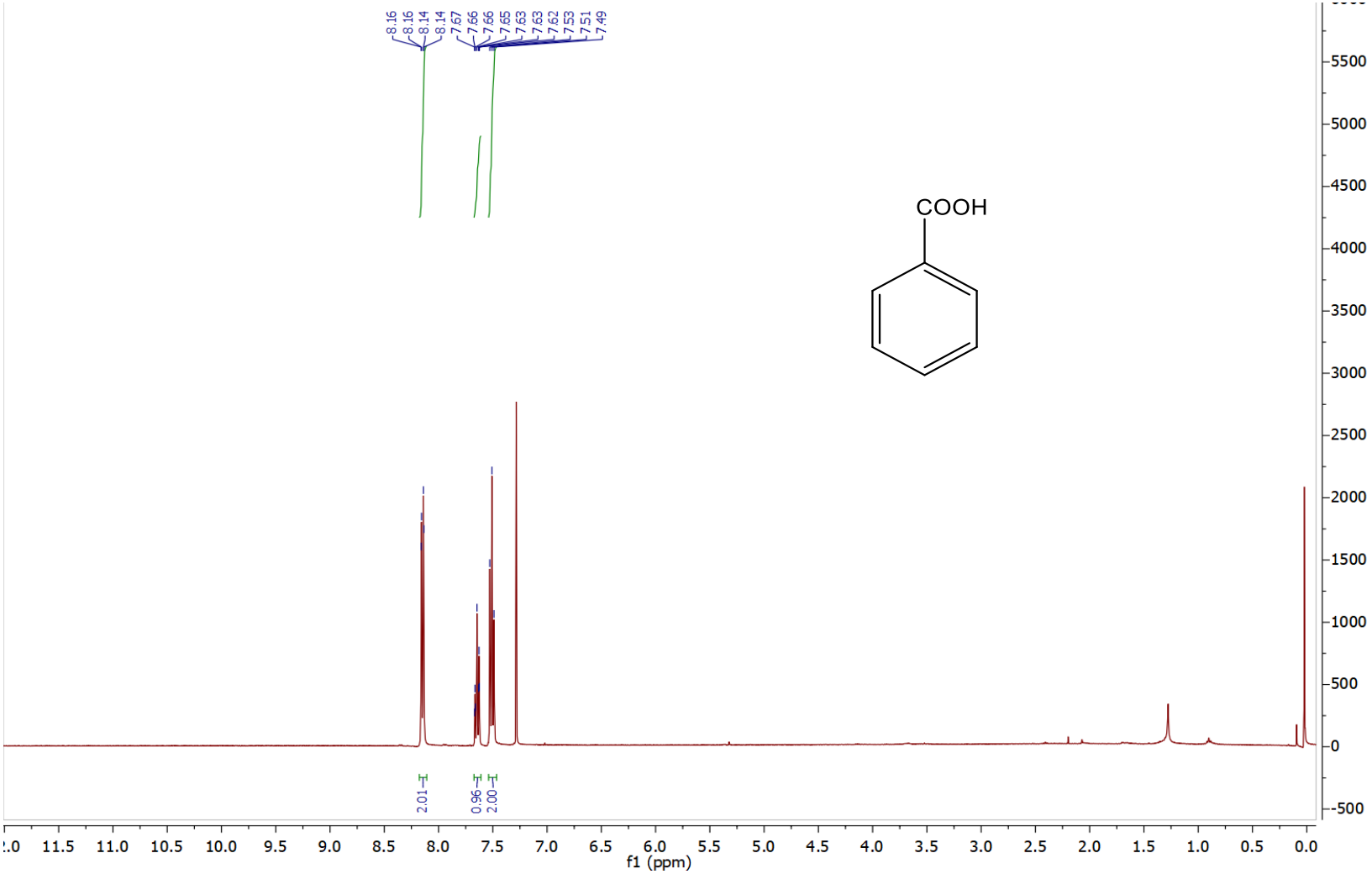

$^{13}C\{^{1}H\}$ NMR spectrum of compound 1.

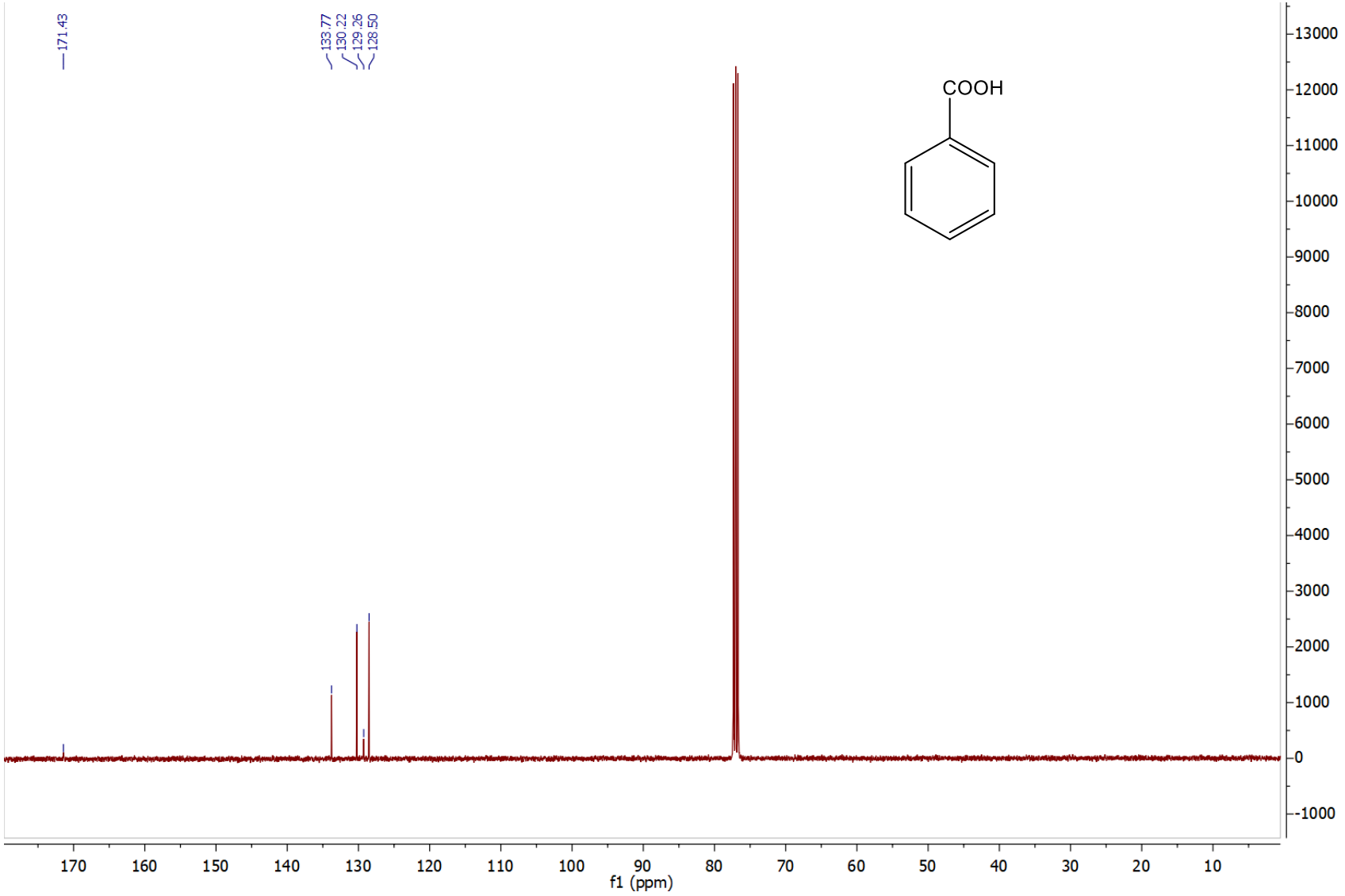

^{1}H NMR spectrum of compound 2.

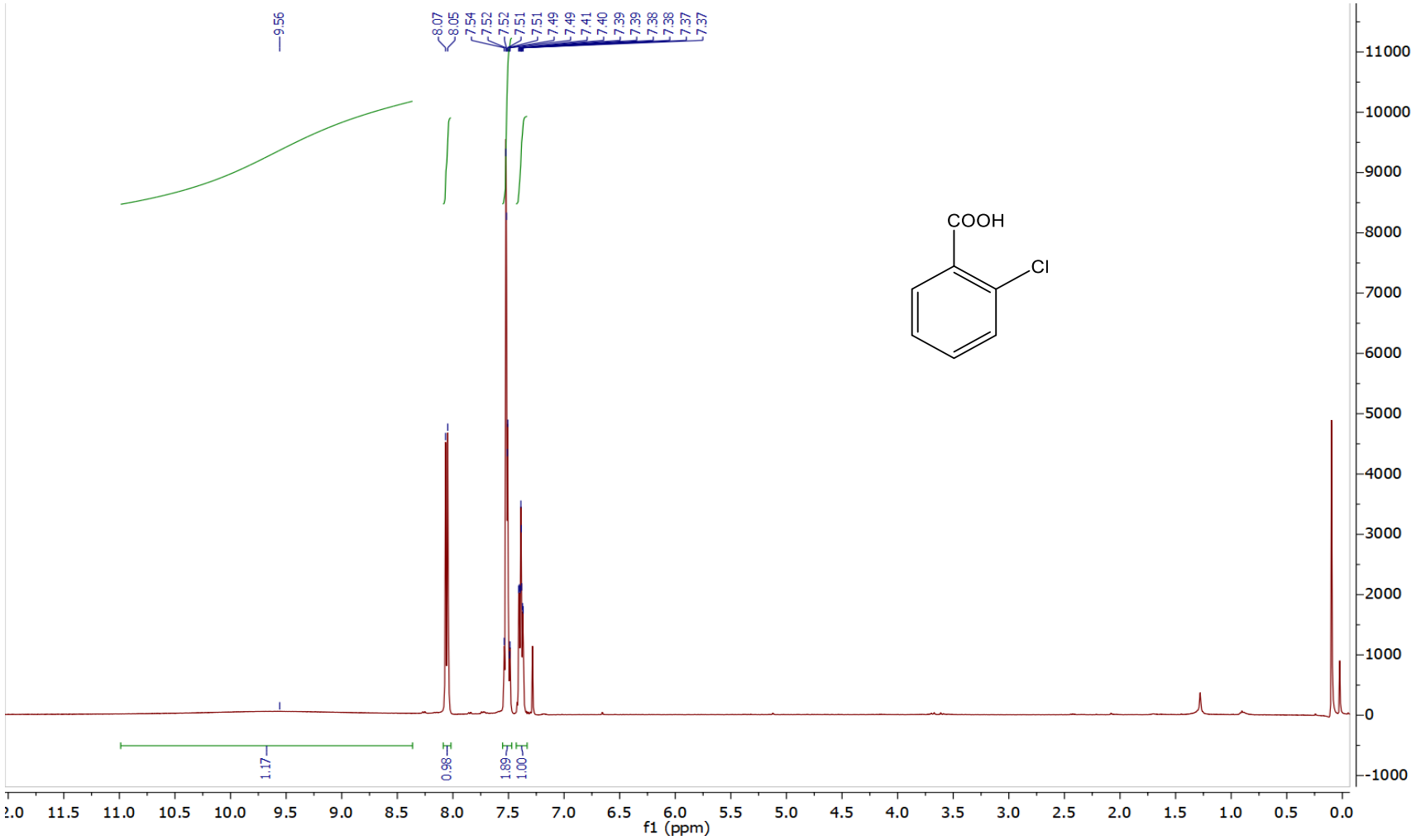

$^{13}C\{^{1}H\}$ NMR spectrum of compound 2.

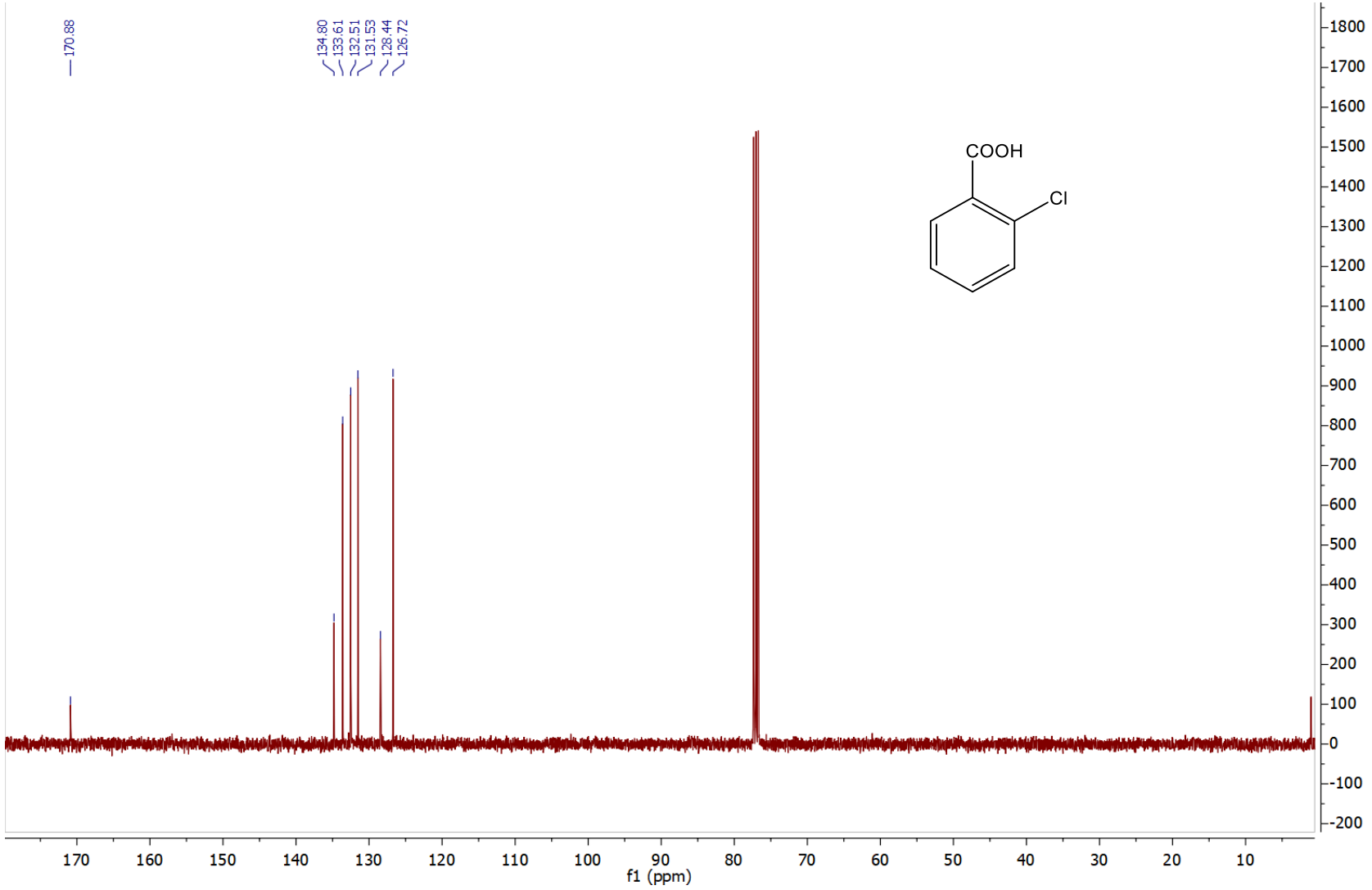

^{1}H NMR spectrum of compound 3.

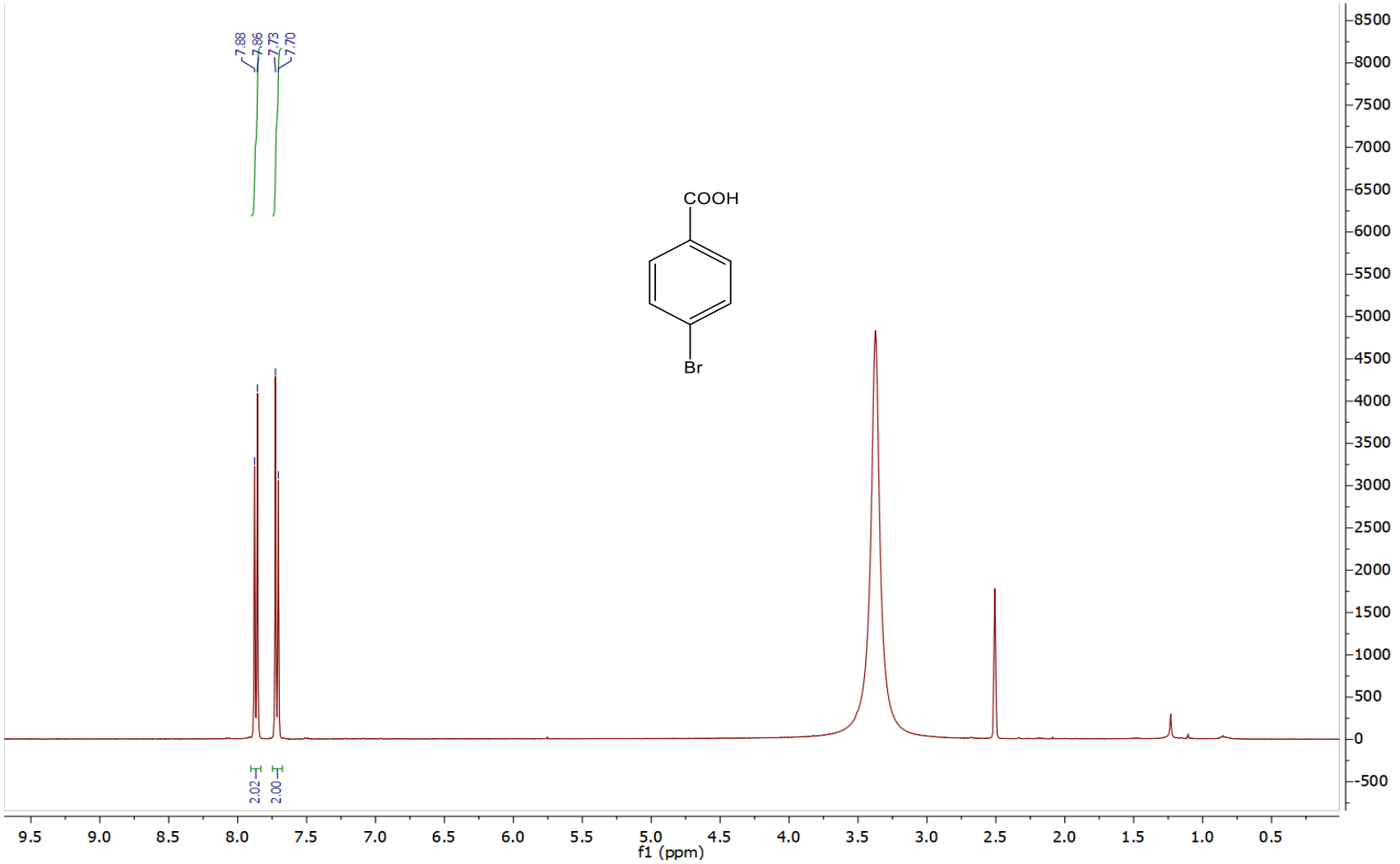

$^{13}C\{^{1}H\}$ NMR spectrum of compound 3.

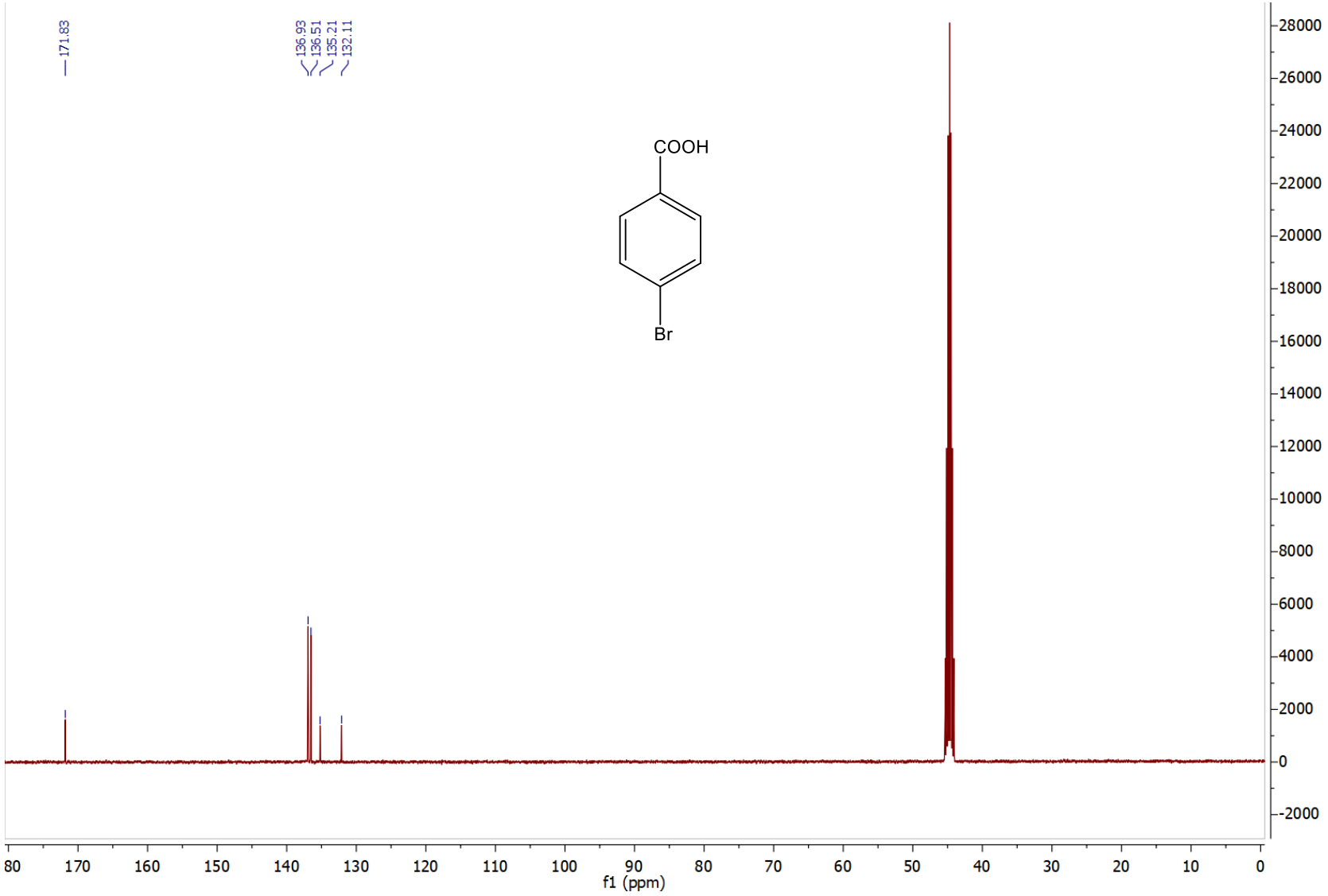

^{1}H NMR spectrum of compound 4.

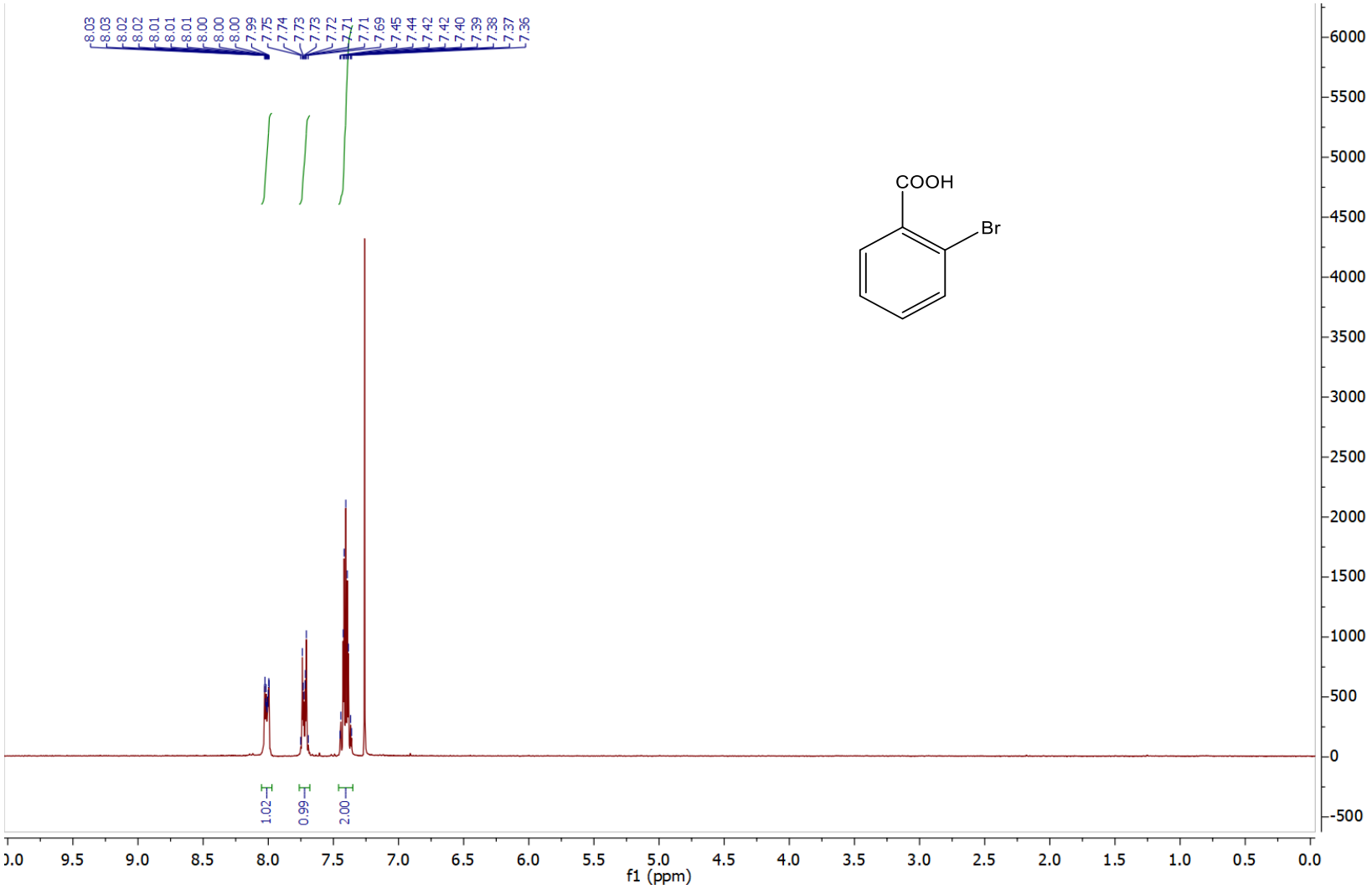

$^{13}C\{^{1}H\}$ NMR spectrum of compound 4.

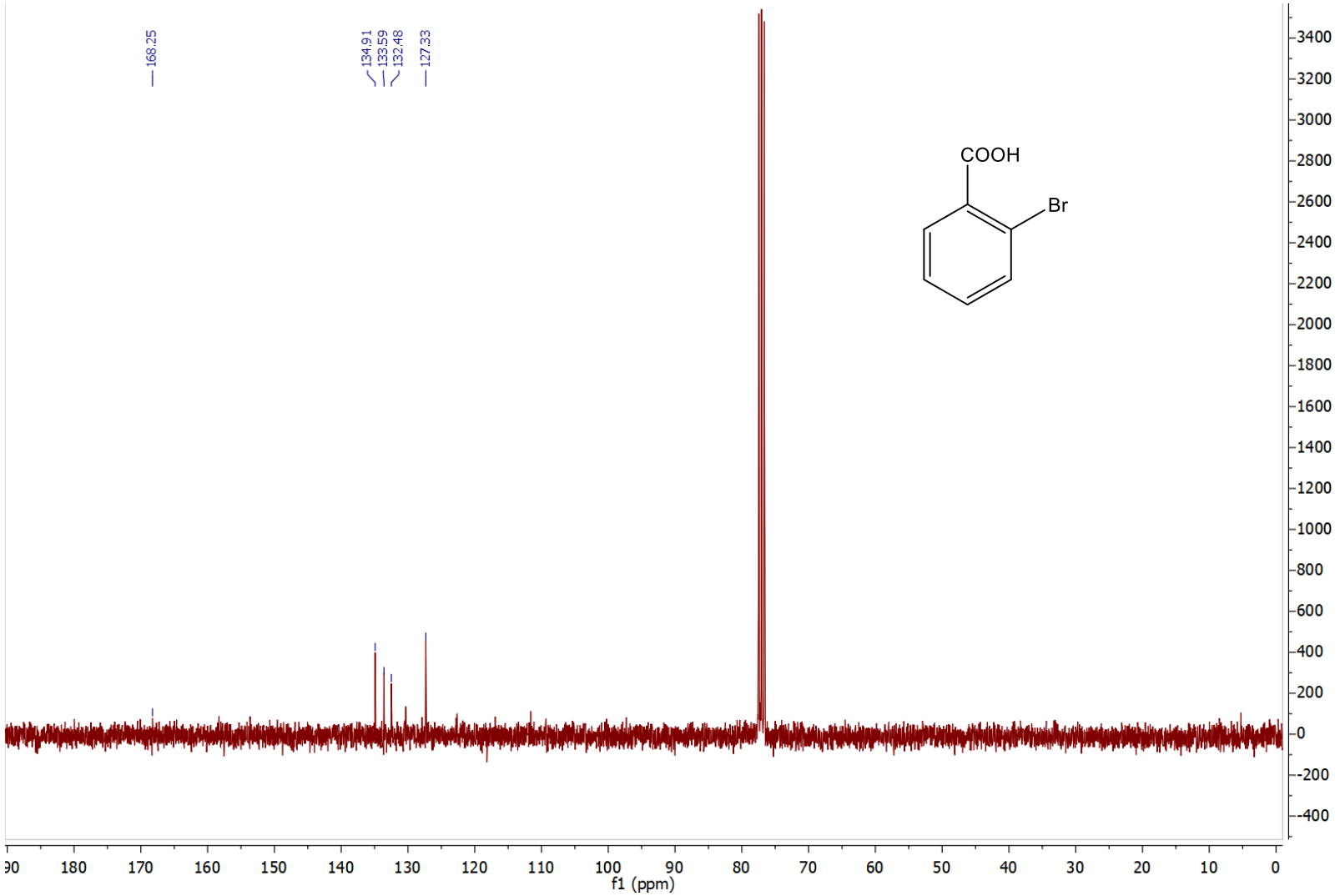

[1]H NMR spectrum of compound 5.

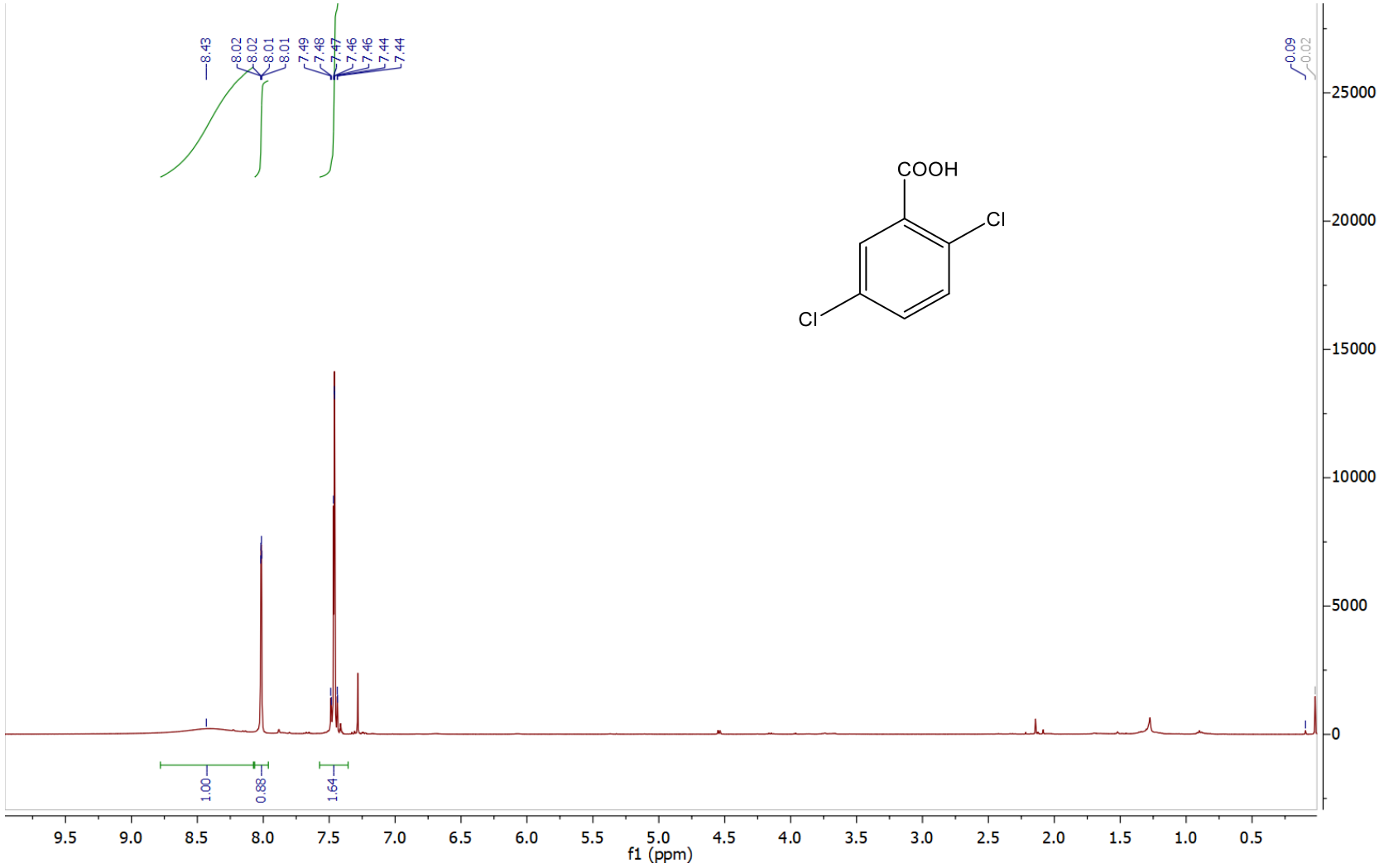

$^{13}C\{^{1}H\}$ NMR spectrum of compound 5.

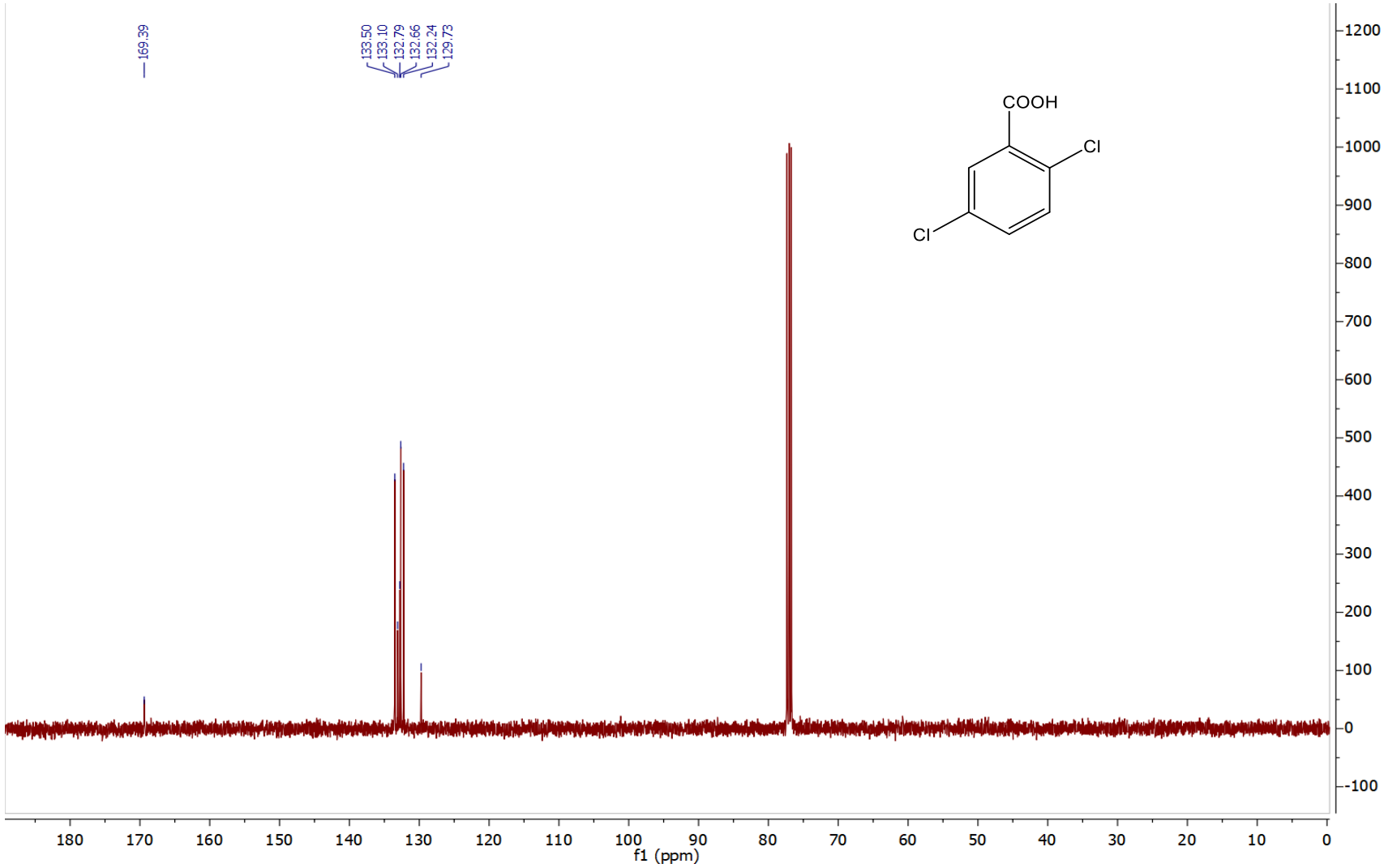

^{1}H NMR spectrum of compound 6.

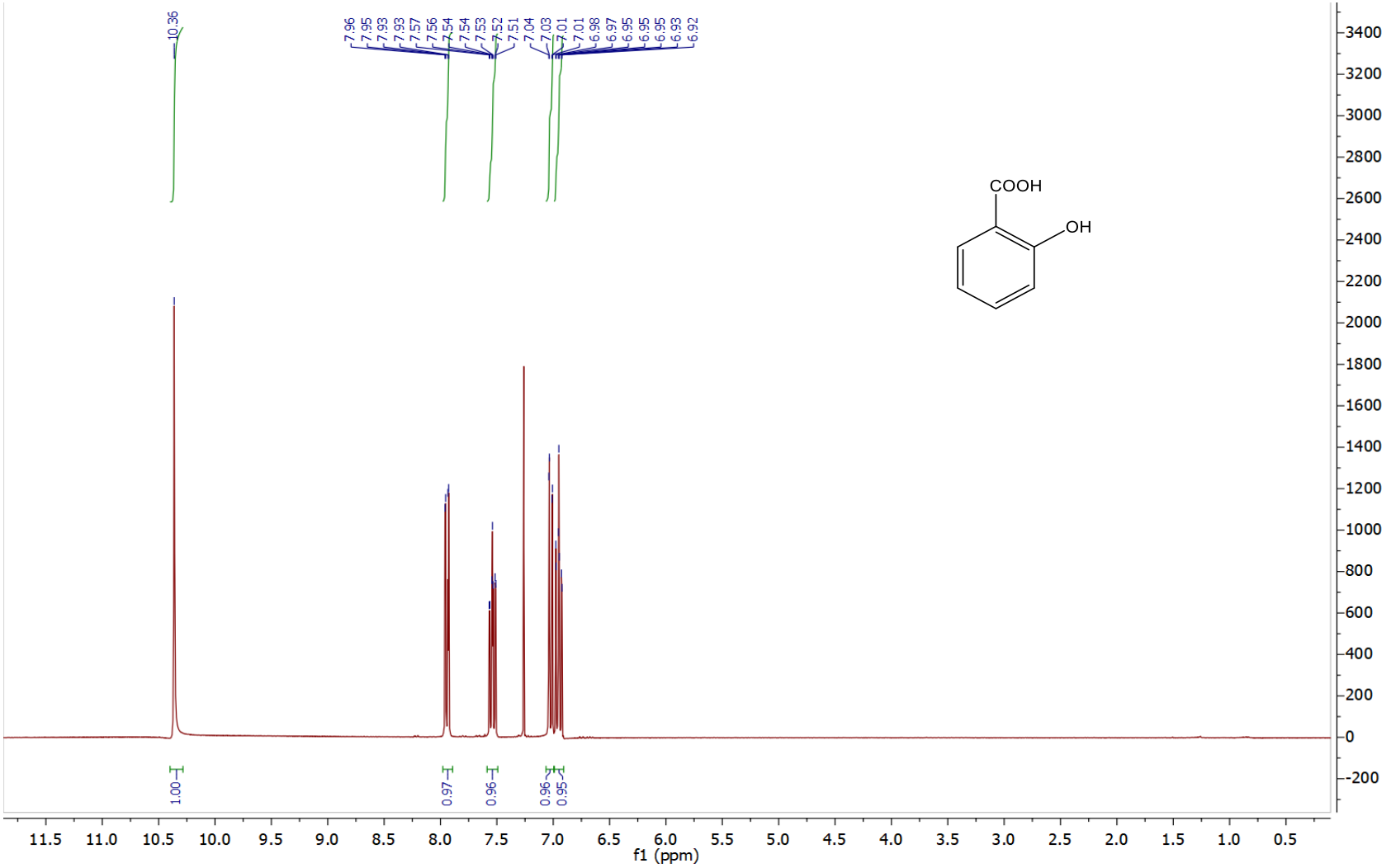

$^{13}C\{^{1}H\}$ NMR spectrum of compound 6.

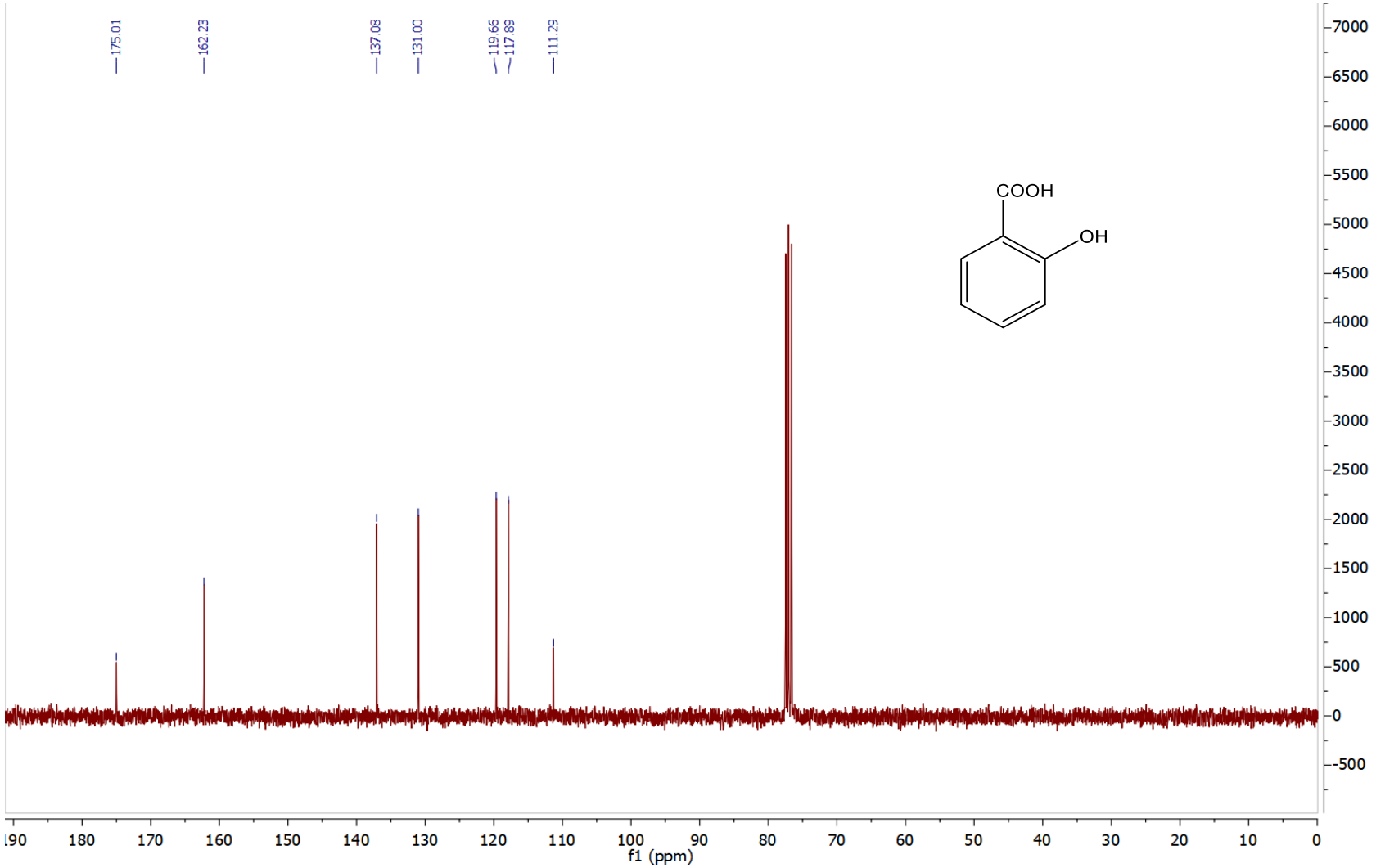

^{1}H NMR spectrum of compound 7.

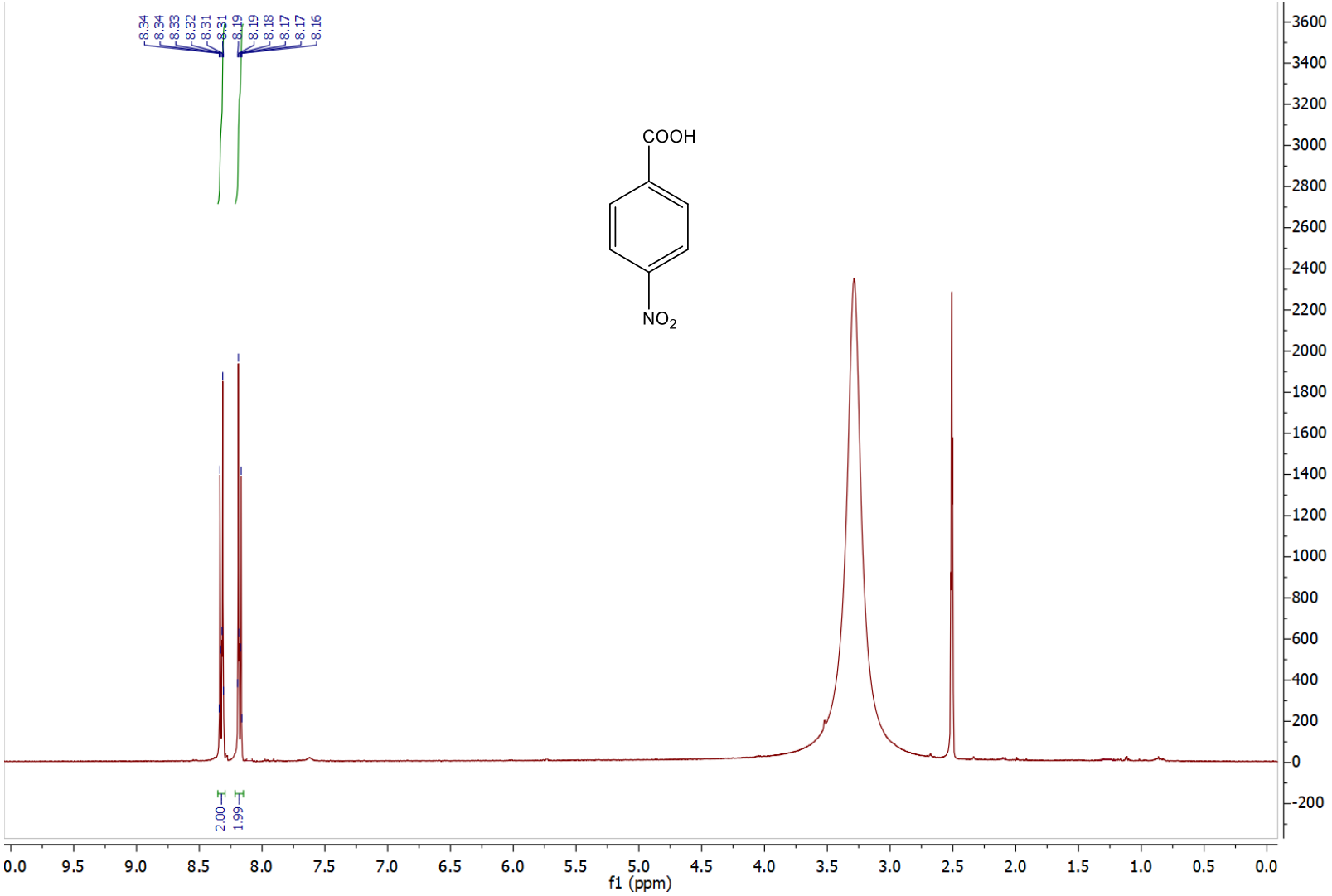

$^{13}C\{^{1}H\}$ NMR spectrum of compound 7.

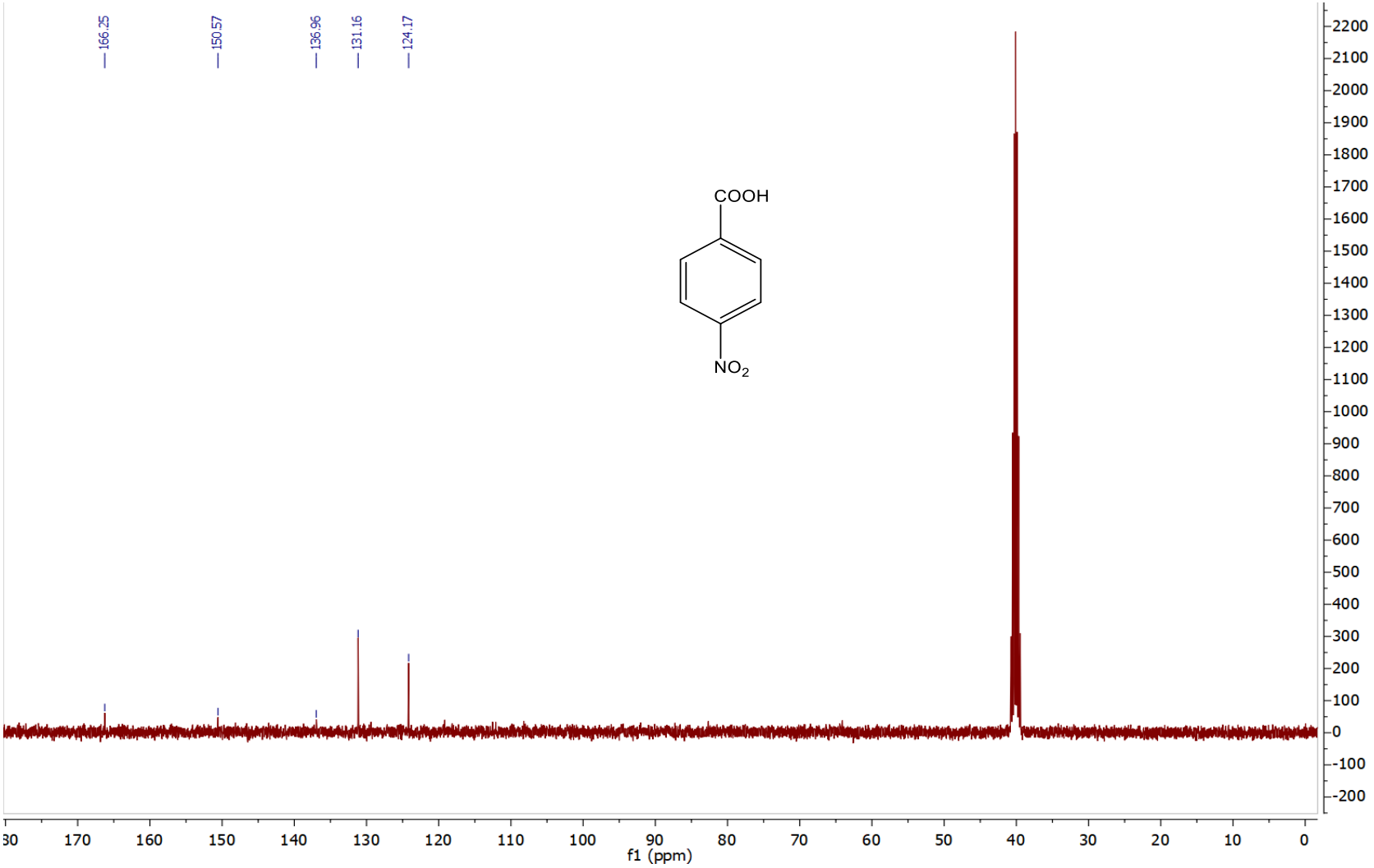

^{1}H NMR spectrum of compound 8.

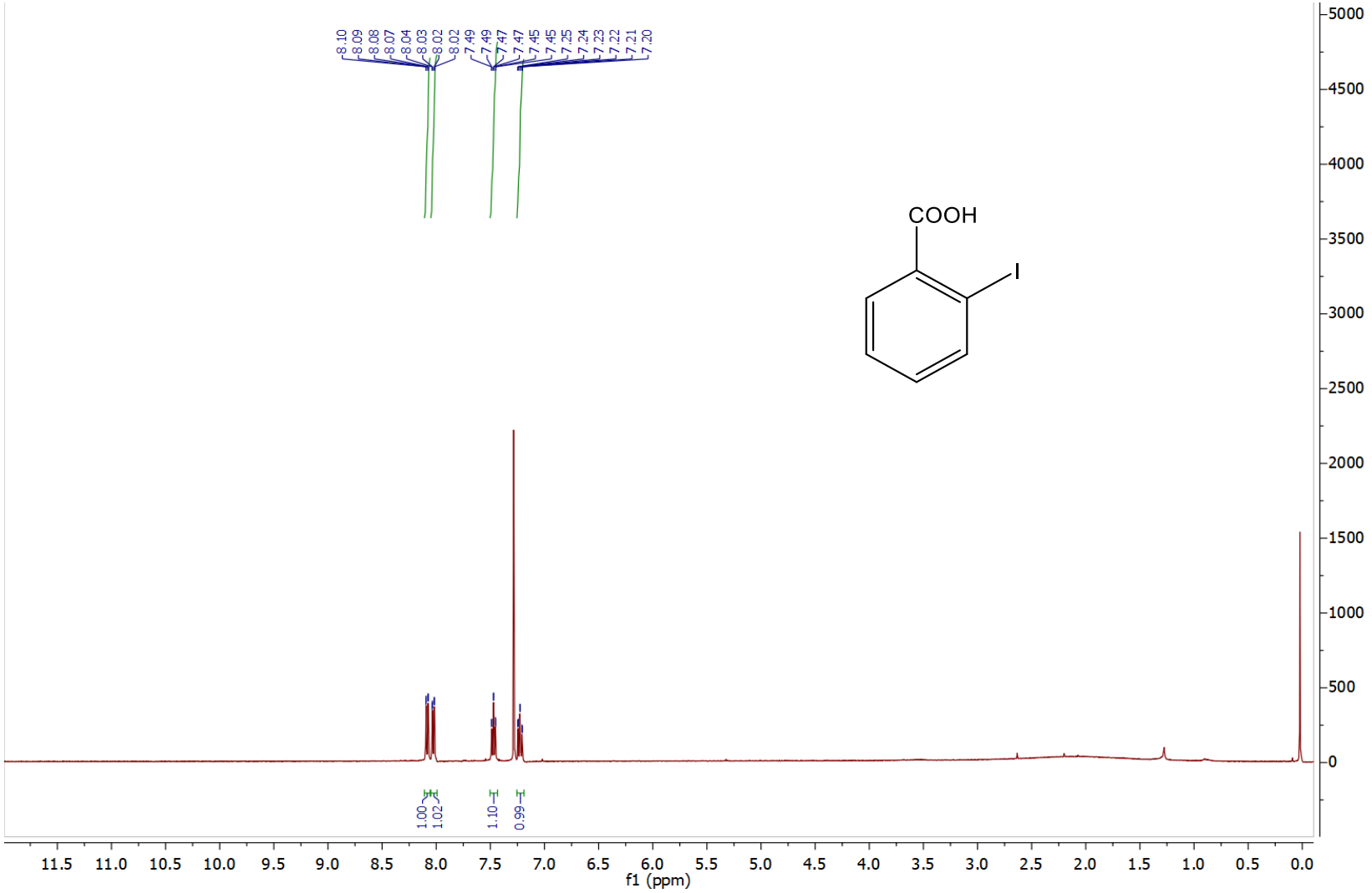

$^{13}C\{^{1}H\}$ NMR spectrum of compound 8.

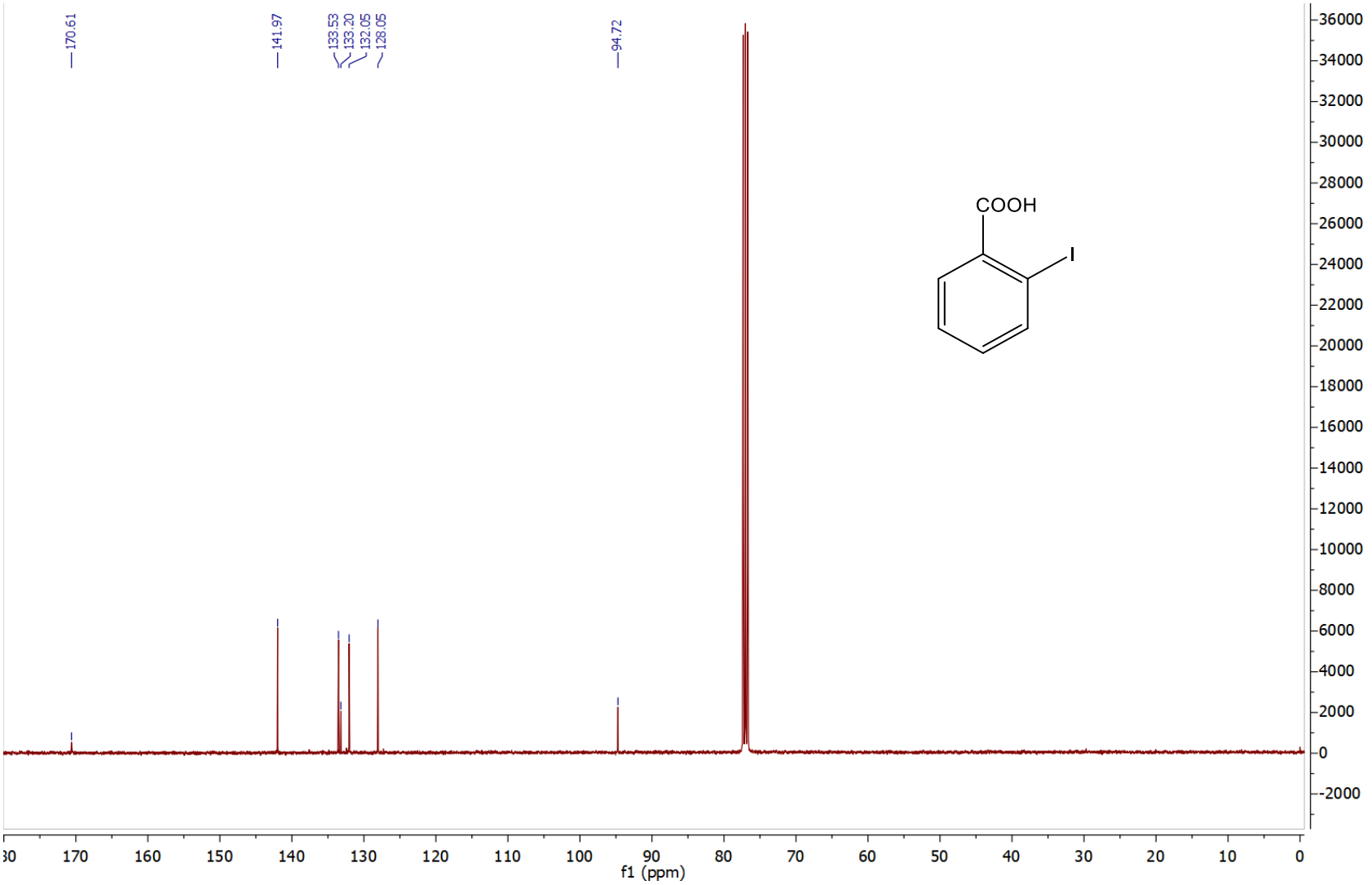

^{1}H NMR spectrum of compound 9.

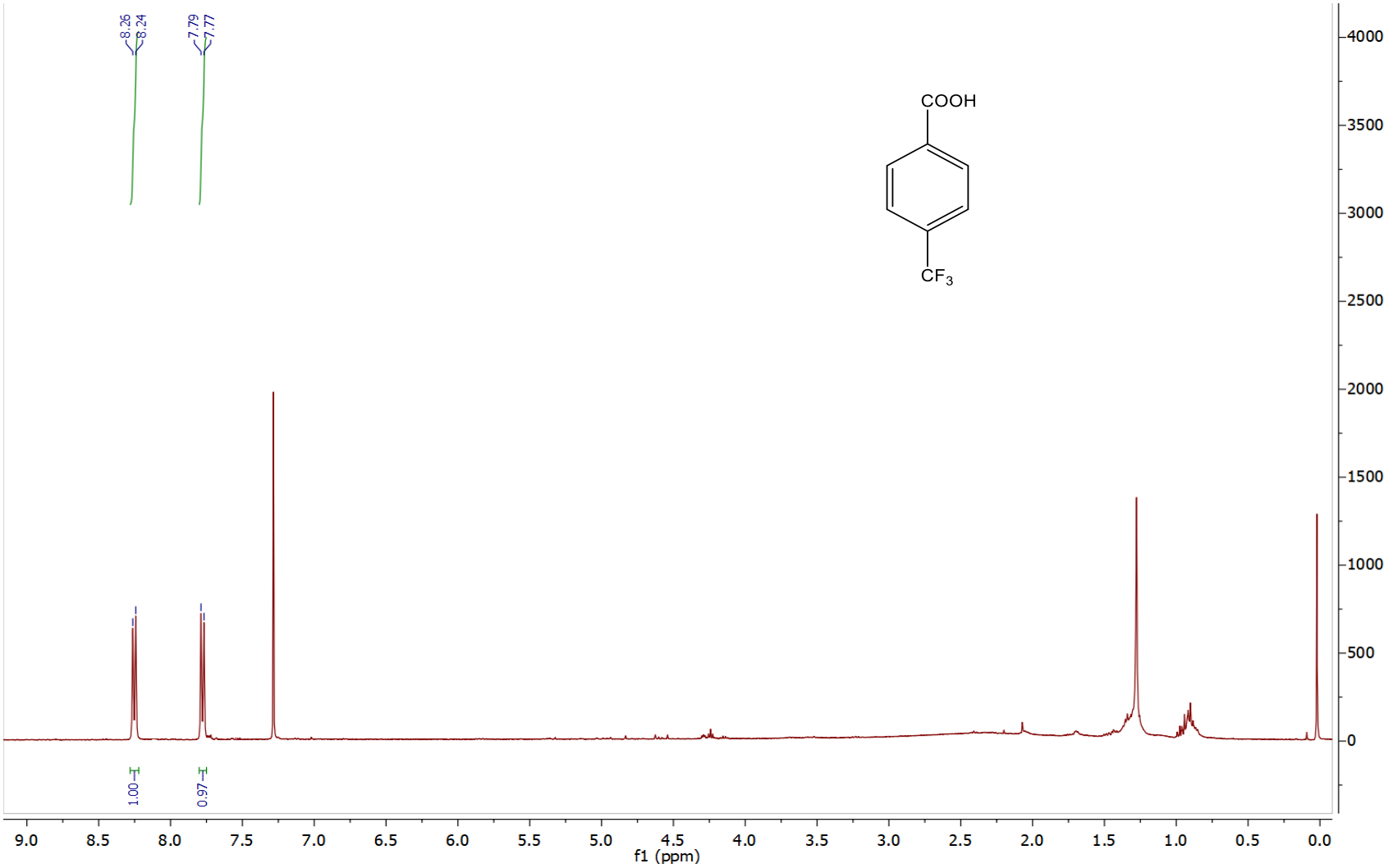

$^{13}C\{^{1}H\}$ NMR spectrum of compound 9.

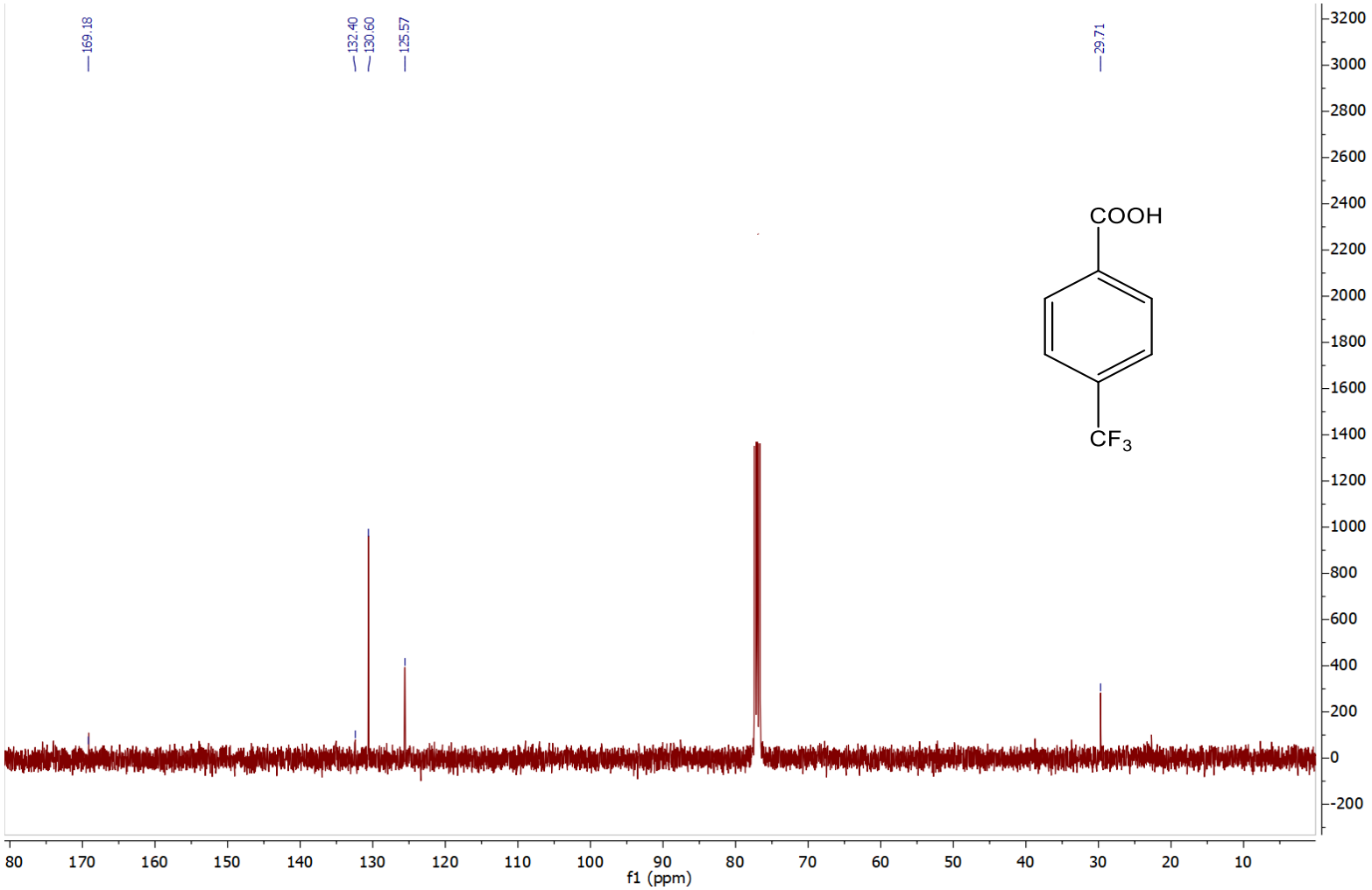

[1]H NMR spectrum of compound 12.

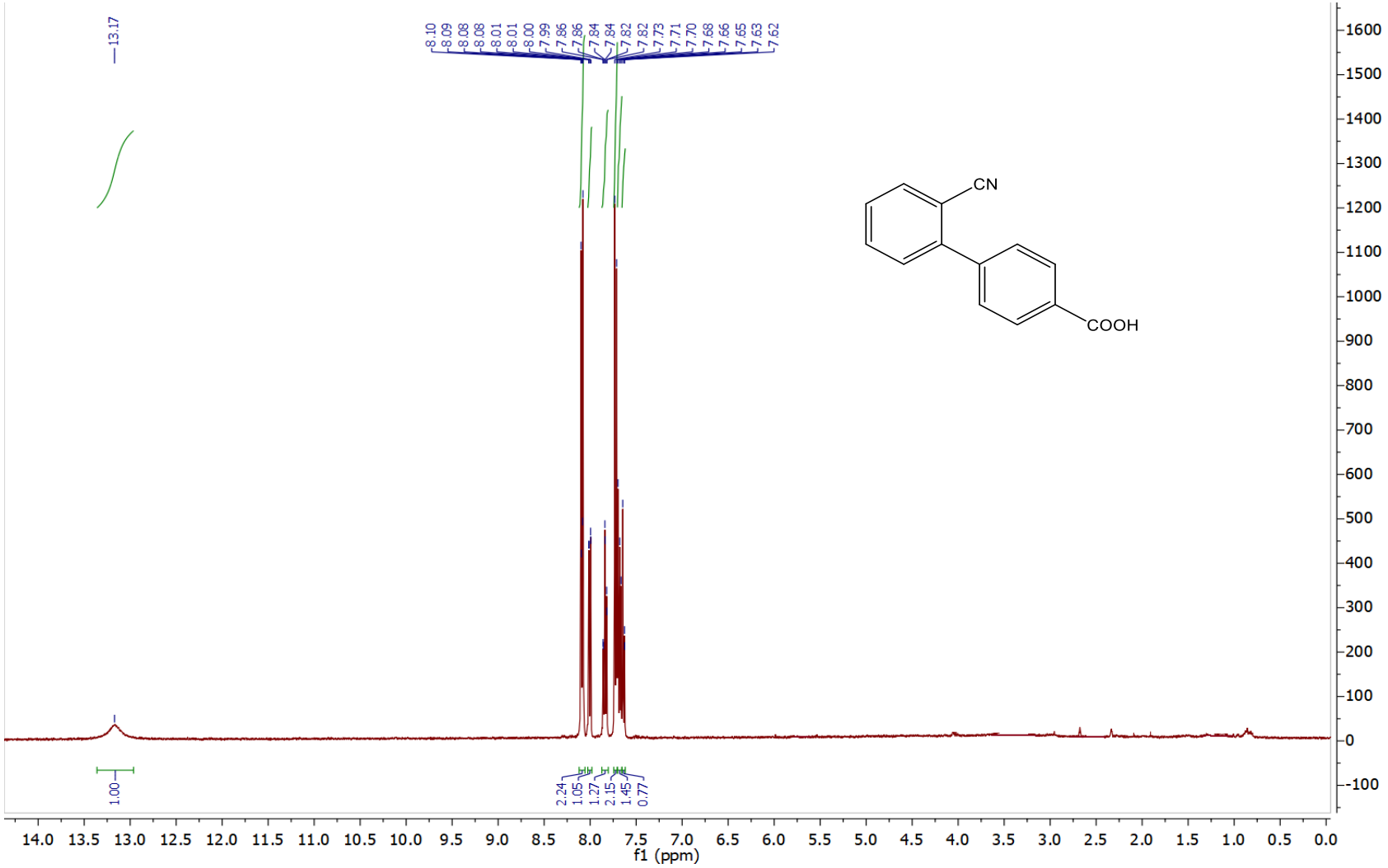

$^{13}C\{^{1}H\}$ NMR spectrum of compound 12.

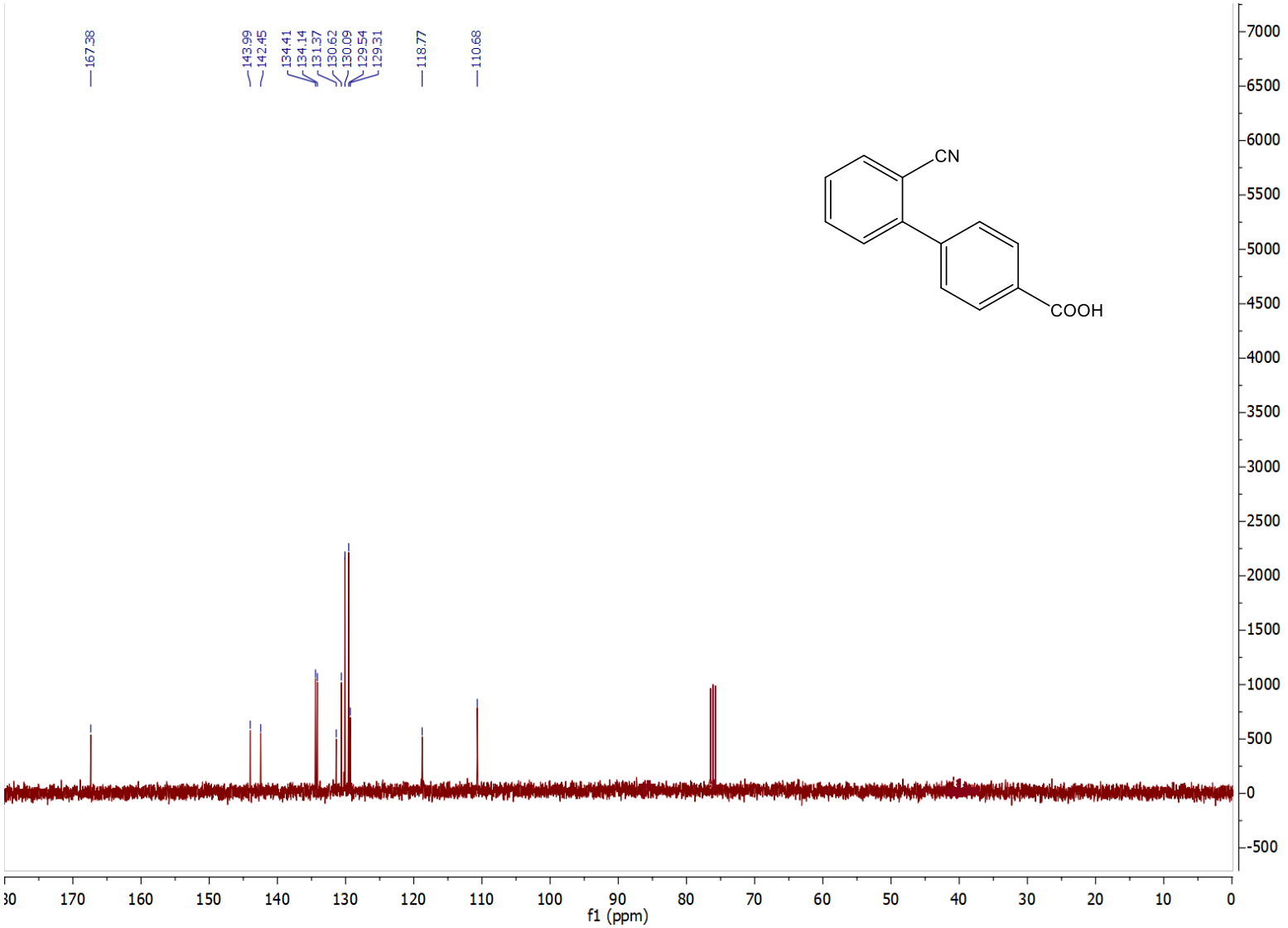

^{1}H NMR spectrum of compound 14.

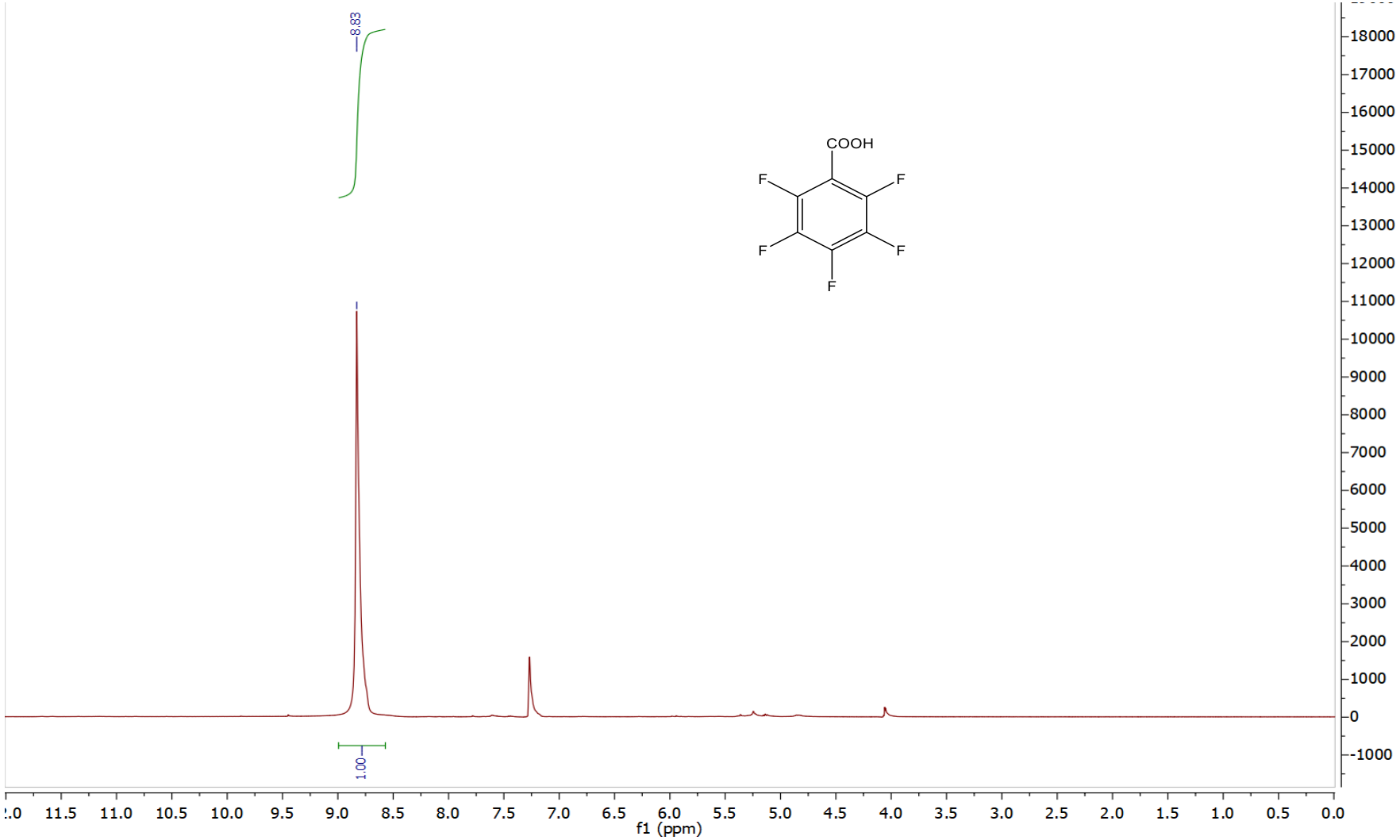

$^{13}C\{^{1}H\}$ NMR spectrum of compound 14.

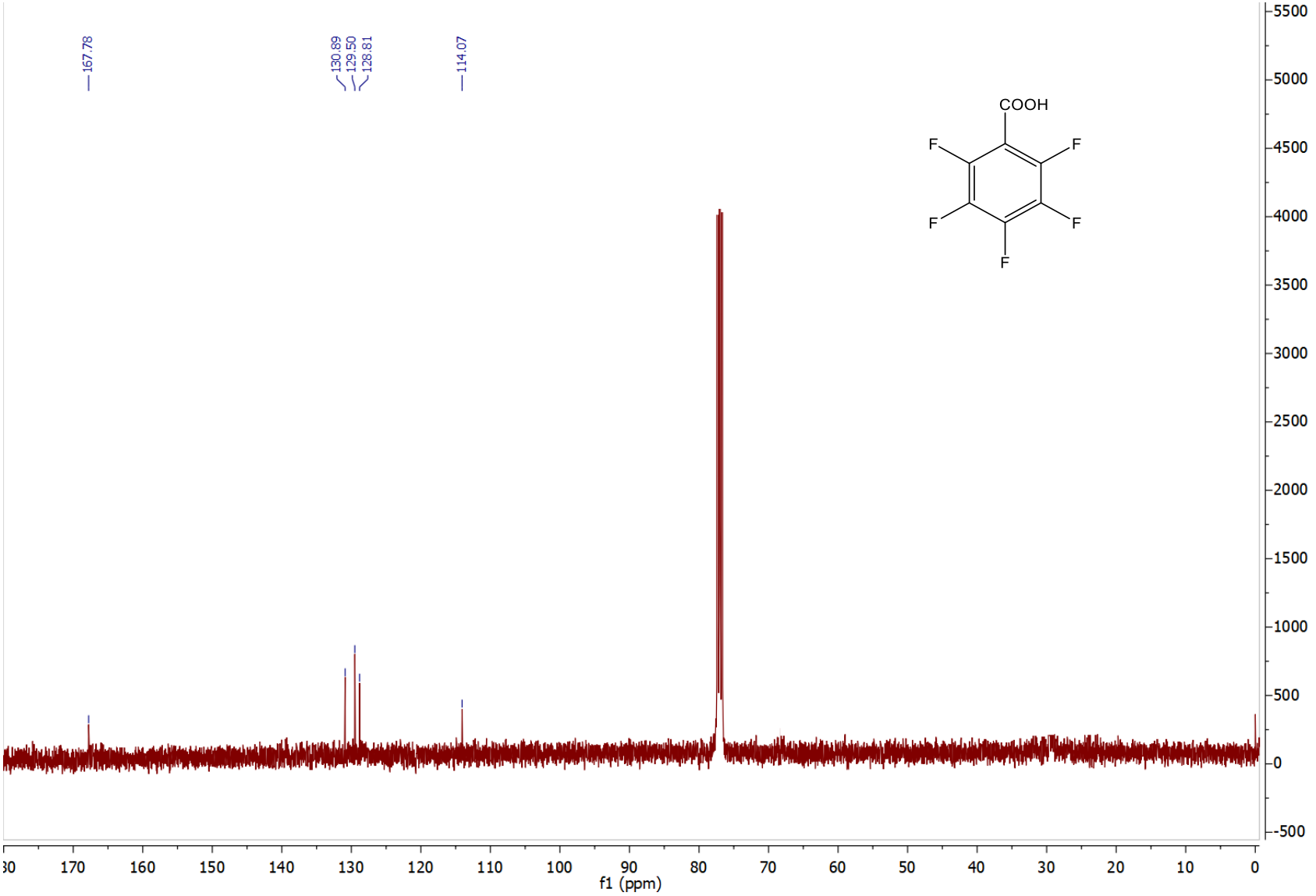

^{1}H NMR spectrum of compound 22.

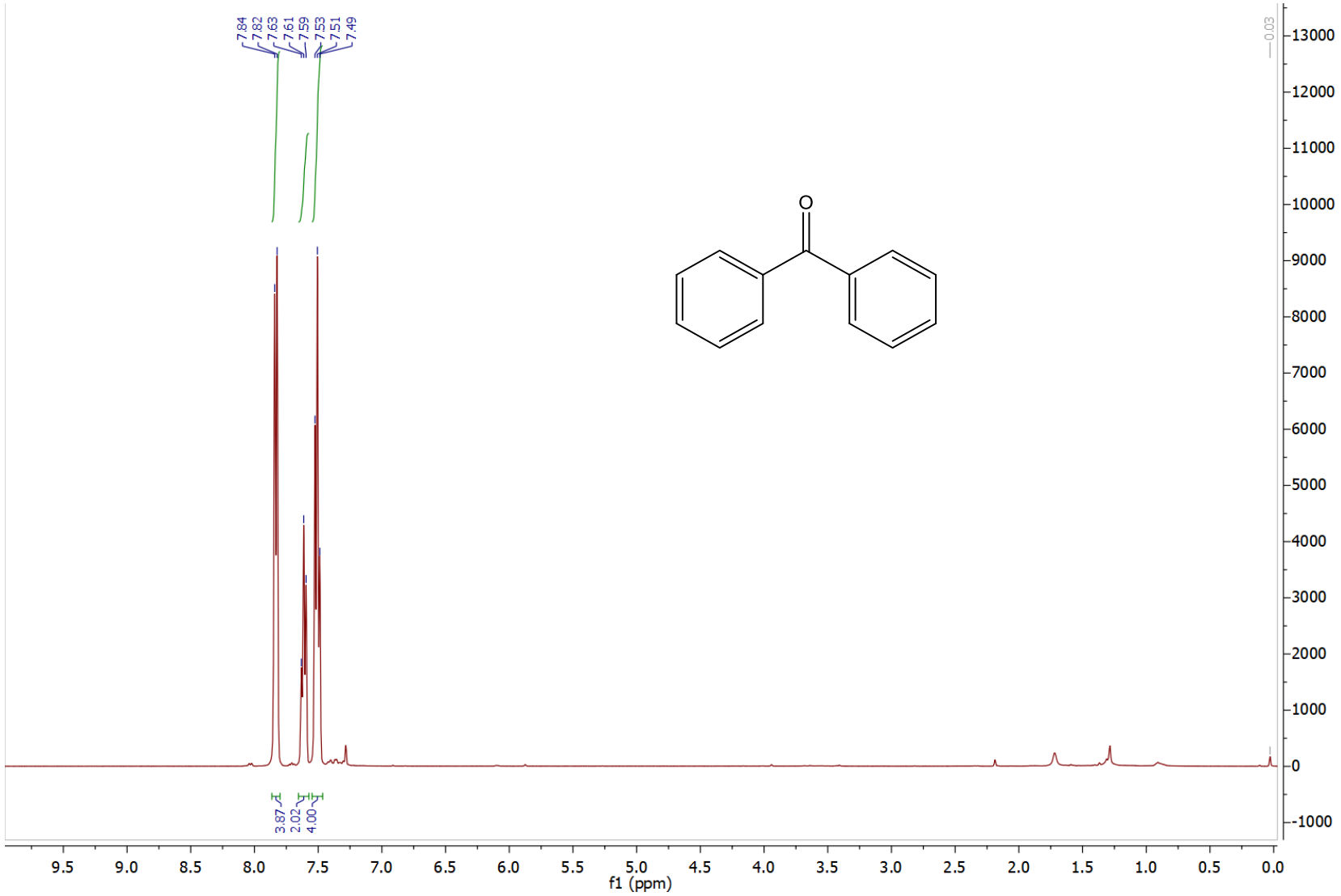

$^{13}C\{^{1}H\}$ NMR spectrum of compound 22.

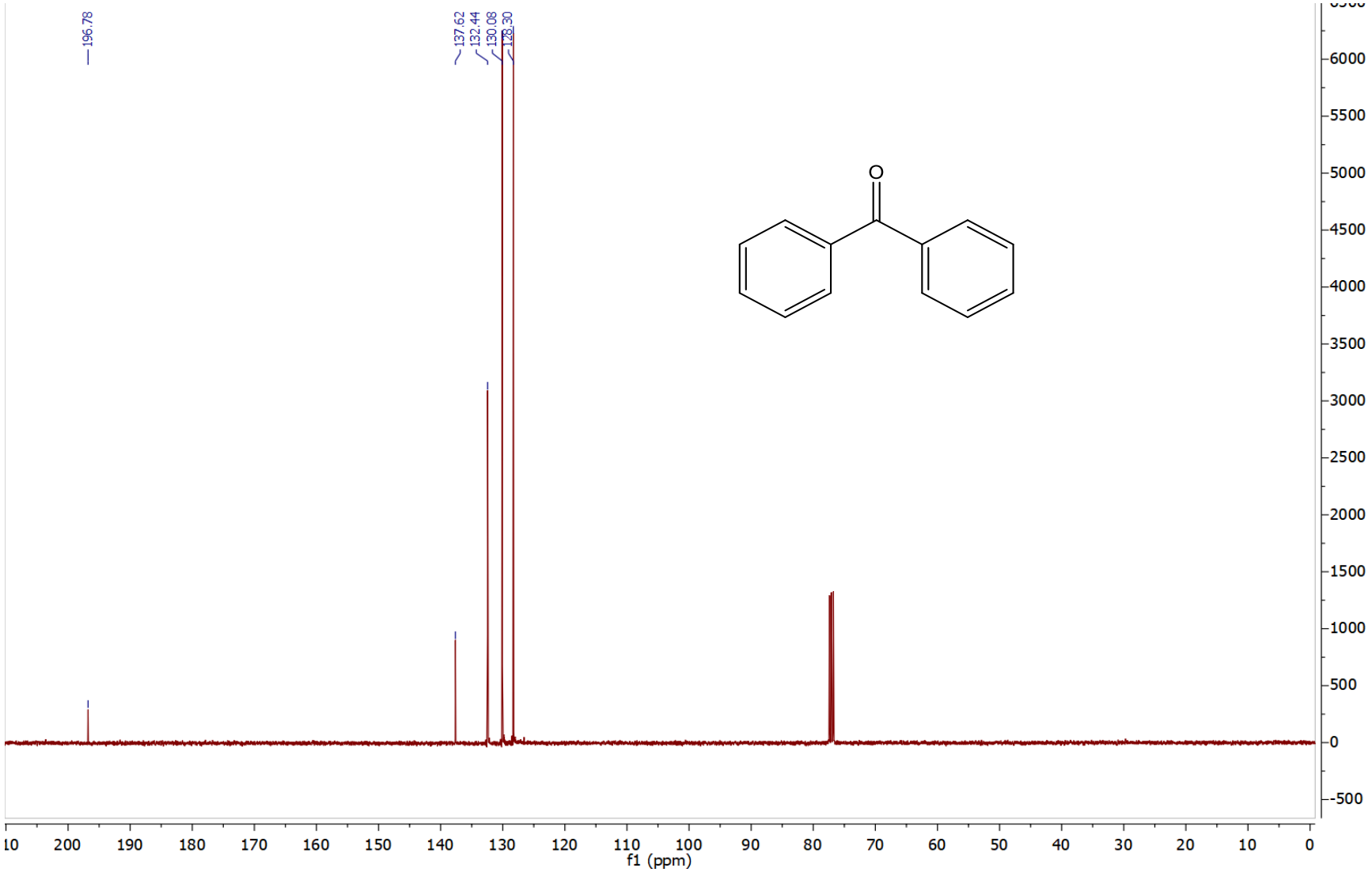

[1]H NMR spectrum of compound 23.

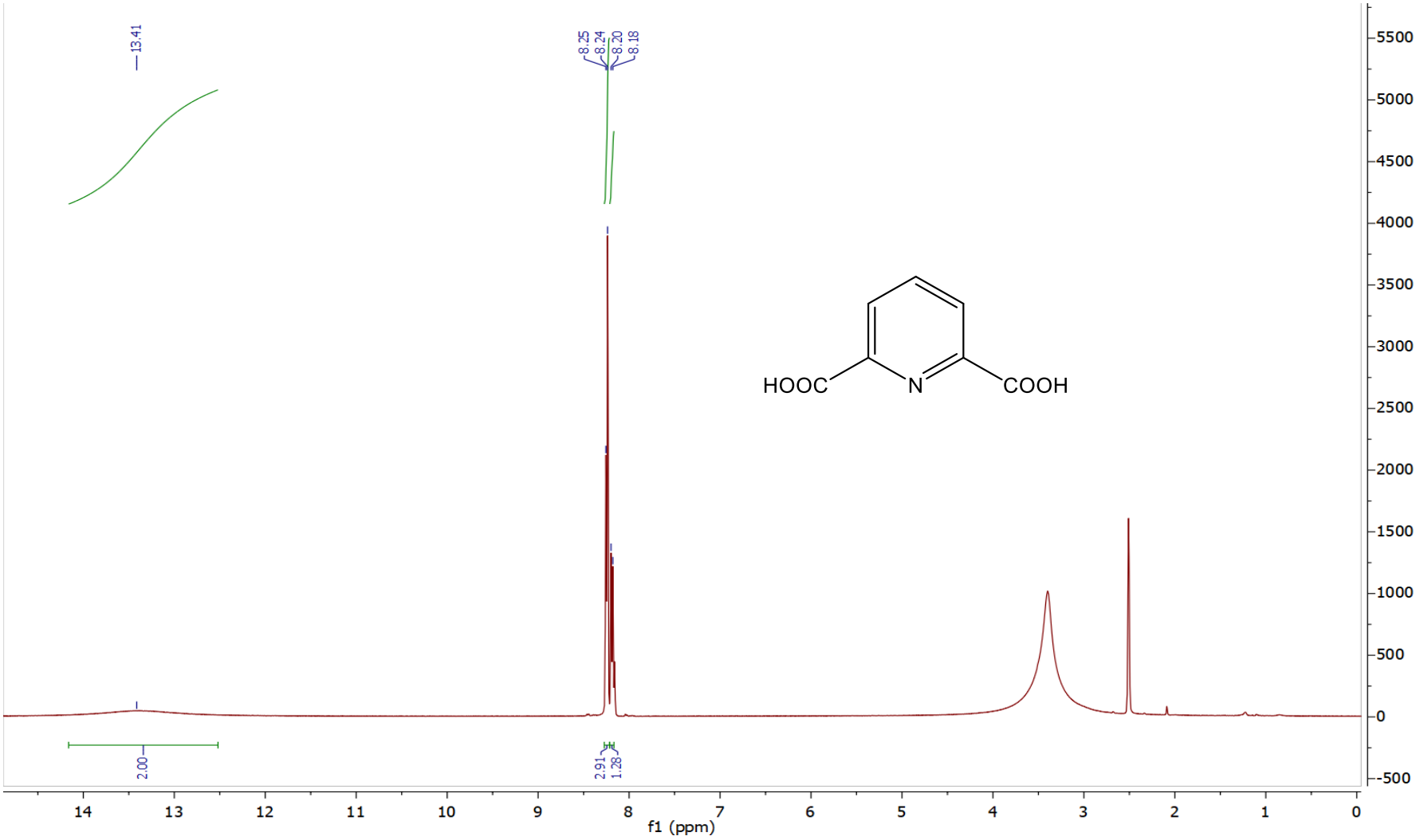

$^{13}C\{^{1}H\}$ NMR spectrum of compound 23.

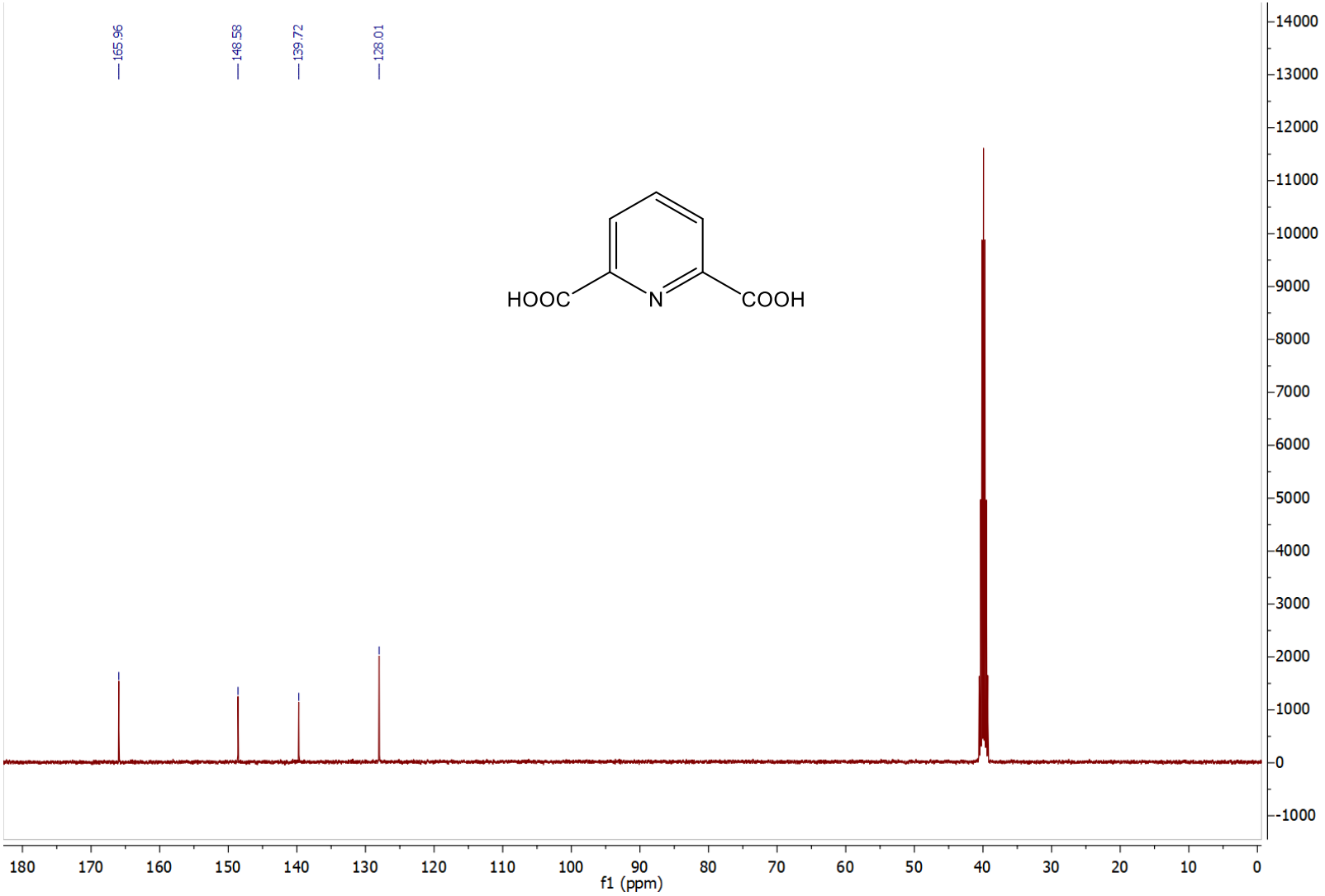

[1]H NMR spectrum of compound 25.

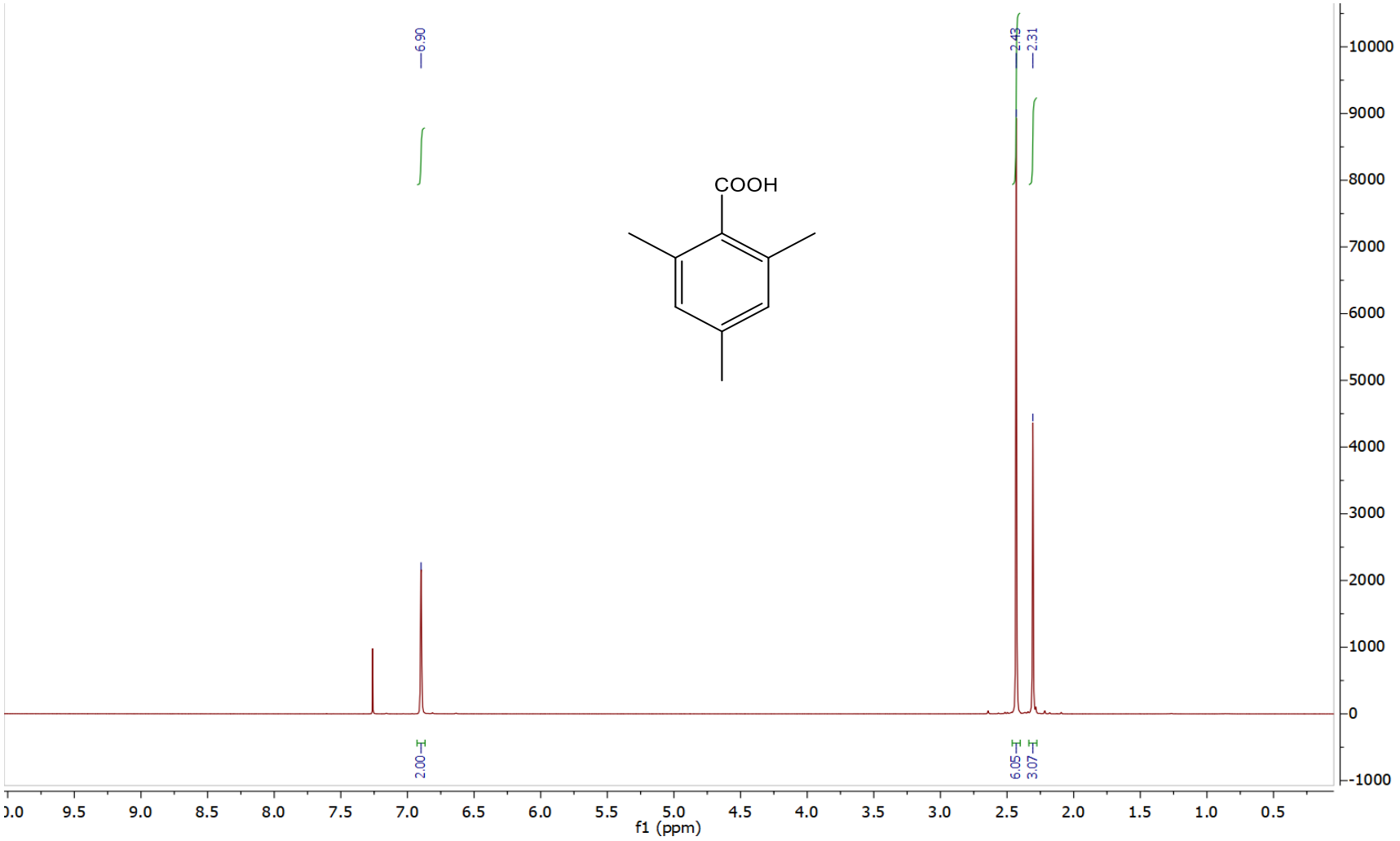

$^{13}C\{^{1}H\}$ NMR spectrum of compound 25.

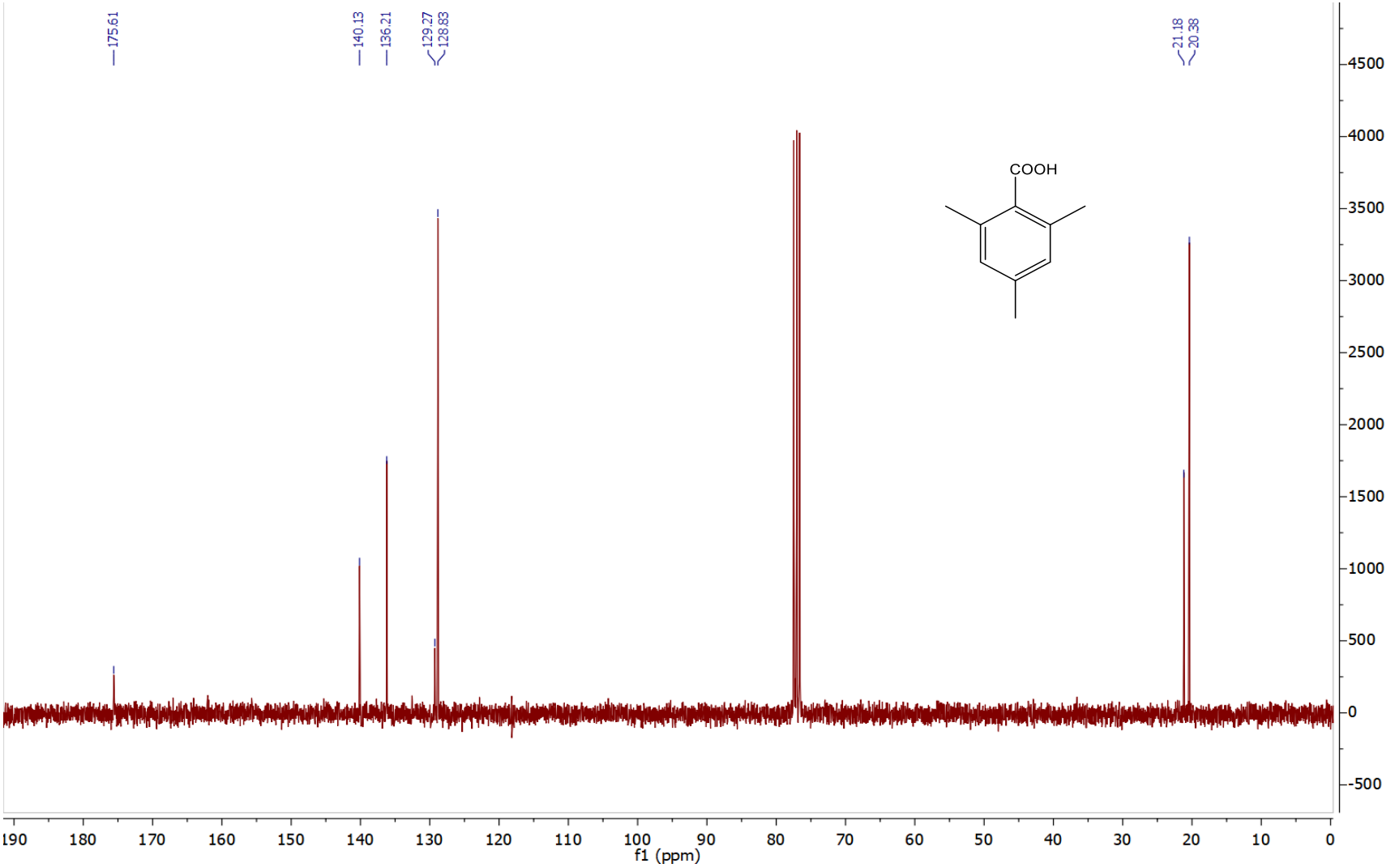

^{1}H NMR spectrum of compound 26.

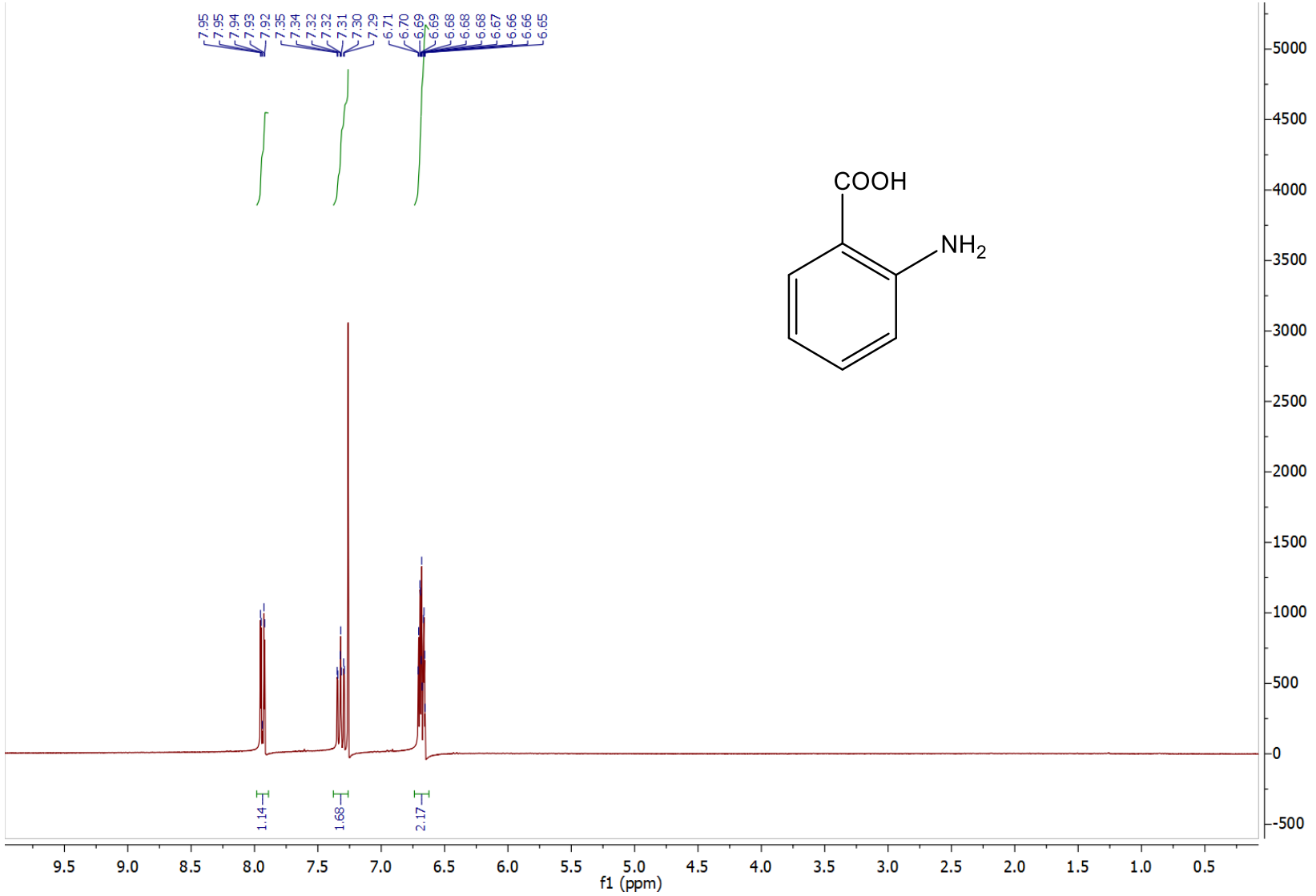

$^{13}C\{^{1}H\}$ NMR spectrum of compound 26.

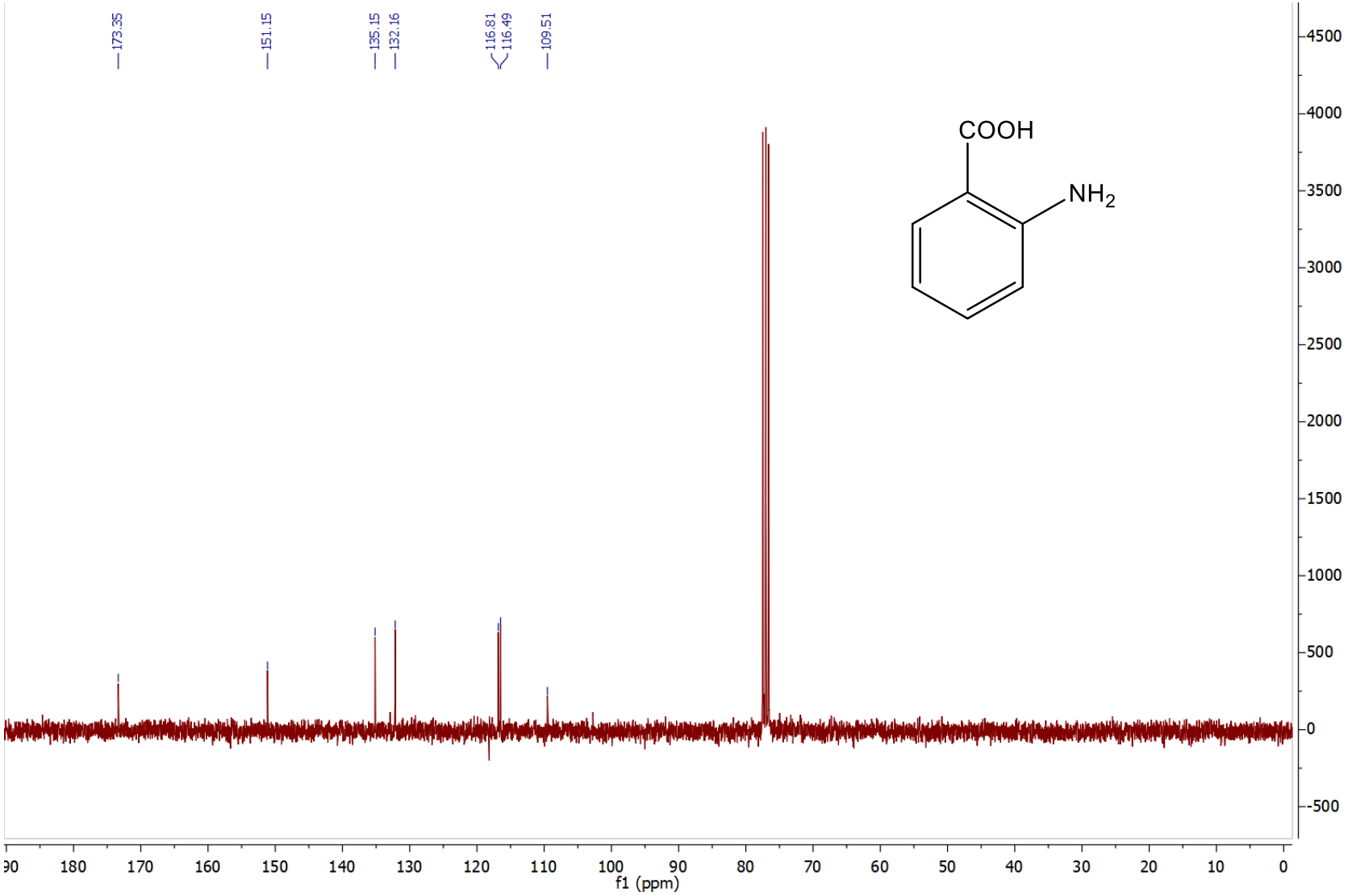

^{1}H NMR spectrum of compound 27.

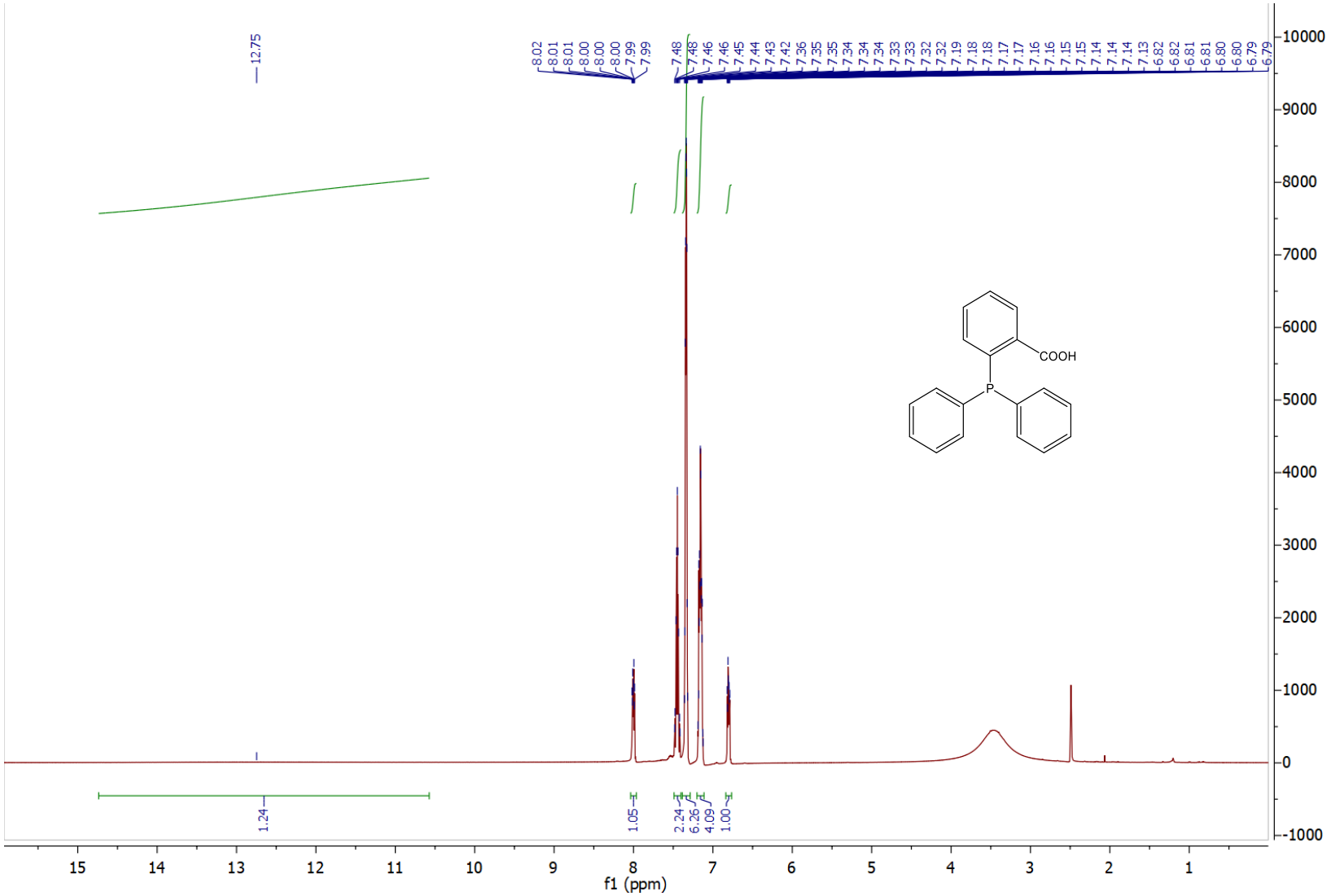

$^{13}C\{^{1}H\}$ NMR spectrum of compound 27.

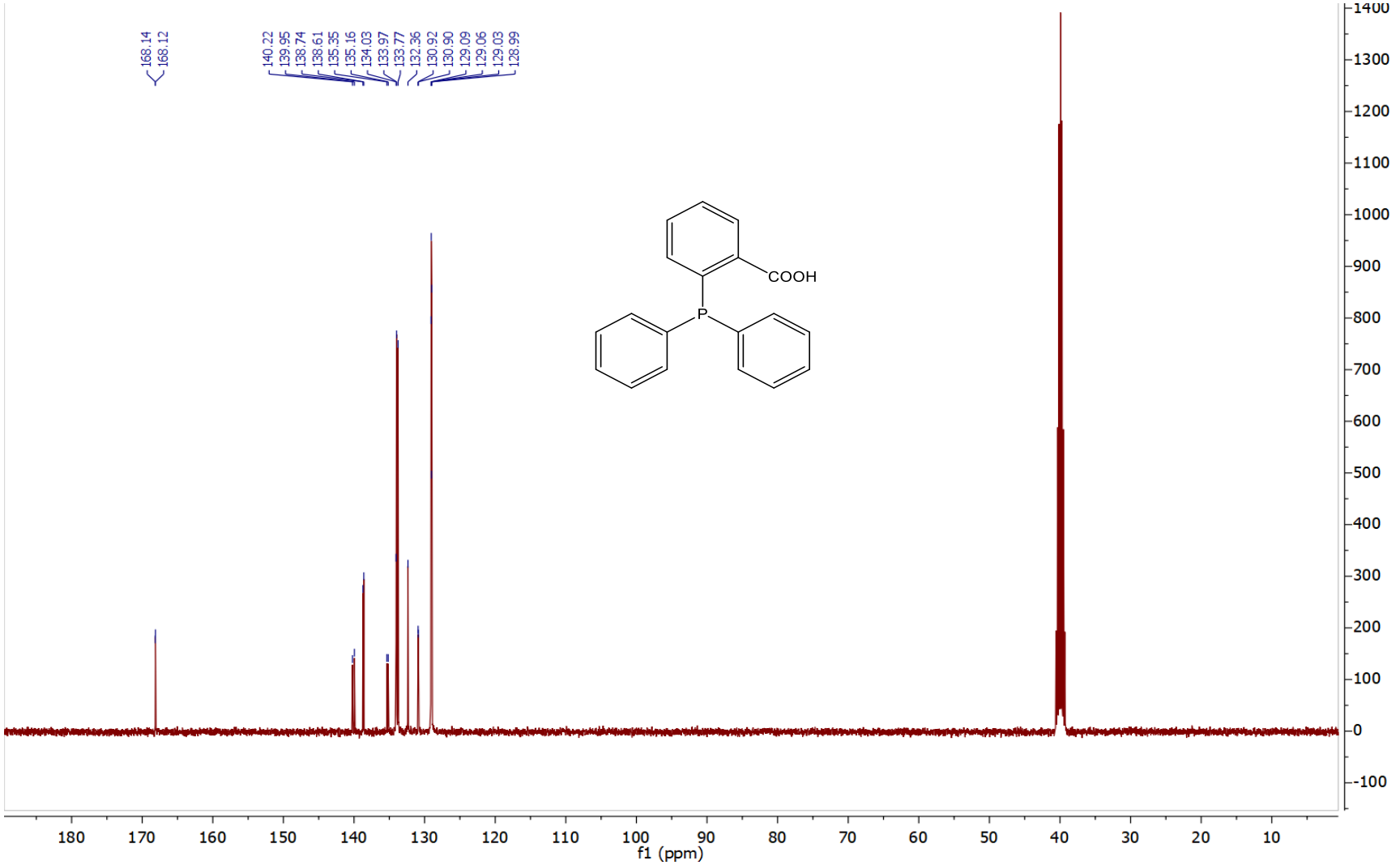

^{31}P NMR spectrum of compound 27.

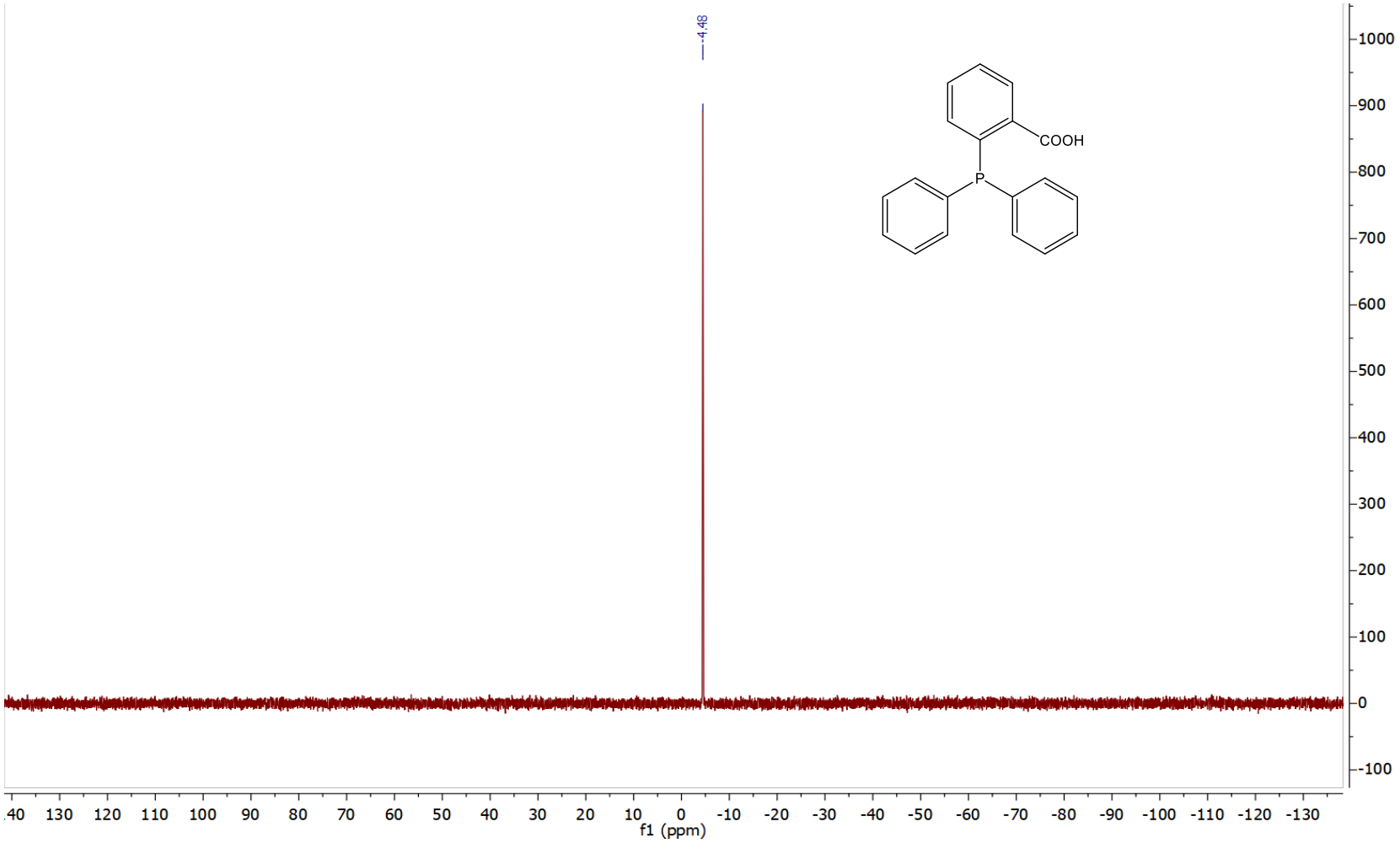

[1]H NMR spectrum of compound 28.

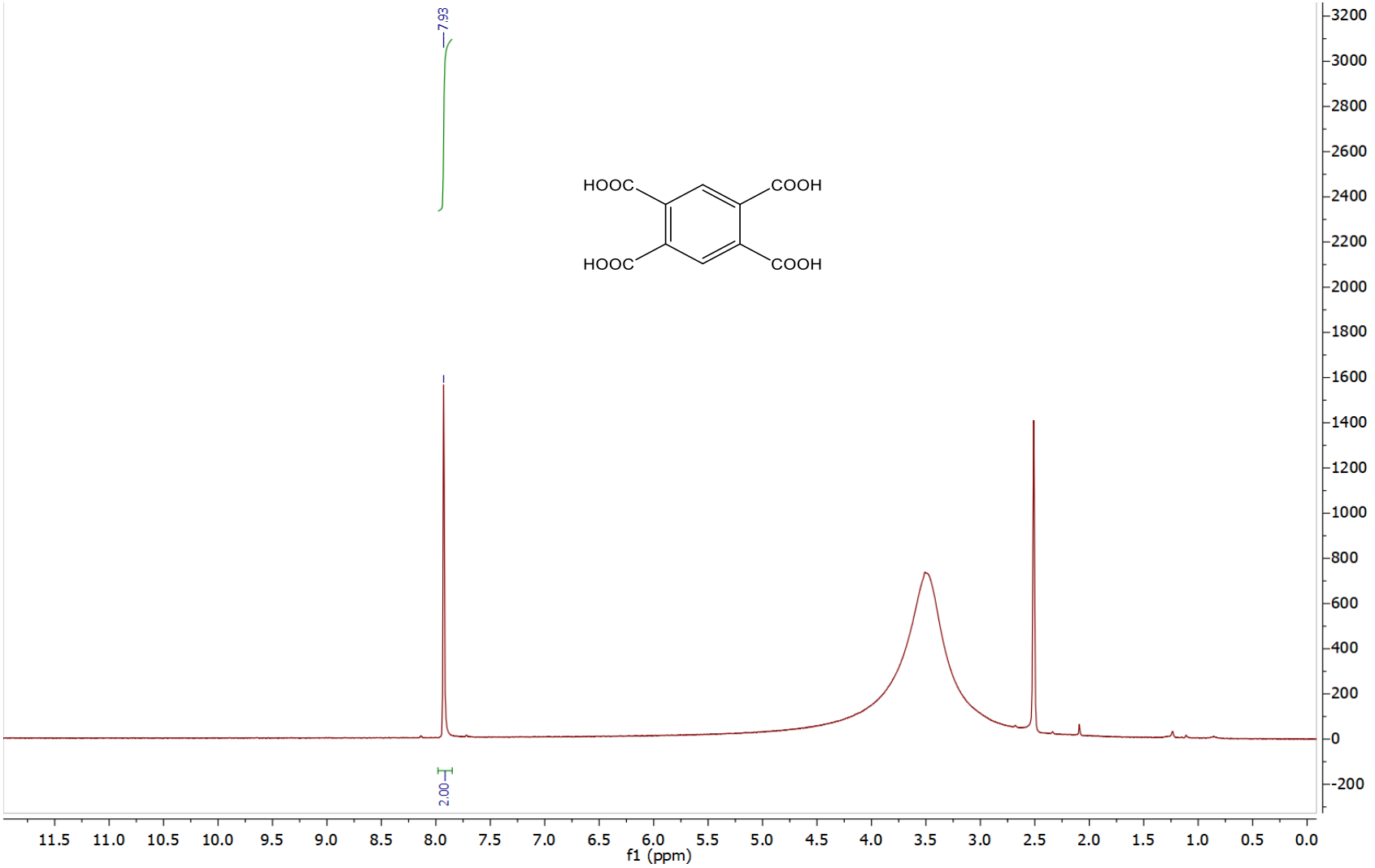

$^{13}C\{^{1}H\}$ NMR spectrum of compound 28.

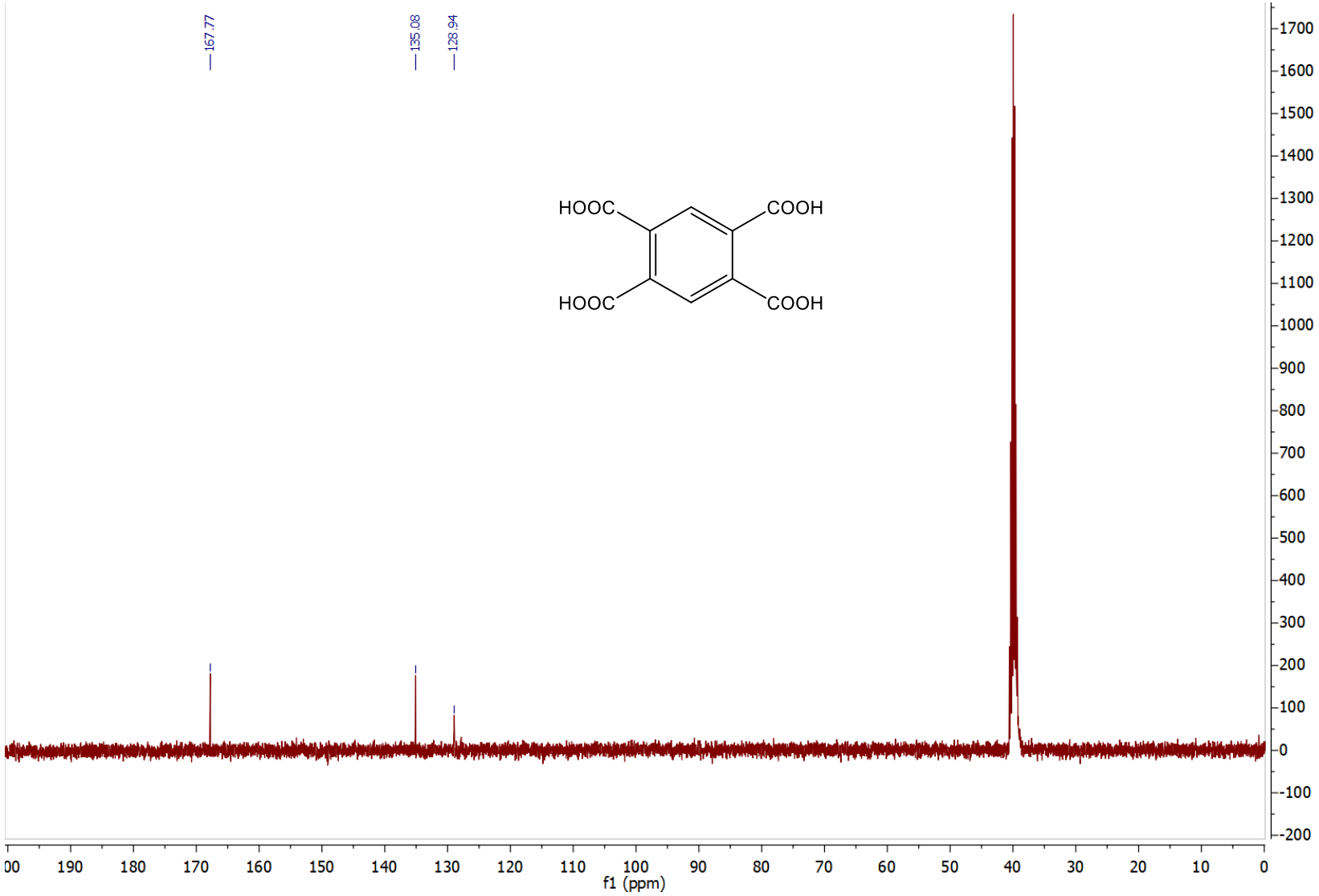

^{1}H NMR spectrum of compound 29.

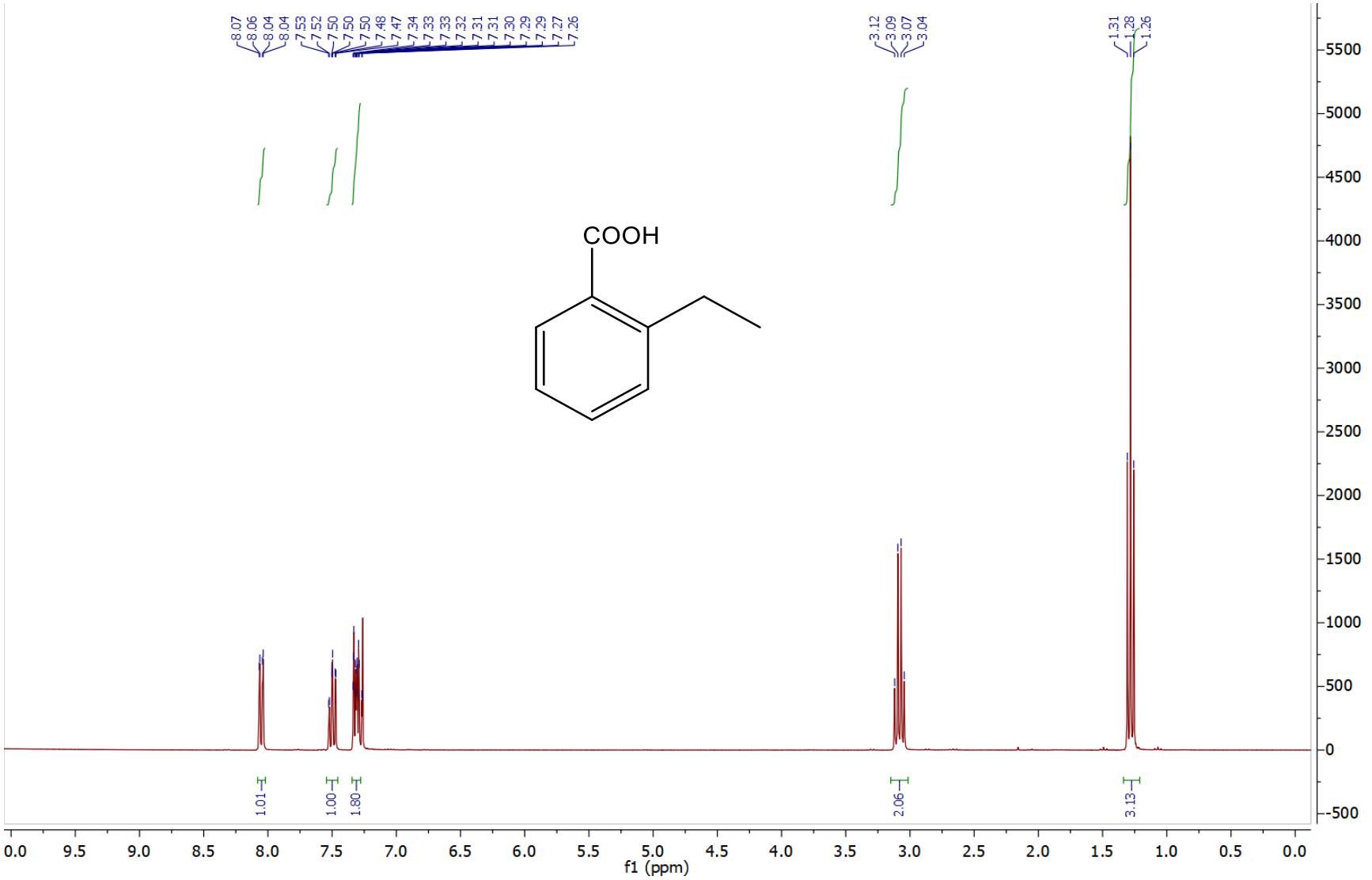

$^{13}C\{^{1}H\}$ NMR spectrum of compound 29.

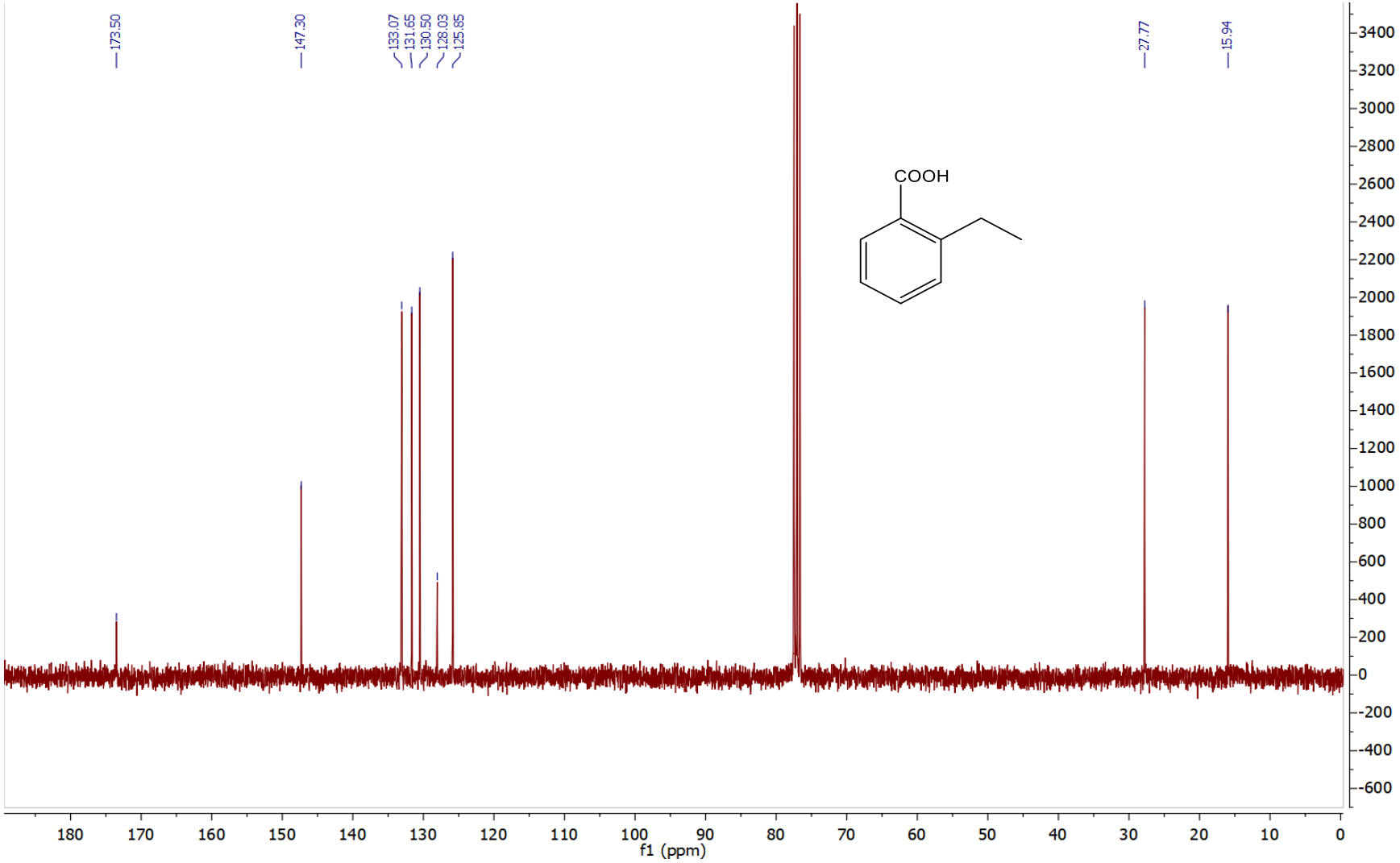

[1]H NMR spectrum of compound 30.

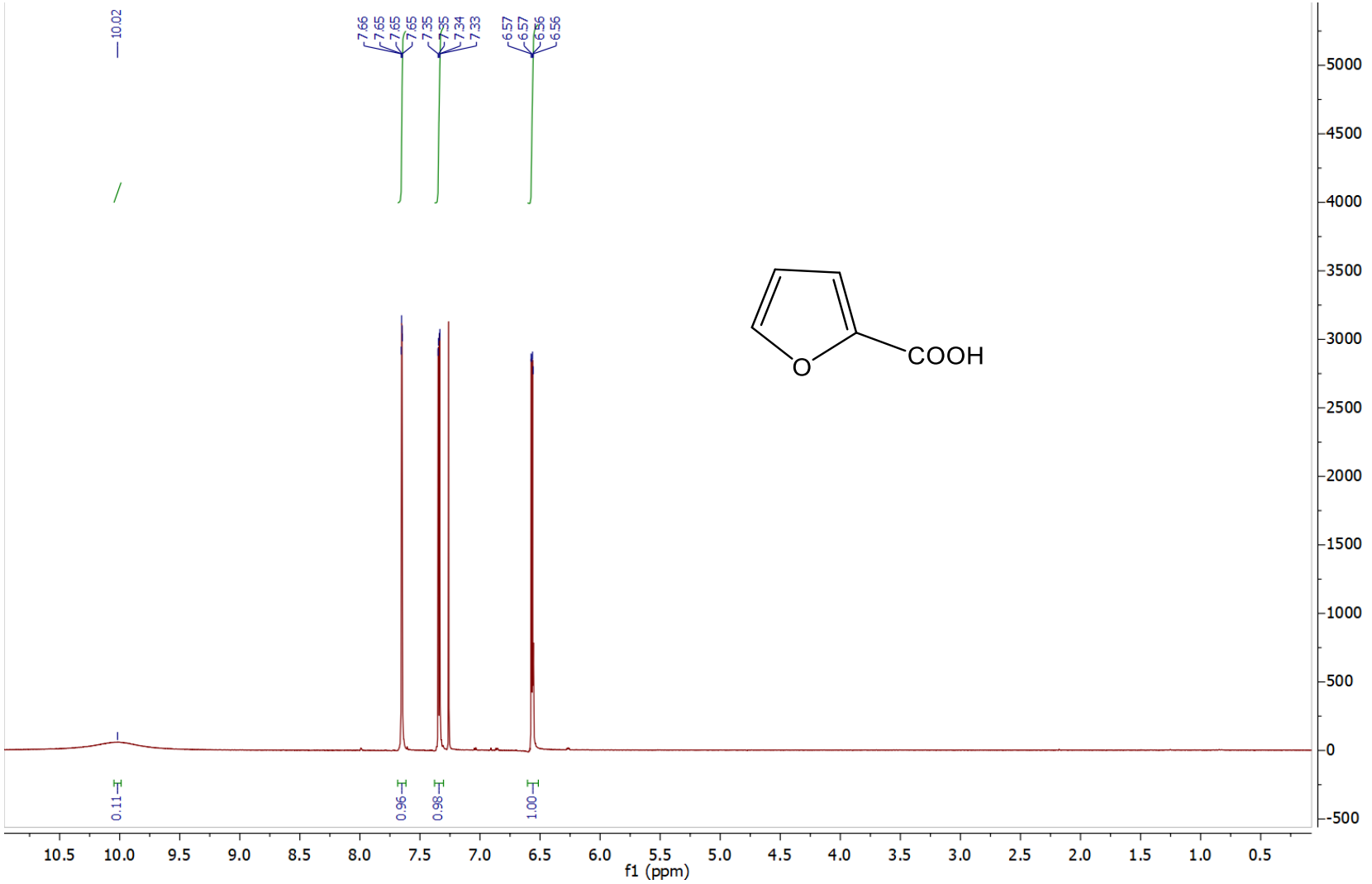

$^{13}C\{^{1}H\}$ NMR spectrum of compound 30.

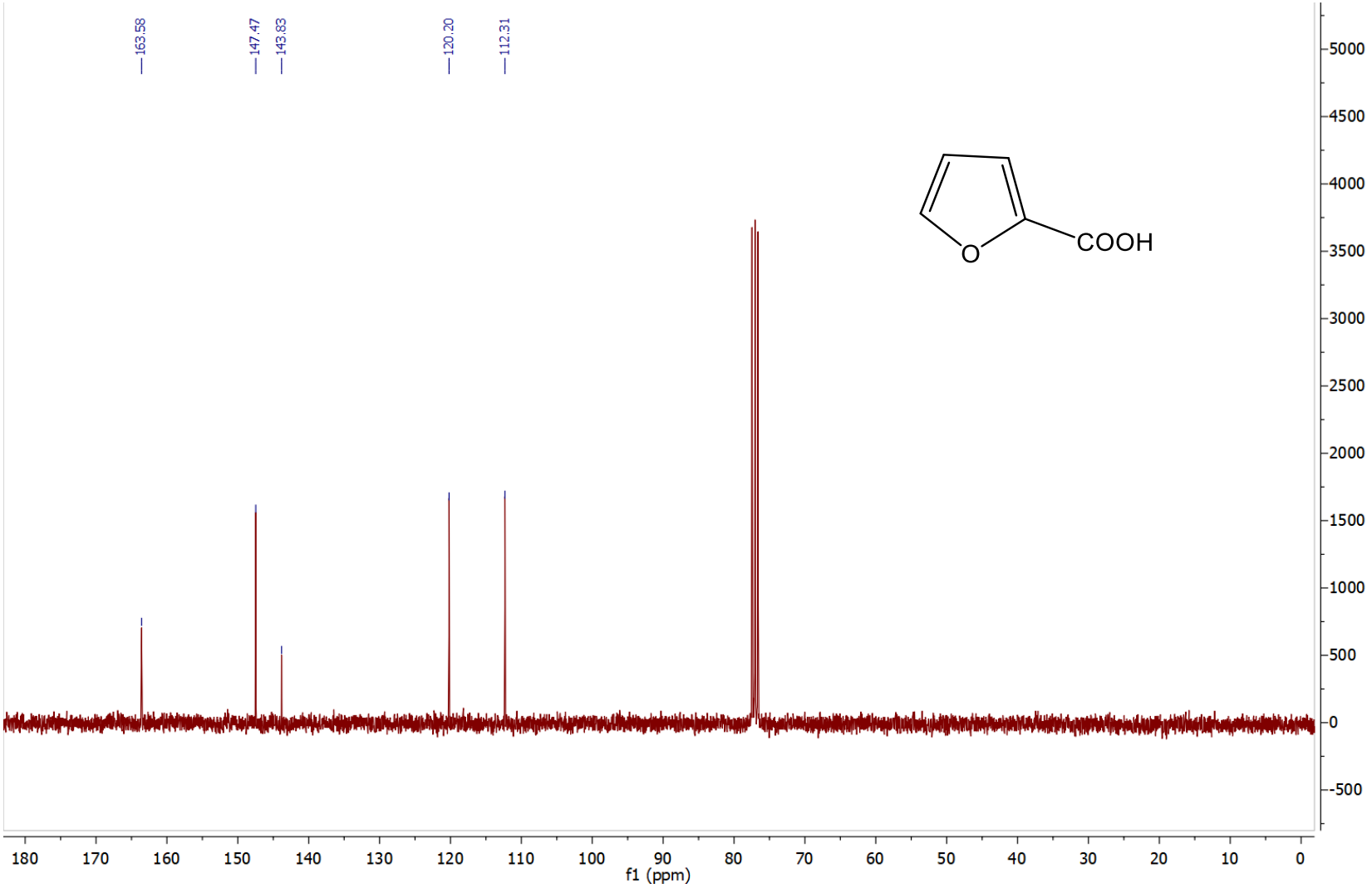

[1]H NMR spectrum of compound 31.

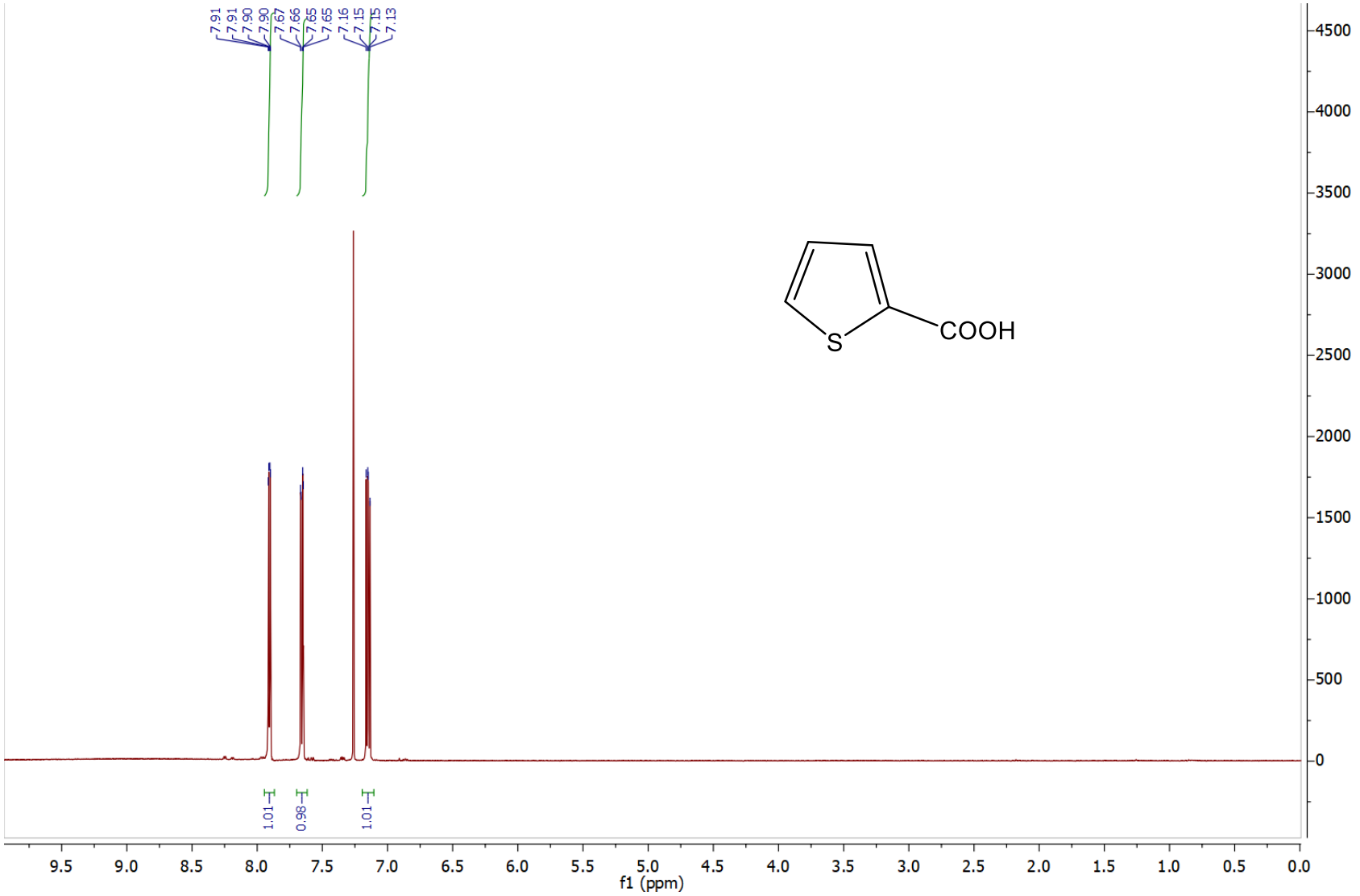

$^{13}C\{^{1}H\}$ NMR spectrum of compound 31.

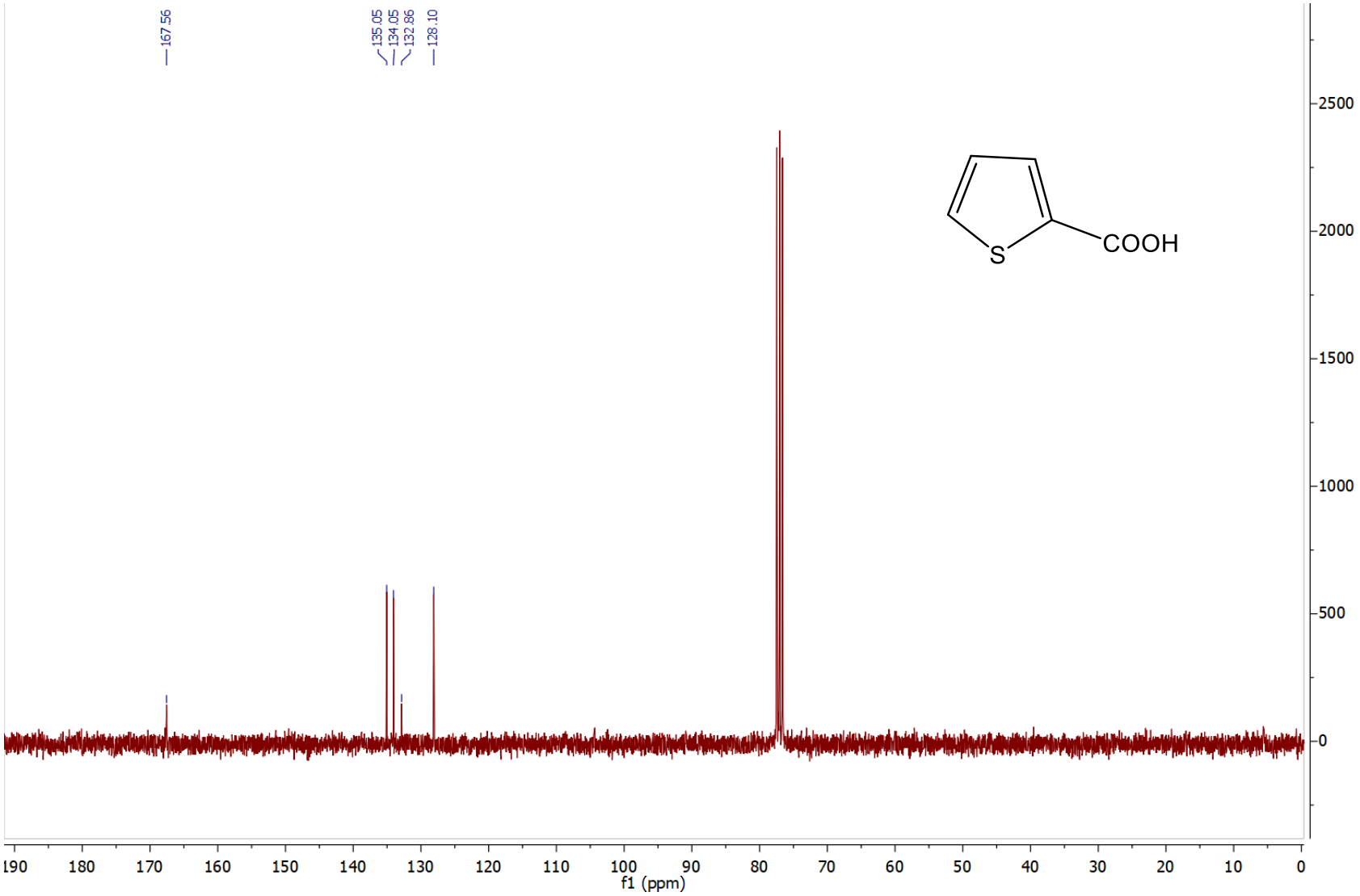

13. Identification of α-bromo ketones.

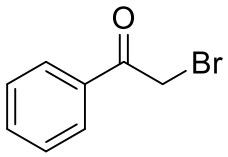

(2-bromo-1-phenylethan-1-one)

^{1}H NMR (400 MHz, Chloroform-*d*) δ 8.04 – 8.00 (m, 2H), 7.67 – 7.61 (m, 1H), 7.55 – 7.50 (m, 2H), 4.49 (s, 2H).
^{13}C NMR (101 MHz, Chloroform-*d*) δ 191.31, 133.99, 128.96, 128.89, 128.50, 30.93.

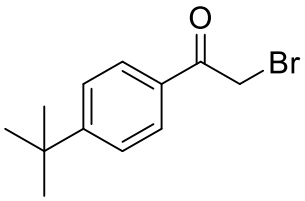

(2-bromo-1-(4-(tert-butyl) phenyl) ethan-1-one)

^{1}H NMR (400 MHz, Chloroform-*d*) δ 7.97 – 7.93 (m, 2H), 7.61 – 7.47 (m, 2H), 4.46 (s, 2H), 1.37 (s, 9H).
^{13}C NMR (101 MHz, Chloroform-*d*) δ 190.90, 157.89, 128.94, 125.97, 125.83, 35.24, 31.07, 31.02.

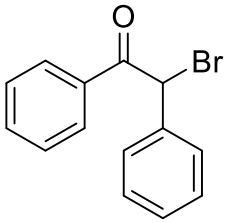

(2-bromo-1,2-diphenylethan-1-one)

^{1}H NMR (400 MHz, Chloroform-*d*) δ 8.04 – 7.99 (m, 2H), 7.57 (t, *J* = 1.8 Hz, 1H), 7.48 (dd, *J* = 8.4, 7.1 Hz, 2H), 7.42 – 7.35 (m, 5H), 6.40 (s, 1H).
^{13}C NMR (101 MHz, Chloroform-*d*) δ 191.09, 135.92, 134.18, 133.73, 129.16, 129.04, 128.83, 128.58, 125.52, 51.05.

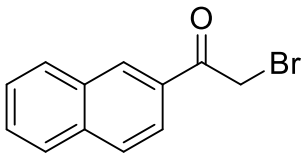

(2-bromo-1-(naphthalen-2-yl) ethan-1-one)
^{1}H NMR (400 MHz, Chloroform-*d*) δ 8.55 – 8.46 (m, 1H), 8.04 (dd, *J* = 8.7, 1.8 Hz, 1H), 8.01 – 7.98 (m, 1H), 7.92 (dd, *J* = 10.4, 8.1 Hz, 2H), 7.65 (ddd, *J* = 8.2, 6.9, 1.4 Hz, 1H), 7.60 (ddd, *J* = 8.2, 6.9, 1.4 Hz, 1H), 4.60 (s, 1H).
^{13}C NMR (101 MHz, Chloroform-*d*) δ 191.32, 135.90, 132.41, 131.30, 130.99, 129.73, 129.08, 128.85, 127.88, 127.10, 124.18, 31.02.

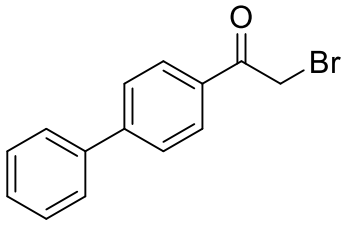

(1-([1,1'-biphenyl]-4-yl)-2-bromoethan-1-one)

^{1}H NMR (400 MHz, Chloroform-*d*) δ 8.13 – 8.03 (m, 2H), 7.77 – 7.72 (m, 2H), 7.68 – 7.64 (m, 2H), 7.52 – 7.49 (m, 2H), 7.47 – 7.44 (m, 1H), 4.51 (s, 2H).
^{13}C NMR (101 MHz, Chloroform-*d*) δ 190.96, 146.69, 139.58, 132.64, 129.59, 129.05, 128.53, 127.50, 127.33, 30.90.

14. NMR spectra of α-bromo ketones.

^{1}H NMR spectrum of 2-bromo-1-phenylethan-1-one in $CDCl_3$ solvent (400 MHz, T = 300 K).

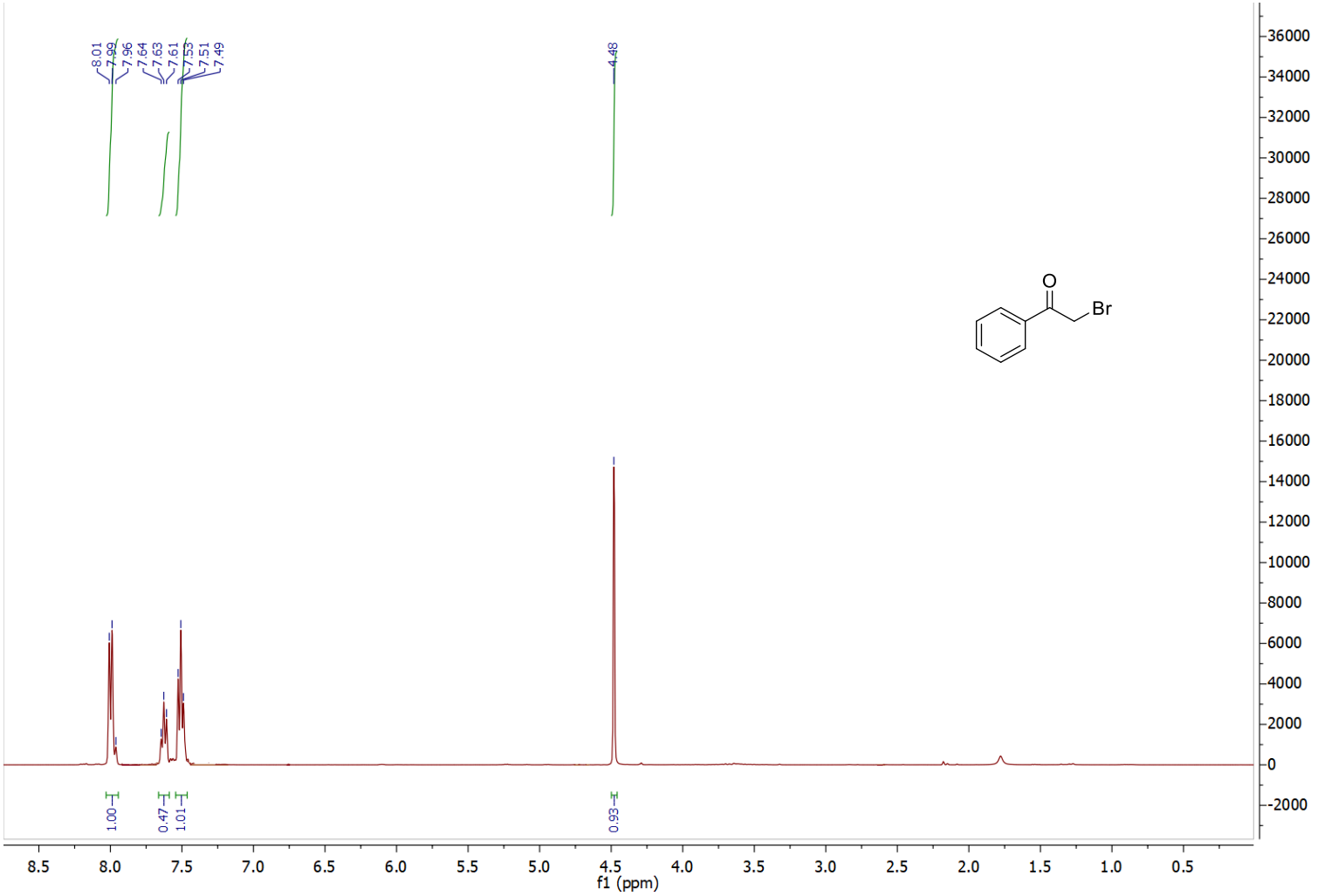

^{13}C NMR spectrum of 2-bromo-1-phenylethan-1-one in $CDCl_3$ solvent (100 MHz, T = 300 K).

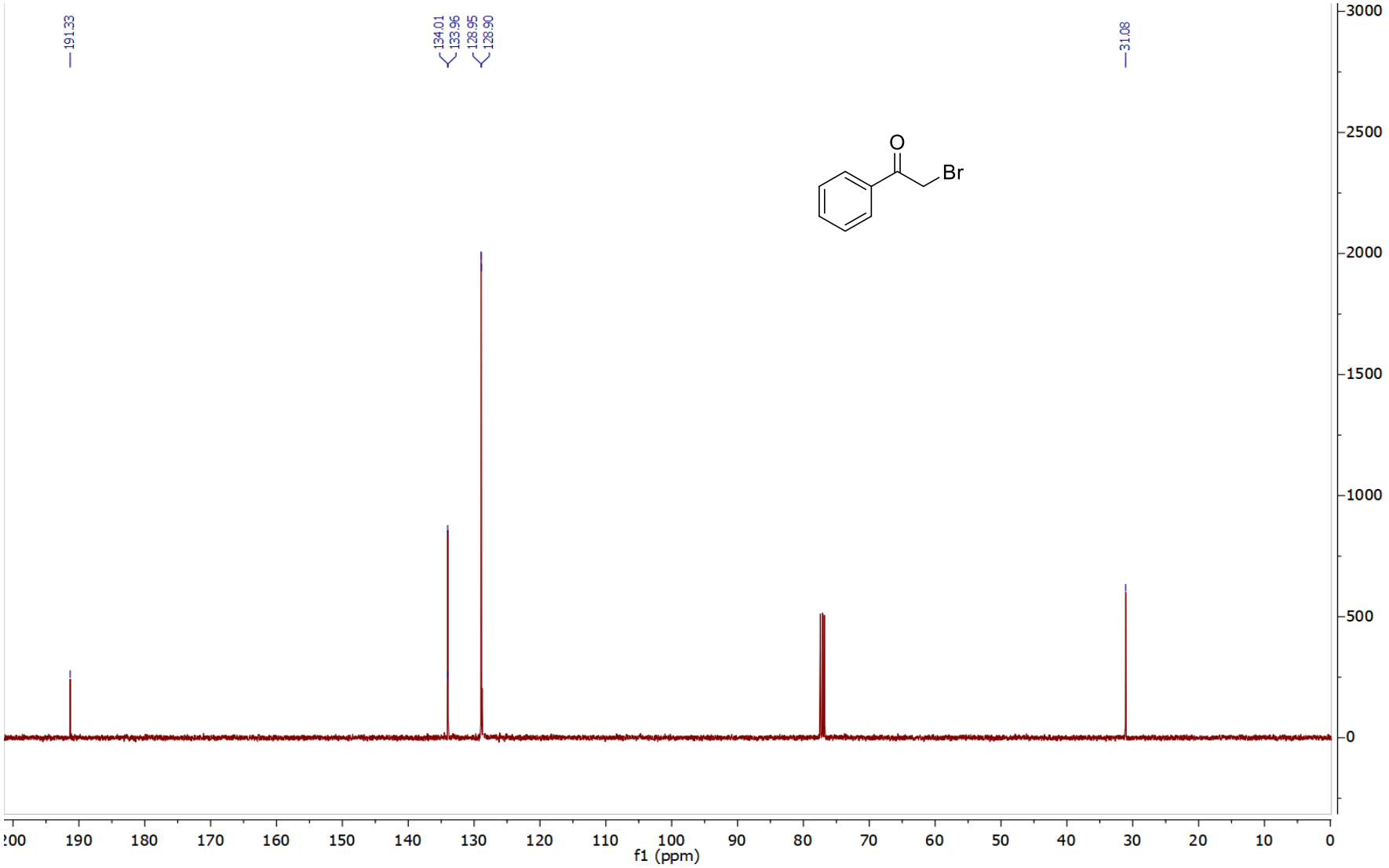

^{1}H NMR spectrum of 2-bromo-1-(4-(tert-butyl)phenyl)ethan-1-one in $CDCl_3$ solvent (400 MHz, T = 300 K).

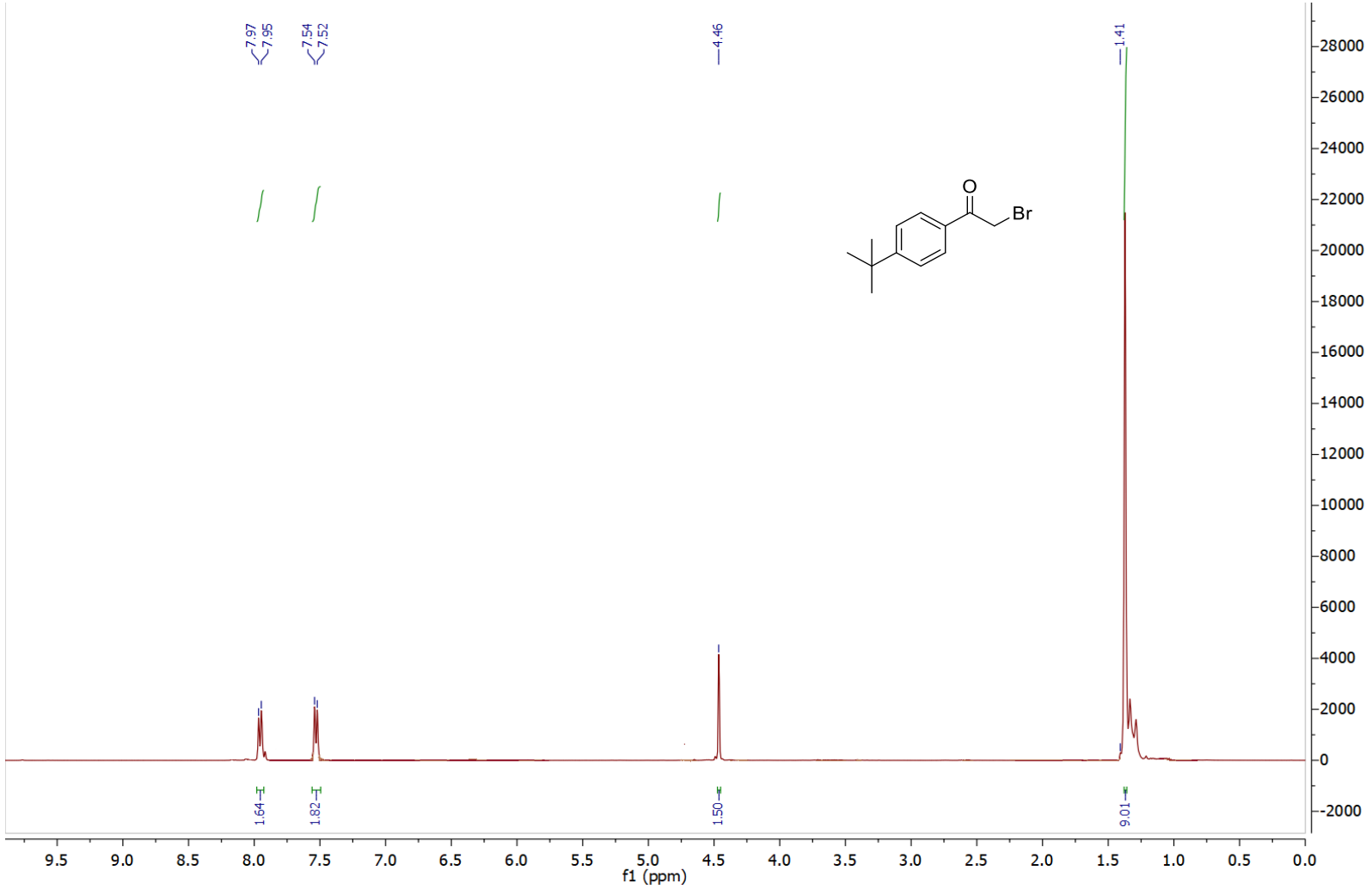

^{13}C NMR spectrum of 2-bromo-1-(4-(tert-butyl)phenyl)ethan-1-one in $CDCl_3$ solvent (100 MHz, T = 300 K).

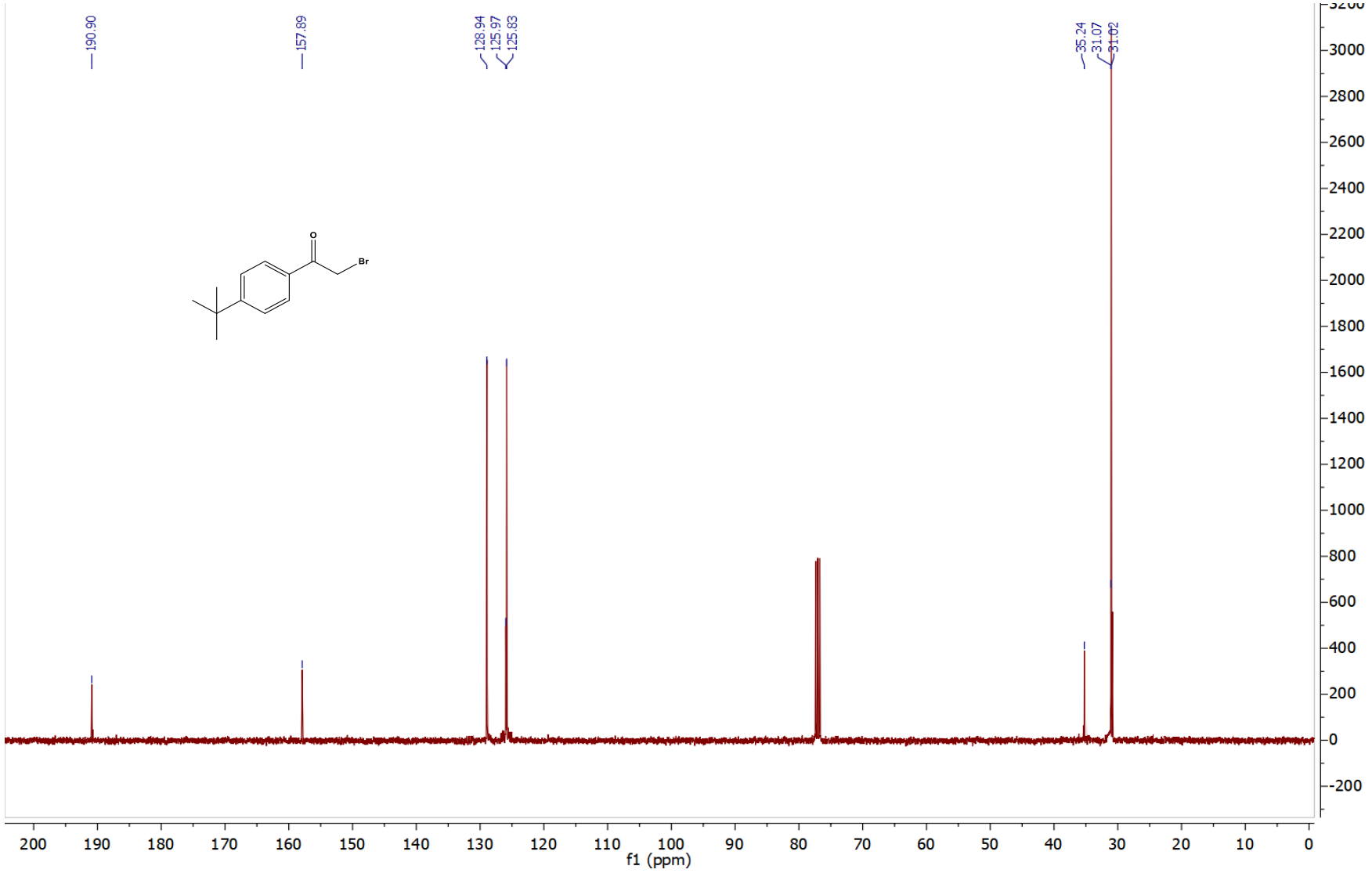

^{1}H NMR spectrum of 2-bromo-1,2-diphenylethan-1-one in $CDCl_3$ solvent (400 MHz, T = 300 K).

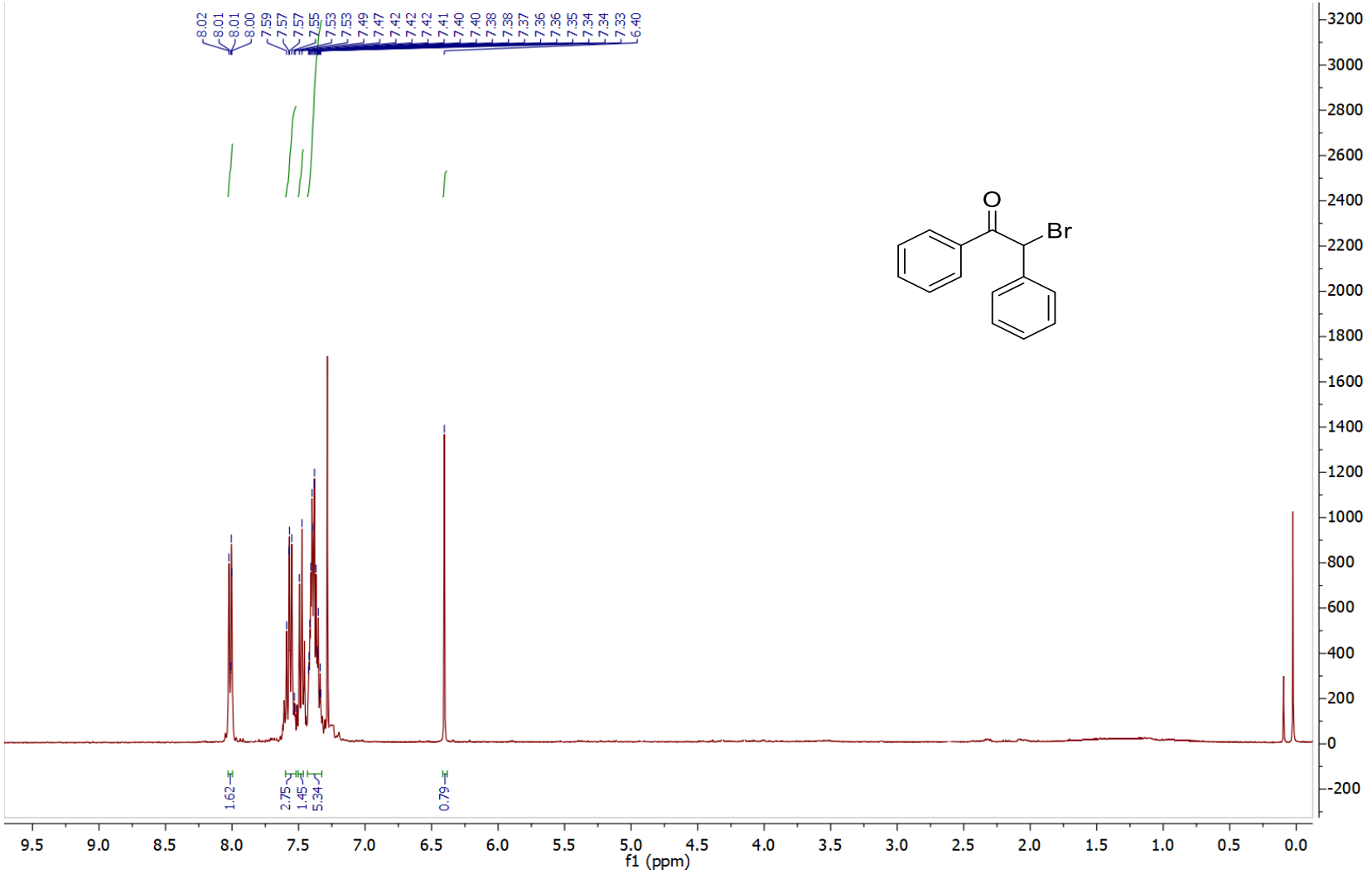

^{13}C NMR spectrum of 2-bromo-1,2-diphenylethan-1-one in $CDCl_3$ solvent (100 MHz, T = 300 K).

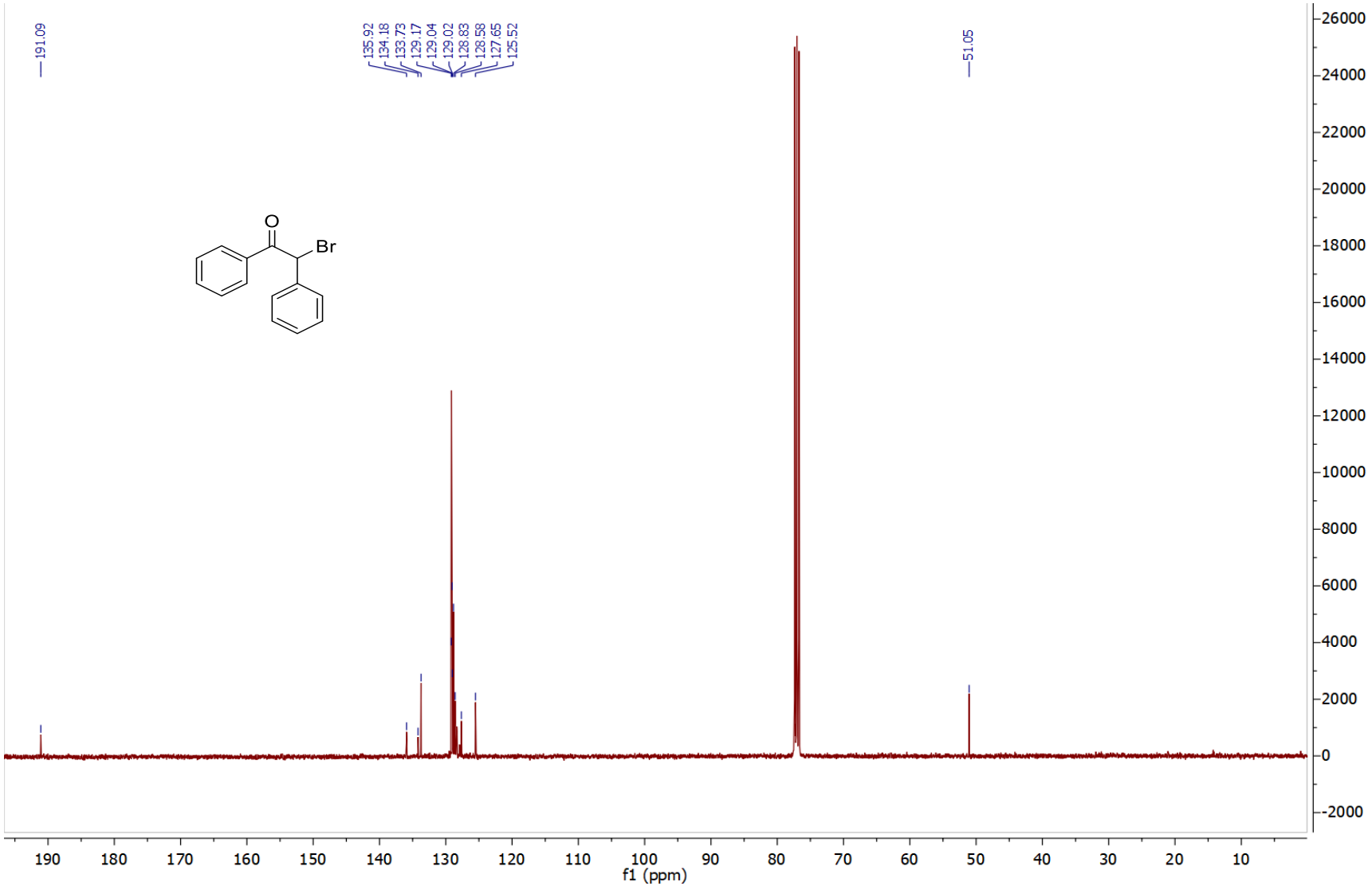

^{1}H NMR spectrum of 2-bromo-1-(naphthalen-2-yl)ethan-1-one in $CDCl_3$ solvent (400 MHz, T = 300 K).

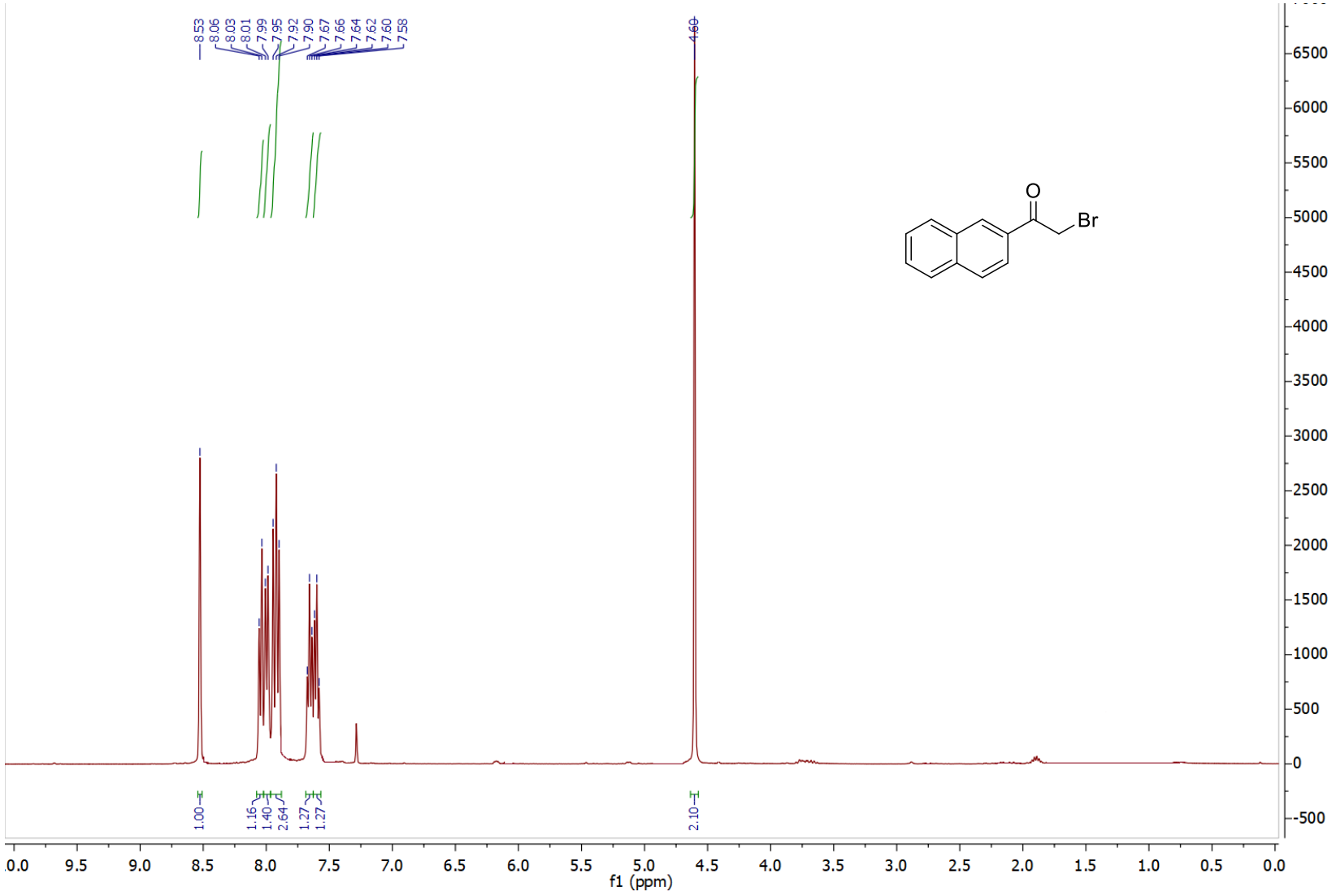

^{13}C NMR spectrum of 2-bromo-1-(naphthalen-2-yl)ethan-1-one in $CDCl_3$ solvent (100 MHz, T = 300 K).

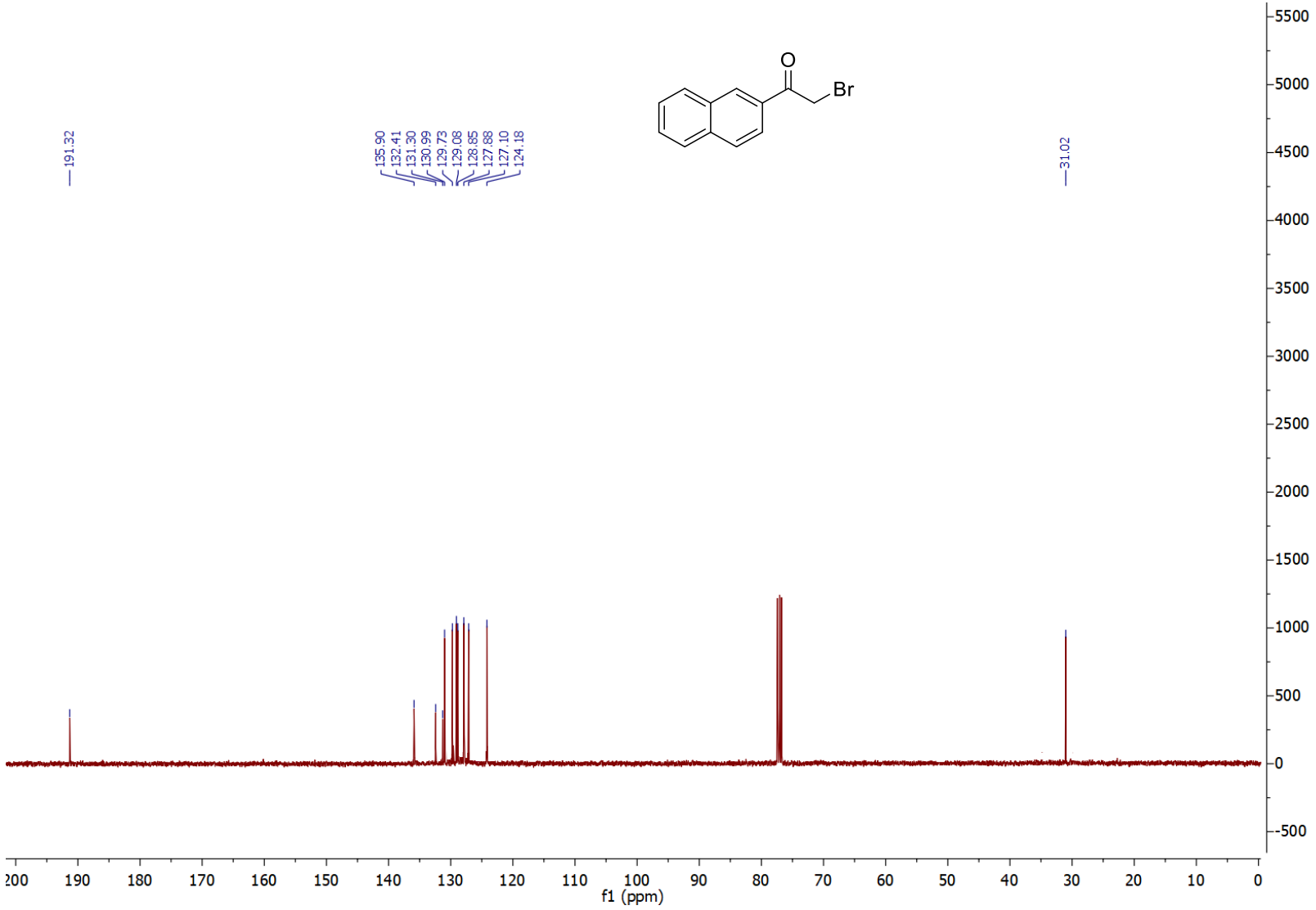

^{1}H NMR spectrum of 1-([1,1'-biphenyl]-4-yl)-2-bromoethan-1-one in $CDCl_3$ solvent (400 MHz, T = 300 K).

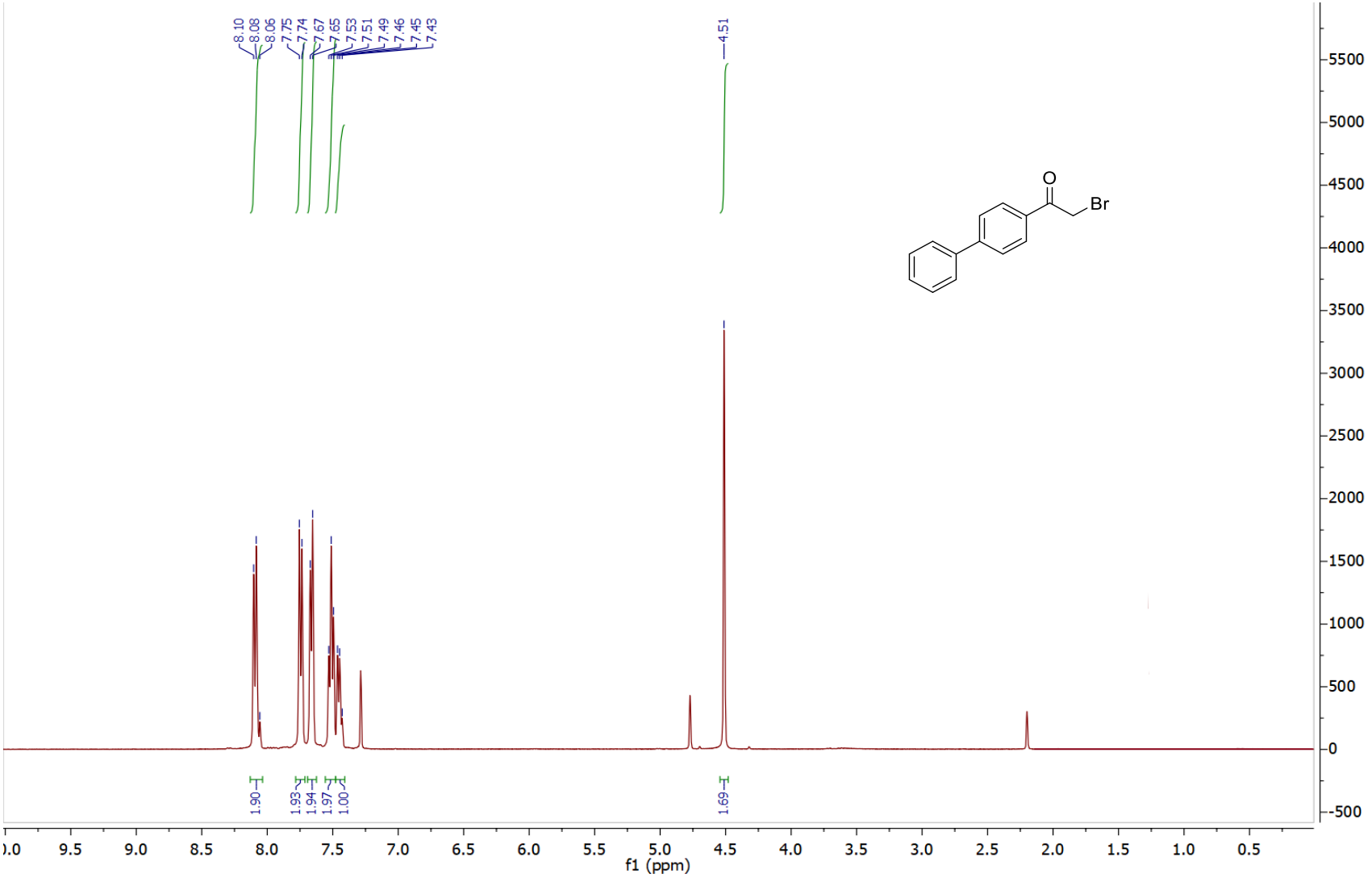

^{13}C NMR spectrum of 1-([1,1'-biphenyl]-4-yl)-2-bromoethan-1-one in $CDCl_3$ solvent (100 MHz, T = 300 K).